INFORMATION TO USERS

This manuscript has been reproduced from the microfilm master. UMI films the text directly from the original or copy submitted. Thus, some thesis and dissertation copies are in typewriter face, while others may be from any type of computer printer.

The quality of this reproduction is dependent upon the quality of the copy submitted. Broken or indistinct print, colored or poor quality illustrations and photographs, print bleedthrough, substandard margins, and improper alignment can adversely affect reproduction.

In the unlikely event that the author did not send UMI a complete manuscript and there are missing pages, these will be noted. Also, if unauthorized copyright material had to be removed, a note will indicate the deletion.

Oversize materials (e.g., maps, drawings, charts) are reproduced by sectioning the original, beginning at the upper left-hand corner and continuing from left to right in equal sections with small overlaps.

Photographs included in the original manuscript have been reproduced xerographically in this copy. Higher quality 6" x 9" black and white photographic prints are available for any photographs or illustrations appearing in this copy for an additional charge. Contact UMI directly to order.

Bell & Howell Information and Learning
300 North Zeeb Road, Ann Arbor, MI 48106-1346 USA

UMI®
800-521-0600

Probing the Redox-Active Residues in Cytochrome *c* Peroxidase

George Tsaprailis

A Thesis

in

The Department

of

Chemistry and Biochemistry

Presented in Partial Fulfillment of the Requirements
for the Degree of Doctor of Philosophy at
Concordia University
Montreal, Quebec, Canada

May 1997

National Library of Canada
Acquisitions and Bibliographic Services
395 Wellington Street
Ottawa ON K1A 0N4
Canada

Bibliothèque nationale du Canada
Acquisitions et services bibliographiques
395, rue Wellington
Ottawa ON K1A 0N4
Canada

Your file Votre référence

Our file Notre référence

0-612-39775-0

Canada

CONCORDIA UNIVERSITY

School of Graduate Studies

This is to certify that the thesis prepared

By: Mr. George Tsaprailis

Entitled: Probing the Redox-Active Residues in Cytochrome *c* Peroxidase

and submitted in partial fulfillment of the requirements for the degree of

Doctor of Philosophy (Biochemistry)

complies with the regulations of this University and meets the accepted standards with respect to originality and quality.

Signed by the final examining committee:

_____ External Examiner

_____ Examiner

_____ Examiner

_____ Examiner

_____ Examiner

Approved by _____

Chair of Department or Graduate Program Director

_____ 19____ _____

Dean of Faculty

ABSTRACT

Probing The Redox-Active Residues in Cytochrome *c* Peroxidase

George Tsaprailis, Ph.D.
Concordia University, 1997.

The reaction of cytochrome *c* peroxidase (CCP) with H_2O_2 results in compound I formation, where the two oxidizing equivalents of H_2O_2 are stored as an oxyferryl heme and a Trp191 radical. Ferrocytochrome *c* *normally* reduces compound I back to the resting enzyme, but in the absence of exogenous donors, CCP can reduce up to 20 equivalents of H_2O_2. Compound I of horseradish peroxidase (HRP) does not form a protein radical, and is unlikely to store oxidizing equivalents on its polypeptide. The conformational states in denaturants of recombinant CCP [CCP(MI)], HRP and their CN-ligated forms were investigated to probe the structural basis of peroxidase polypeptide vs heme reactivity. Despite similar structures, the kinetic stabilities and conformational states of CCP(MI) and HRP were found to be significantly different.

The role of Trp residues as endogenous electron donors in yeast CCP, CCP(MI), and two active site mutants (W51F and W191F) was examined by protein steady-state fluorescence. Compound I and more highly oxidized forms were formed by adding 2, 6, and 20 equivalents of H_2O_2 to the proteins in the absence of exogenous donors. Loss of protein fluorescence following protein denaturation in 8 M urea at pH 1.5 was correlated with Trp oxidation. The fluorescence data confirmed Trp191 radical formation in compound I, suggested that Trp51 becomes redox active when > 2

equivalents of H_2O_2 are reduced, and that ~ 3, 4, 2.5 and 2 Trps were lost in CCP, CCP(MI), W51F and W191F, respectively, following addition of 20 equivalents of H_2O_2. Activity loss in the H_2O_2-oxidized proteins paralleled Trp loss, and correlated with their H_2O_2 titers. SDS-PAGE revealed 40 - 75% *crosslinking* in H_2O_2-oxidized W51F, 0 - 35% in CCP and CCP(MI), and 30 - 35% in W191F.

On-line HPLC-ESI-MS analysis of proteolytic digests of crosslinked W191F revealed that peptides T_6 (residues 30-48) and T_{26} (residues 227-243) formed T_6—T_6 and T_6—T_{26} crosslinks, suggesting that oxidation of exposed Tyr residues in T_6 (Tyr36, 39, 42) is necessary for crosslinking. H_2O_2 oxidation of CCP(MI) in the presence of the spin trap, MNP, revealed that spin adducts were formed on peptides T_6, T_{21} (residues 150-155; Tyr153) and T_{26} (Tyr229, 236). Tyr236 was identified as the major site of spin adduct formation in CCP(MI) by MS sequencing.

ACKNOWLEDGMENTS

I would like to acknowledge first and foremost Dr. Ann English for her support and guidance throughout the course of my studies. I thank her for her scientific excellence and wisdom. Her dedication to her students is something that I will carry with me always and it has been a great pleasure to work and learn from her.

I am grateful to the members of my committee, Drs. John Capobianco and Justin Powlowski. I would like to especially thank Dr. Joanne Turnbull for agreeing to serve as an alternate examiner and for her support and advice with some of the experimental work.

During my time at Concordia I had the pleasure to work with a terrific and talented group of faculty, students and staff. Notable mentions are extended to Dr. Ted Fox, Stephen Marmor, Marco DiFrucio, Antonella Badia, Rina Carlini, Line D'Astous, Ines Holzbaur, Pina Teoli, Angelo Filosa, Iolie Bakas, Yazhen Hu, Haizi Bu, Greg Huyer, Susan Aitkens and Kelly Millan. A very special thank you is directed to Dr. Craig Fenwick who over the years gave me a lot of support and encouragement. I would like to express my gratitude for his friendship and for all those coffee breaks. It has an honor to work and learn from him.

I am especially appreciative for the effort and friendship provided to me by Mr. Bernie Gibbs who initiated me to biological mass spectrometry. I would also like to thank the collective technical staff of the Chemistry and Biochemistry Department for their help during the 1995/1996 academic year.

Finally, I would like to express my gratitude to mom, dad, and Mike.

DEDICATION

Αφιερώνω αυτή την εργασία στους γονείς μου και τον αδερφό μου για την ανεκτίμητη υποστήριξη, βοήθεια και αγάπη που απλόχερα μου χάρισαν ολα αυτά τα χρόνια.

I dedicate this thesis to my parents and brother for their constant and unyielding love, support, and encouragement throughout the years.

TABLE OF CONTENTS

LIST OF FIGURES

LIST OF TABLES

LIST OF ABBREVIATIONS

ABTS;	2,2'-azinobis(3-ethylbenzothiazoline-6-sulfonate)
apoCCP;	CCP from which the heme has been removed
apoHRP;	HRP from which the heme has been removed
apoMb;	Mb from which the heme has been removed
APX;	ascorbate peroxidase (EC 1.11.1.11)
ARP;	*Arthromyces ramosus* peroxidase (EC 1.11.1.7)
ARP-CN;	cyanide-ligated ARP
CCP;	yeast cytochrome *c* peroxidase (EC 1.11.1.5)
CCP-CN;	cyanide adduct of CCP or CCP(MI)
CCP-I;	compound I of CCP
CCP(MI);	recombinant cytochrome *c* peroxidase from *E coli*. (EC 1.11.1.5)
CCP(MI)-I;	compound I of CCP(MI)
CD;	circular dichroism
CID;	collision induced dissociation
CIP;	*Coprinus cinereus* peroxidase (EC 1.11.1.7)
compound I;	two-electron oxidized species formed when stoichiometric (2 *redox* equivalents) H_2O_2 reacts with a peroxidase

compound II;	species formed on one-electron reduction of compound I
cyt *c*;	cytochrome *c*
DETPA;	diethylenetriamine- *N,N,N',N'',N''*-pentaacetic acid
DTT;	dithiothrietol
EDTA;	ethylenediamine tetraacetic acid
ENDOR;	electron-nuclear double resonance
EOP;	eosinophil peroxidase (EC 1.11.1.7)
EPR;	electron paramagnetic resonance
ESI-MS;	electrospray ionization mass spectrometry
EXAFS;	extended X-ray absorption fine structure
Fe^{IV}=O;	oxyferryl iron
FPLC;	fast protein liquid chromatography
FTIR;	Fourier transform infrared spectroscopy
GdHCl;	guanidine hydrochloride
hemin;	ferric protoporphyrin IX heme
HPLC;	high performance liquid chromatography
HPLC-ESI-MS;	high performance liquid chromatography with electrospray ionization mass spectrometric detection

HRP;	horseradish peroxidase isoenzyme C (EC 1.11.1.7)
HRP-CN;	cyanide ligated form of ferric (Fe^{III}) HRP
LC-MS;	liquid chromatography with mass spectrometric detection
LIP;	lignin peroxidase (EC 1.11.1)
LIP-I;	compound I of lignin peroxidase
LPO;	lactoperoxidase (EC 1.11.1.7)
Mb;	myoglobin
Mb-CN;	cyanometmyoglobin
MCD;	magnetic circular dichroism
MNP;	2-methyl-2-nitrosopropane
MnP;	manganese peroxidase (EC 1.11.1)
MPO;	myeloperoxidase (EC 1.11.1.7)
MS/MS;	tandem mass spectrometry
NATA;	*N*-acetyltryptophanamide
NAYA;	*N*-acetyltyrosinamide
NMR;	nuclear magnetic resonance
PGHS;	prostaglandin H synthase or prostaglandin endoperoxidase residues 290-510 (EC 1.11.1)
PNP;	peanut peroxidase (EC 1.11.1.7)
RNase T_1;	ribonuclease T_1 (EC 3.1.27.3)

RR;	Resonance Raman
SDS-PAGE;	sodium dodecyl sulfate polyacrylamide gel electrophoresis
TPO;	thyroid peroxidase
$[D]_{½}$;	denaturant concentration at half maximum ellipticity or relative fluorescence
$P^{+\cdot}$ or $X^{\cdot}$;	organic radical in the form of a porphyrin π-cation radical or an amino acid radical
R_o;	Förster distance, defined as the donor-acceptor separation at which the donor fluorescence is quenched by 50%
$\Delta\varepsilon$;	molar circular dichroic absorption
$\Delta G_{d,aq}$;	Free energy of denaturation under aqueous conditions (0 M denaturant)
$[\theta]$;	molar ellipticity
λ_{ex}	excitation wavelength
m;	slope of the linear dependence of ΔG_d on denaturant concentration

CHAPTER 1

GENERAL INTRODUCTION

1.0 Introduction

Heme peroxidases are plentiful in nature and possess diverse functions and specificities.[1] They catalyze the oxidation of a wide variety of organic and inorganic substrates by hydrogen peroxide (H_2O_2) according to:

$$H_2O_2 + 2AH \rightharpoonup 2H_2O + 2A \qquad 1.1$$

Examples include horseradish peroxidase (HRP), peanut peroxidase (PNP), seed specific ascorbate peroxidase (APX), yeast cytochrome *c* peroxidase (CCP), *Coprinus cinereus* peroxidase (CIP), *Arthromyces ramosus* peroxidase (ARP), lignin peroxidase (LIP), manganese peroxidase (MnP), myeloperoxidase (MPO), thyroid peroxidase (TPO), eosinophil peroxidase (EOP), lactoperoxidase (LPO), and prostaglandin endoperoxidase residues 290-510 (PGHS). Notable among them is CCP since this was the first heme peroxidase for which a high-resolution X-ray structure was available.[2,3] Also, CCP has been studied for over 50 years following its initial discovery by Altschul et al. in 1940.[4] CCP is found in the intermembrane space of yeast mitochondria and its biosynthesis is induced under aerobic growth conditions.[5] CCP catalyzes the oxidation of ferrocyt *c* to ferricyt *c* by H_2O_2:

$$2 \text{ cyt } c \ (Fe^{II}) + H_2O_2 + 2H^+ \rightarrow 2 \text{ cyt } c \ (Fe^{III}) + 2H_2O \qquad 1.2$$

Heme peroxidases are found in plants, fungi, bacteria,[6] and animals.[7] Peroxidases with ferricyt *c* oxidizing activity have been found only in yeast,[4] *Pseudomonas* bacteria,[8] and in parasites such as the cestodes *Hymenolepis dimimata* and *Moniezia expansa*,[9,10] the trypanosomatid *Crithidia fasciculata*,[11] and the trematodes *Fasciola hepatica*[12] and *Schistosoma mansoni*.[13] The biological role of peroxidases is believed to include plant cell wall metabolism, plant hormone biosynthesis and defense in response to cellular oxidative stress.[14] The latter function has been tentatively assigned to CCP since its biosynthesis is related to the stage when yeast switch from anaerobic to aerobic metabolism and H_2O_2 levels increase. It has also been postulated that CCP might act as a control point in cellular respiration by managing the supply of reducing equivalents of ferrocyt *c* to the terminal oxidase in the respiratory chain.[15]

CCP (Figure 1.1) is made up of a single polypeptide chain of 294 amino acid residues.[16] It is a relatively small protein of molecular weight ~ 34 000 Da.[17] The protein is encoded by nuclear DNA and is synthesized in the cytosol with a 68 residue amino-terminal extension[18] which is believed to contain a signal sequence that specifies translocation of CCP into the mitochondrial matrix. The precursor is eventually processed to yield the mature protein.[19] CCP contains a single non-covalently bound protoporphyrin IX prosthetic group[20] which can be removed to produce the apoenzyme.[21] The electronic absorption spectrum of the holoprotein indicates that CCP contains pentacoordinate high-spin ferric heme iron.[17]

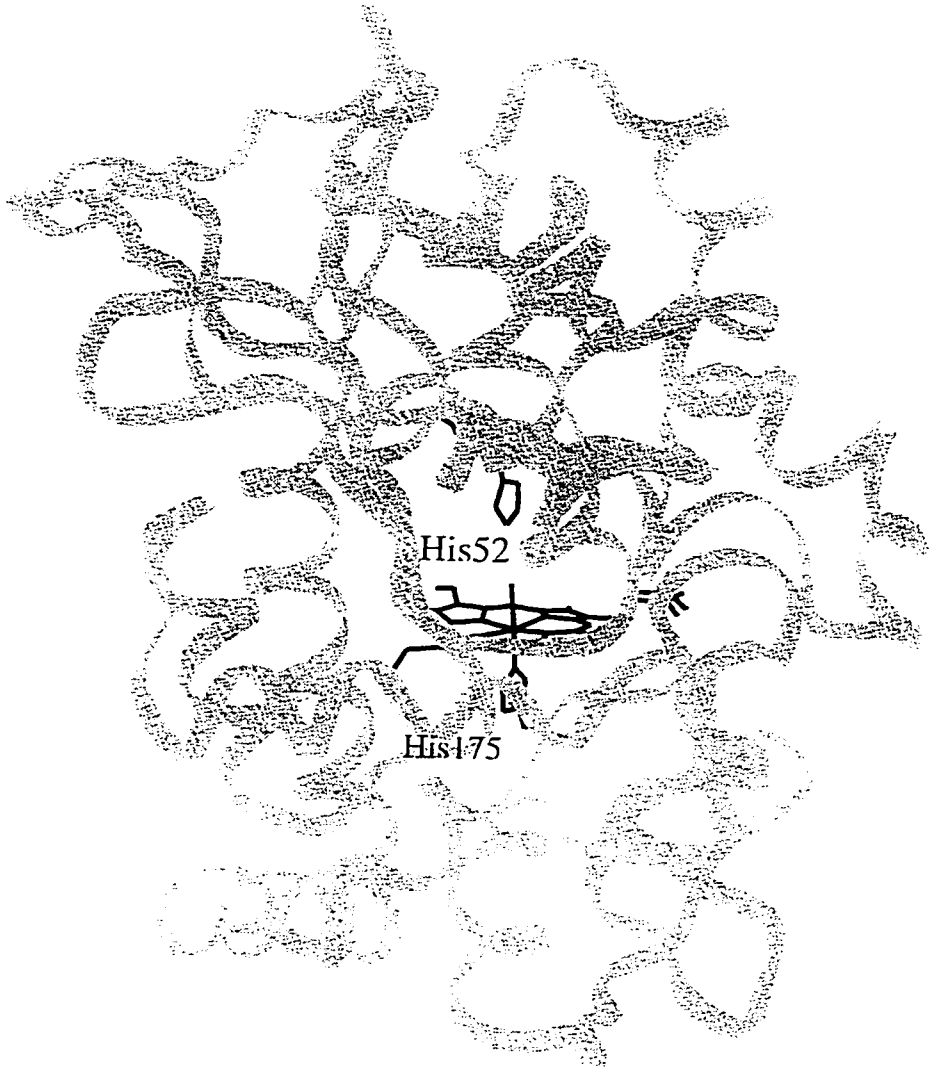

Figure 1.1 The C_α backbone of yeast cytochrome *c* peroxidase generated from the X-ray coordinates.[3] This diagram was prepared using Insight II (v.2.3.0) software (BIOSYM Technologies Inc., San Diego). The heme, distal His52 and proximal His175 are shown in bold.

1.1 Superfamily of Heme Peroxidases

The plant peroxidase superfamily consists of evolutionarily-related heme peroxidases from bacteria, fungi, and plants.[6] The superfamily can be divided into three classes based on sequence alignments and biological origin.[6] Class I is comprised of the intracellular peroxidases and includes CCP and a number of plant and bacterial peroxidases found in the cytosol or chloroplasts. Secretory fungal peroxidases form class II and examples include LIP, MnP, CIP, and ARP. These enzymes are monomeric glycoproteins with four conserved disulfide bridges and two conserved calcium ions. Class III peroxidases include the classical plant secretory peroxidases such as HRP and its isoenzymes, PNP, and barley peroxidase. These are also monomeric glycoproteins with four disulfide bridges and two calcium ions, but the locations of the disulfides differ from those of class II peroxidases, whereas the calcium ions are in the same location in class II and III peroxidases.

Although there is little overall sequence homology within the plant superfamily, the tertiary structures obtained to date (ARP, CCP, CIP, LIP, MnP, and PNP) display considerable structural similarity to CCP shown in Figure 1.1. All possess ten major α-helices and little β-structure, but the loops connecting the helices vary greatly in length between peroxidases. CCP and other class I peroxidases do not contain the four disulfide bridges, the two structural calcium ions nor the glycosylation sites found in class II and III peroxidases. There are nine invariant residues in the plant peroxidase superfamily and most of these are involved in catalysis.[6]

As with the plant peroxidase superfamily and other homologous enzymes,[6,22] it is anticipated that the 3-D structures of the mammalian peroxidases will be shown to be similar. A comparison of the sequences of EPO, LPO, MPO, and TPO reveals that the residues surrounding the heme are highly conserved,[23,24] suggesting a common heme environment for these four mammalian peroxidases. Moreover, spatial superposition of CCP, LIP, MPO and PGHS revealed that the helices making up the heme pocket are arranged very similarly, suggesting a peroxidase fold.[25]

1.2 Compound I Formation

The reaction of H_2O_2 with resting ferric CCP (eq 1.3) is very fast with a second-order rate constant (k_1) of 1.4 x 10^8 $M^{-1}s^{-1}$ between pH 4.5 and 8:[26]

$$CCP(Fe^{III}) + H_2O_2 \xrightarrow{k_1} \text{Compound I}(Fe^{IV}{=}O,\ P^{\bullet+}) + H_2O \qquad 1.3$$

The first step in peroxidase catalysis is the formation of a two-electron oxidized intermediate on reaction of peroxide (ROOH, R=H, alkyl or aryl) with the resting ferric form of the enzyme. This intermediate, which stores the two oxidizing equivalents of the peroxide, is known as compound I. In most peroxidases known to date, except for CCP, both oxidizing equivalents reside on the heme in the form of an oxyferryl iron (Fe^{IV}=O) and a porphyrin π-cation radical ($P^{\bullet+}$).[27] Following the elucidation of the X-ray structure of CCP,[2,3] a detailed mechanism of compound I formation was proposed.[20] This (Figure 1.2) involved binding of H_2O_2 to the Fe^{III} ion

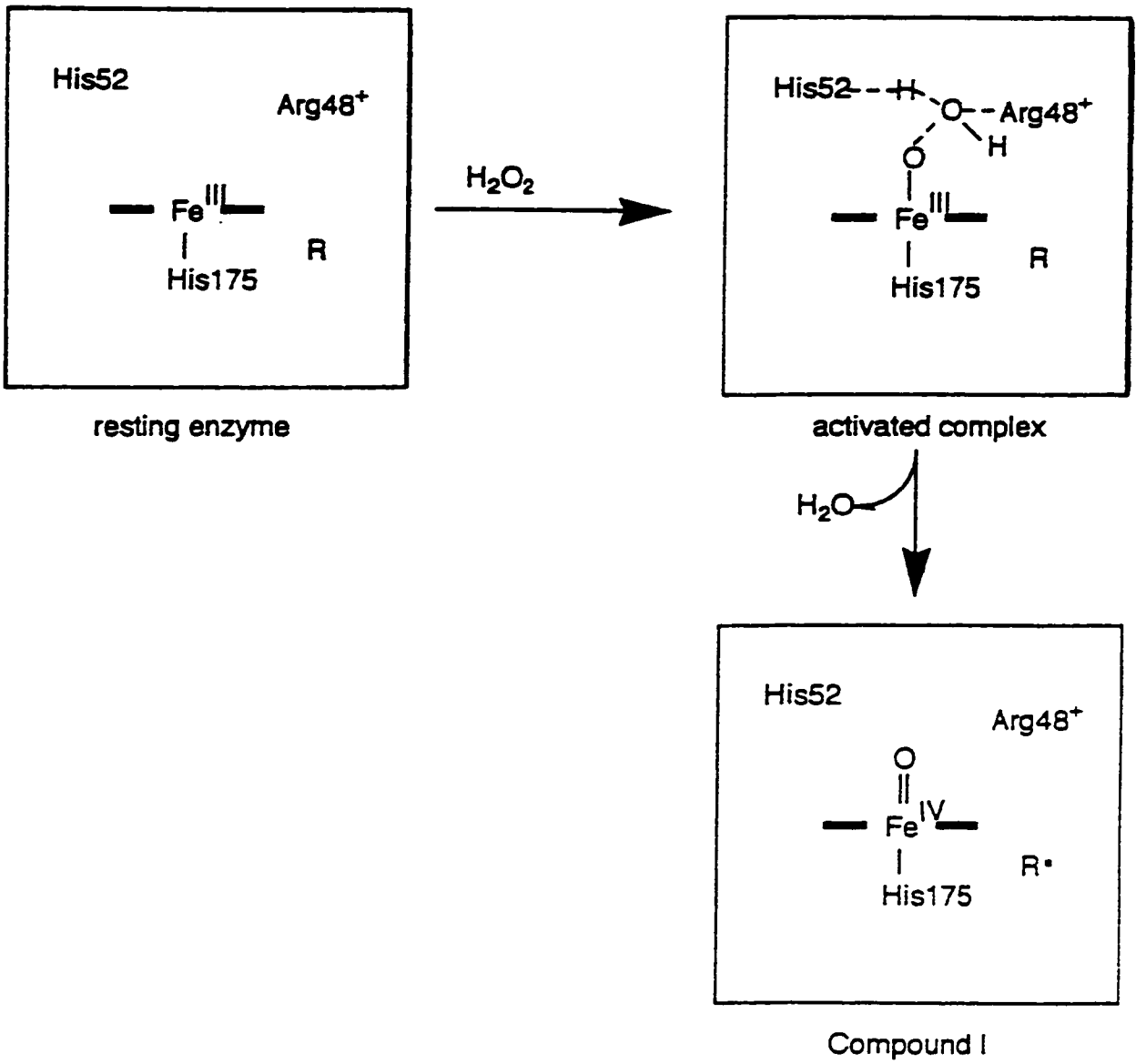

Figure 1.2 Formation of compound I in CCP based on the first proposed mechanism.[20] Adapted from Reference 20.

with the concomitant donation of a proton to the distal His52 from the α-oxygen of H_2O_2. In addition to His52, CCP contains other active-site residues (Figure 1.3) which are poised to aid in the heterolytic cleavage of peroxide.[20] In the model of Poulos and Finzel (Figure 1.2),[20] the positively-charged guanidinium side-chain of Arg48 moved to directly interact with the anionic peroxide ligand, thus promoting the build up of negative charge on the β-oxygen atom. The reorientation of Arg48 coupled with back proton transfer from His52 to the β-oxygen resulted in general acid-catalyzed heterolytic cleavage of the peroxide O—O bond, and the formation of H_2O and a "Fe^{V}=O" species. The latter is rapidly reduced via intramolecular electron transfer from an amino acid residue to form Fe^{IV}=O; thus, one oxidizing equivalent remains at the heme iron and one is stored on the polypeptide as an amino acid radical in CCP compound I.

More recently, the mechanism for compound I formation in CCP has been revised (Figure 1.4). This is largely based on the elucidation of the X-ray structure of the Fe^{II}-O_2 adduct of the Trp191→Phe mutant of CCP (W191F), which serves as a model for the Fe^{III}-OOH, or ES complex.[28] The refined structure reveals two distinct binding sites for oxygen close to the iron. These are stabilized by H-bonding between the O_2 ligand and Trp51 and His52 (Figure 1.4), but no interaction is observed between Arg48 and the bound O_2. Following the transfer of a proton from the α-oxygen of H_2O_2 to His52 to yield the activated complex (Figure 1.2), His52 donates the proton to the β-oxygen giving rise to a water molecule as the leaving group. This water is dispelled from the heme pocket by nonbonded interactions with the nascent

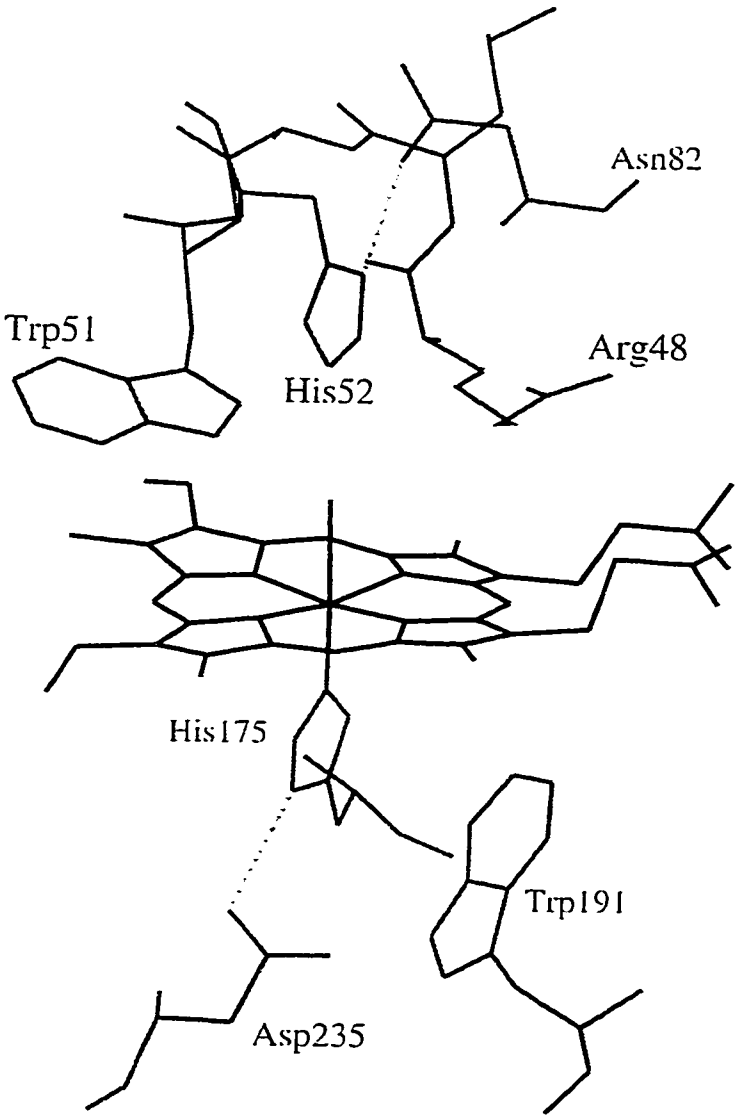

Figure 1.3 Active-site structure of yeast cytochrome *c* peroxidase. The dashed lines represent H-bonds between N1 of the distal His52 and the side-chain carbonyl of Asn82, and N1 of the proximal His175 and the side-chain carboxylate of Asp235. This diagram was generated using the X-ray coordinates for the 1.7-Å structure of CCP.[3]

Figure 1.4 Fe^{III}-OOH (ES) complex of CCP and its decay to compound I. **(A)** The proposed structure of the ES complex showing H-bonding between the α-oxygen and Trp51, and the β-oxygen and His52. The active-site water (Wat648) is depicted as an asterisk. **(B)** The activated complex showing proton donation from His52 to the β-oxygen, partial cleavage of the O—O bond, and the reorientation of Arg48 to H-bond donate to the nascent oxene ligand, which dispels Wat648 from the active site. **(C)** The oxyferryl center of compound I showing H-bonding between the oxene ligand and Trp51 and Arg48. This diagram was generated using the X-ray coordinates for the 2.2-Å structure of the O_2 adduct of CCP(W191F),[28] which were kindly provided by Mark Miller (University of California, San Diego).

A

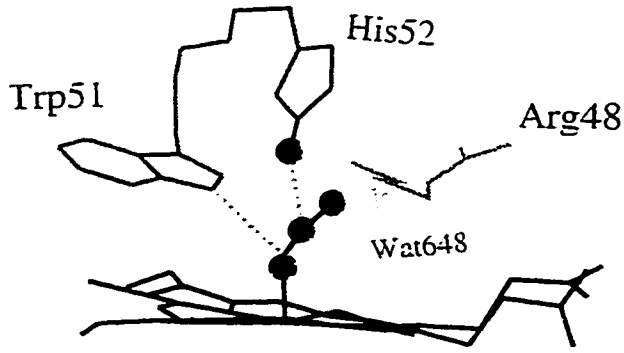

B

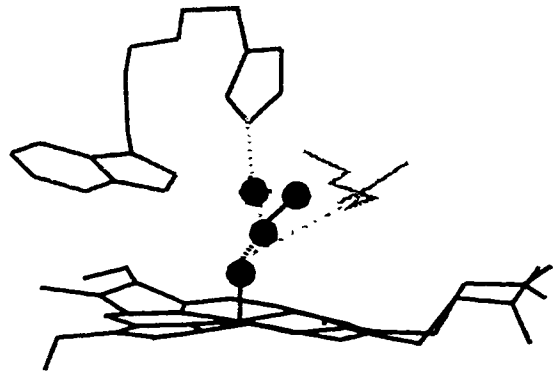

C

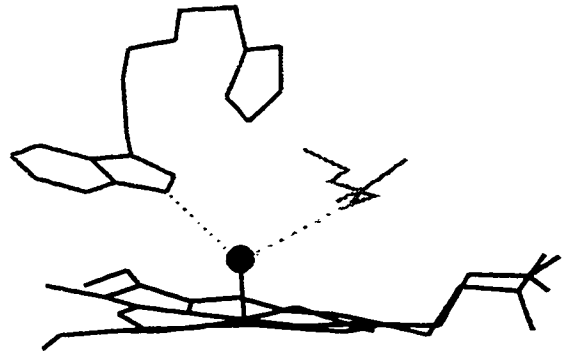

oxene ligand. As the O—O bond is being cleaved, Arg48 moves towards the iron, forms a H-bond with the oxene atom and displaces an active-site water molecule (Wat648) (Figure 1.4B). Together, these processes lead to the formation of compound I (Figure 1.4C).

Myoglobin (Mb) also forms a Fe^{IV}=O intermediate with a rate constant of 1.4 x 10^2 $M^{-1}s^{-1}$.[29] In Mb, Phe43 takes the place of Arg48, and the proximal His93 is weakly H-bonded to a carbonyl group of the peptide backbone.[20] Approximately 30% of the peroxide bond-breaking occurs via homolytic cleavage in sperm whale Mb compared to 100% heterolytic cleavage in peroxidases,[30] suggesting that the more polar pocket of CCP promotes charge separation whereas in the nonpolar heme cavity of Mb, $OH^{\cdot}$ radical formation may be competitive with deprotonation of H_2O_2, the first step in heterolytic cleavage.

1.3 Exogenous Reduction of Compound I

Peroxidases utilize a large variety of substrates to reduce compound I (Fe^{IV}=O, $P^{\cdot +}$) back to the resting ferric form according to:

$$(Fe^{IV}=O, P^{+}) + 1e^{-} \rightarrow (Fe^{IV}=O, P) \qquad 1.4$$

$$(Fe^{IV}=O, P) + 1e^{-} + 2H^{+} \rightarrow (Fe^{III}, P) + H_2O \qquad 1.5$$

As indicated by eqs 1.4 and 1.5, most peroxidase undergo one-electron reduction to

generate the intermediate compound II (Fe^{IV}=O, P), with the single oxidizing equivalent stored as Fe^{IV}=O. Reduction of compound II leads to the formation of the ferric enzyme and a water molecule. Restoration of ferric CCP following compound I formation has been divided formally into a minimum of four reaction steps (eqs 1.6 - 1.9):[17]

$$\text{compound I} + \text{cyt } c\ (Fe^{II}) \rightleftharpoons \text{compound I}\bullet\text{cyt } c\ (Fe^{II}) \qquad 1.6$$

$$\text{compound I}\bullet\text{cyt } c\ (Fe^{II}) \rightarrow \text{compound II} + \text{cyt } c\ (Fe^{III}) \qquad 1.7$$

$$\text{compound II} + \text{cyt } c\ (Fe^{II}) \rightleftharpoons \text{compound II}\bullet\text{cyt } c\ (Fe^{II}) \qquad 1.8$$

$$\text{compound II}\bullet\text{cyt } c\ (Fe^{II}) \rightarrow \text{CCP}(Fe^{III}) + \text{cyt } c\ (Fe^{III}) \qquad 1.9$$

Eq 1.6 describes the association equilibrium of compound I with ferrocyt *c*. This association is followed by the first of two, one-electron transfer steps between ferrocyt *c* and CCP, resulting in the formation of compound II (eq 1.7). Ferric (Fe^{III}) CCP is restored following the association of the second molecule of ferrocyt *c* with compound II (eq 1.8) and the second one-electron transfer step from ferrocyt *c* to compound II (eq 1.9).

The CCP-cyt *c* complex represents an intriguing scenario of protein-protein interaction, complex formation, and intracomplex electron transfer. Moreover, as a result of the availability of the X-ray structures of CCP[3] and cyts *c* from many different sources,[31] a vast amount of research effort has been dedicated to this macromolecular interaction,[20,32-39] and to the study of reduction of compound I in CCP

by cyt *c*.[37,38,40-49] A highlight of current work in this area has been the elucidation of the X-ray structure of the CCP-cyt *c* complex by Pelletier and Kraut.[50]

1.4 Endogenous Reduction of Compound I

The precise structural identity of CCP compound I has been widely studied and debated. The formation of compound I is accompanied by a change in the Soret absorption spectrum of the heme[51] (Figure 1.5). Absorption changes in the visible

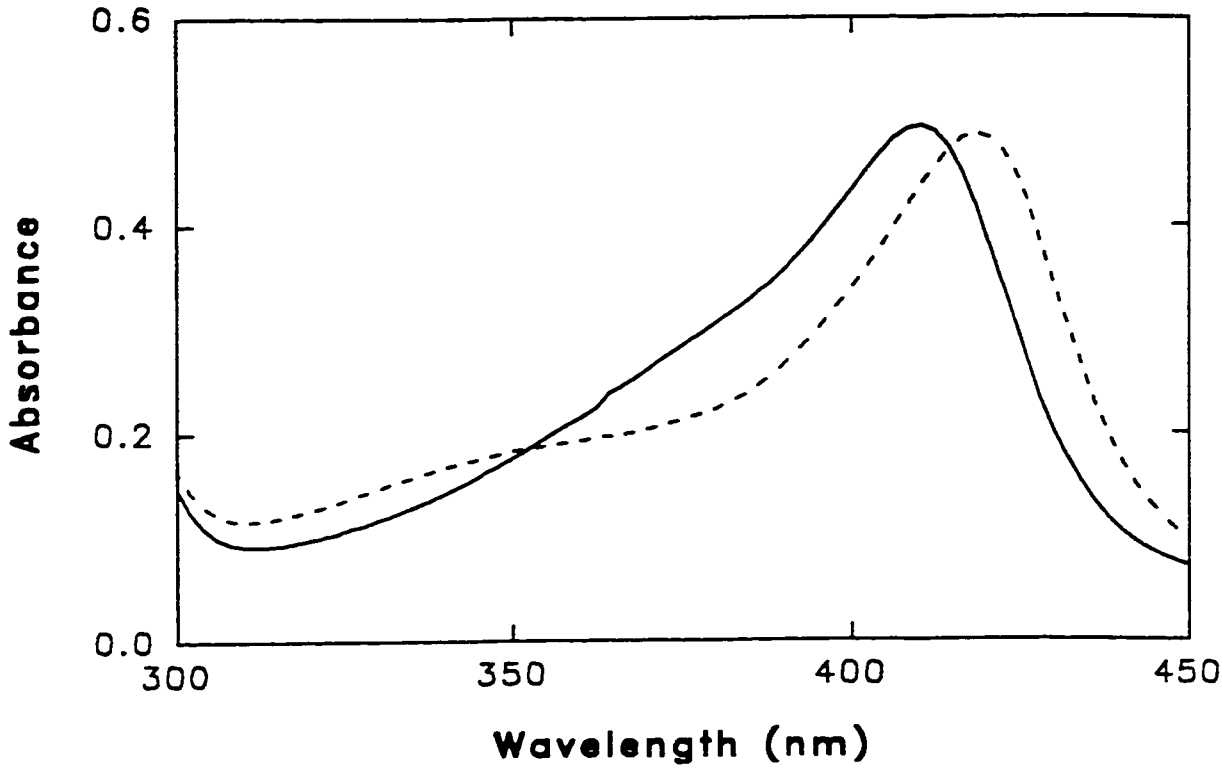

Figure 1.5 Soret absorption of ferric CCP (solid line) and compound I (dashed line).

region (390 - 700 nm) of the spectrum suggest a typical metalloporphyrin without porphyrin modification.[17] Reductive titrations with ferrocyt *c* or ferrocyanide showed that CCP compound I was two oxidizing equivalents above the resting ferric form[52] and EPR studies in 1966 demonstrated that one of these equivalents was in the form of a free radical.[53] It was then proposed that compound I contained two oxidizing equivalents, one in the form of Fe^{IV}=O heme and the other as a protein-based radical (P^{+} in eq 1.3 is an amino acid residue in CCP). The presence of a Fe^{IV}=O heme iron was strongly supported by data from magnetic susceptibility,[54] Mössbauer absorption,[55] MCD,[56] EXAFS,[57] and RR spectroscopy.[58]

The search for the identity of the protein-based radical in CCP compound I began in 1966 with the EPR studies of Yonetani and co-workers.[53] A very intense free radical signal at g = 2.00, flanked by broad wings spanning several thousand gauss at 77 K, was observed and attributed to a protein-based free radical. Wittenberg and co-workers in 1968 excluded a carbon or oxygen-based free radical on residues such as Tyr,[59] while in 1979 Hoffman and co-workers[60] suggested a sulfur-based radical in the form of a dimeric cation radical $(R_2SSR_2)^{+}$. However, the X-ray structure of CCP[2] did not support the Met dimer proposal. Based on the X-ray structure, Trp51, which lies within 4 Å of the heme ring (Figure 1.3), was suggested as the radical site.[61]

Studies on site-directed mutants of CCP in the 1980's brought the debate on the identity of the protein-based radical full circle and a variety of residues were again proposed. These included Trp51,[62-64] Trp191,[62,64,65] Met172,[63,66] Met230 and Met231.[67]

ENDOR measurements on [^{2}H] isotopically labelled CCP[68] identified a tryptophan residue as the radical site. Trp191 (Figure 1.3) appeared to be the most likely candidate since W191F compound I does not exhibit the EPR signal characteristic of native CCP.[65,69] More recently, ENDOR spectroscopy on samples isotopically enriched with [^{13}C]-, [^{15}N]-, and [^{2}H]tryptophan confirmed that the radical is located on Trp191 in CCP.[70] Trp51 was eliminated as the radical site since the Trp51→Phe mutation had no effect on the EPR spectra of compound I.[65]

CCP provided the first example of a redox-active Trp in enzyme catalysis,[71] and a second example has been proposed in ribonucleotide reductase turnover.[72] A Trp radical is also involved in the mechanism of photoactivation of photolyase.[73] The long half-life of the Trp191 radical in CCP compound I ($t_{½}$ ~ 3h),[74] despite the presence of neighboring Tyr residues[75] which rapidly reduce Trp$^{\bullet}$ in aqueous solution,[76] suggests a special radical-stabilizing environment around Trp191. Electrostatic potential calculations have revealed a region of strong negative potential surrounding Trp191 which is sufficient to stabilize the Trp radical in CCP.[77] The W191F mutant shows a transient ($t_{½}$ ~14 ms) porphyrin π-cation radical on reaction with H_2O_2,[64] and the protein-based radicals generated in the Mb(Fe^{III})/H_2O_2 reaction also decay quickly ($t_{½}$ ~ 30 s),[78] emphasizing the stability of the highly-oxidized intermediates in wild-type CCP.

Unlike CCP, most heme peroxidases possess a porphyrin π-cation radical on compound I generation. HRP is archetypical of such enzymes, and the spectrum of HRP compound I is shown in Figure 1.6. The compound I spectra of LIP, ARP and

CIP are almost identical to that shown in Figure 1.6, consistent with the formation of Fe^{IV}=O and a porphyrin π-cation radical.[79-81] In the absence of added electron donors endogenous reduction of the porphyrin π-cation radical occurs and the initial *green* compound I is converted to a brown species, compound II, which has a spectrum like that shown in Figure 1.6 for HRP. ARP, CIP, LIP, PNP and HRP contain a paucity of oxidizable residues (Figures 1.7 and 1.8) and the rates of spontaneous decay of

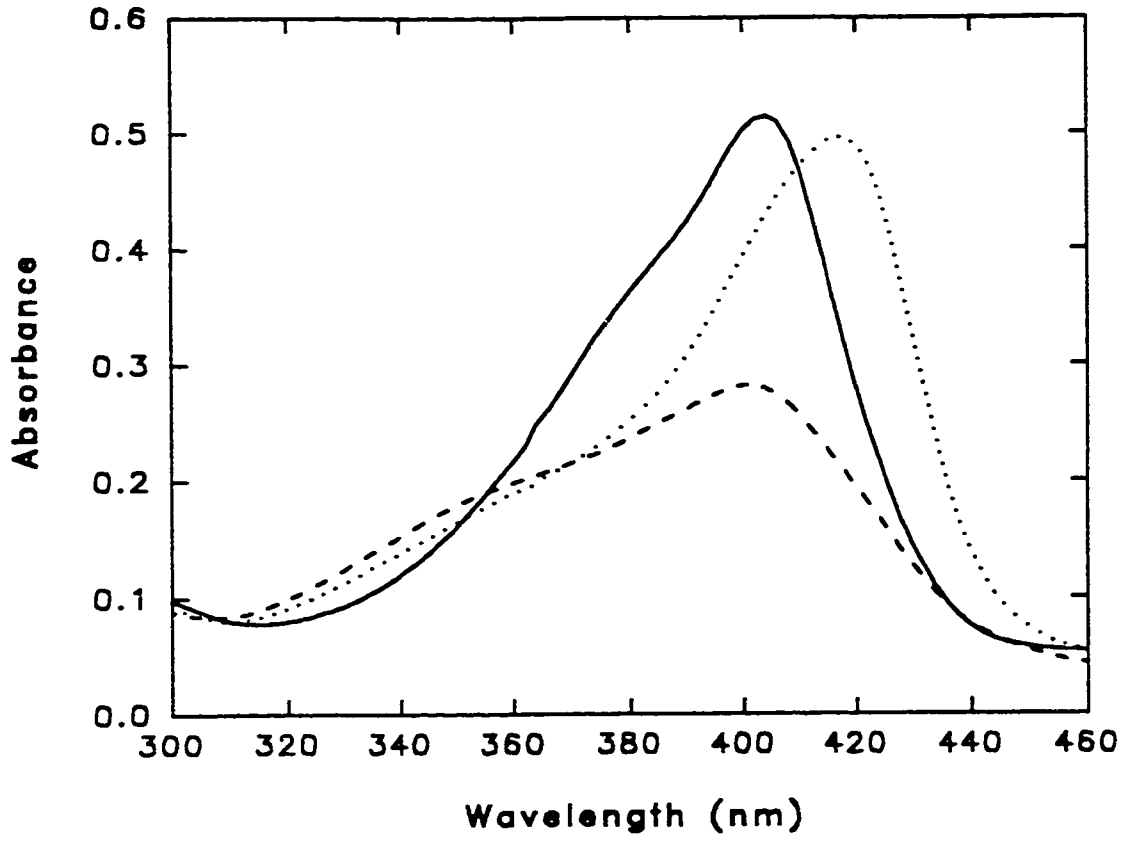

Figure 1.6 Soret absorption at pH 7.0 of ferric HRP (solid line), HRP compound I immediately following addition of 1.2 molar equivalent of H_2O_2 (dashed line) and HRP compound II (dotted line).

compound I to compound II vary between these peroxidases (5 s - 40 min),[80-83] suggesting different redox reactivities of protein residues neighboring the heme. In LIP, oxidizable residues (Met172 & Trp171) are poised close to the heme and may function as radical storage sites similar to Trp191 in CCP which is surrounded by Met230 and Met231 (Figure 1.8).

Compound I-type spectra have also been observed for mammalian peroxidases such as MPO, LPO, and PGHS.[84-86] Rapid conversion to compound II-type spectra (ms - min) occurs in these peroxidases in the absence of exogenous donors.[84,85,87] An EPR signal typical of a tyrosyl radical is observed for PGHS at the same time (1 - 2 min) as the growth of compound II absorbance,[88] and the donation of an electron to the porphyrin π-cation radical of PGHS compound I from Tyr385 has been suggested. The rapid spontaneous conversion ($t_{½} < 7$ s) of MPO compound I to compound II[84] is not surprising given the large number of potential endogenous donors surrounding its heme (Figure 1.9). The species with a compound II like spectrum in LPO accepts two electrons from ferrocyanide, and an amino acid residue has been proposed as the storage site for one of the two oxidizing equivalents[89] so that endogenous heme reduction in LPO results in an intermediate analogous to compound I of CCP (Figure 1.5). The rate of intramolecular oxidation by compound I in peroxidases will depend on the separation between oxidizable residues and the heme and the significance of redox-active residues in peroxidases might be related in part to the control of peroxidase activity and substrate specificity.[7]

In the absence of an oxidizable substrate, the Fe^{IV}=O and protein radical ($P^{+\cdot}$)

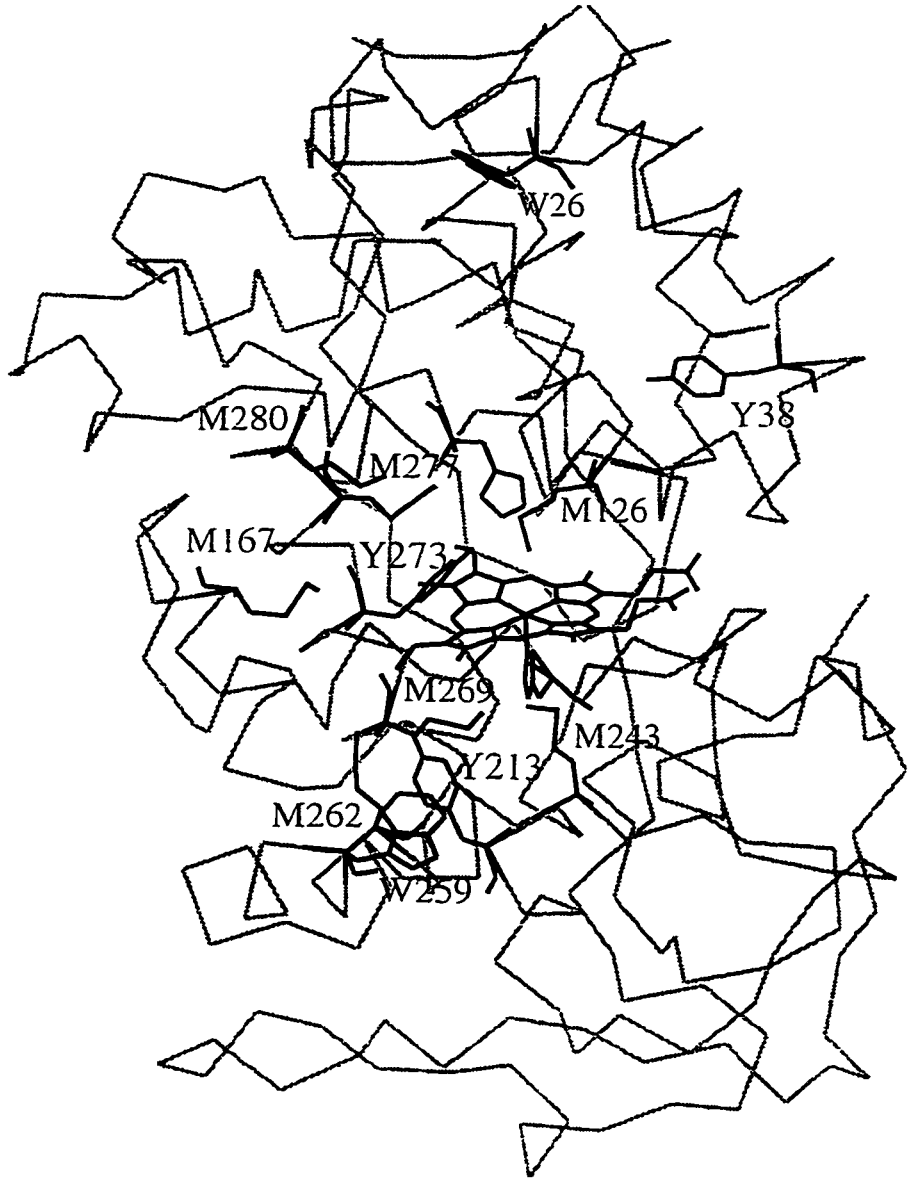

Figure 1.7 The C_α backbone of ARP showing the location of the methionine (M), tryptophan (W) and tyrosine (Y) residues relative to the heme.

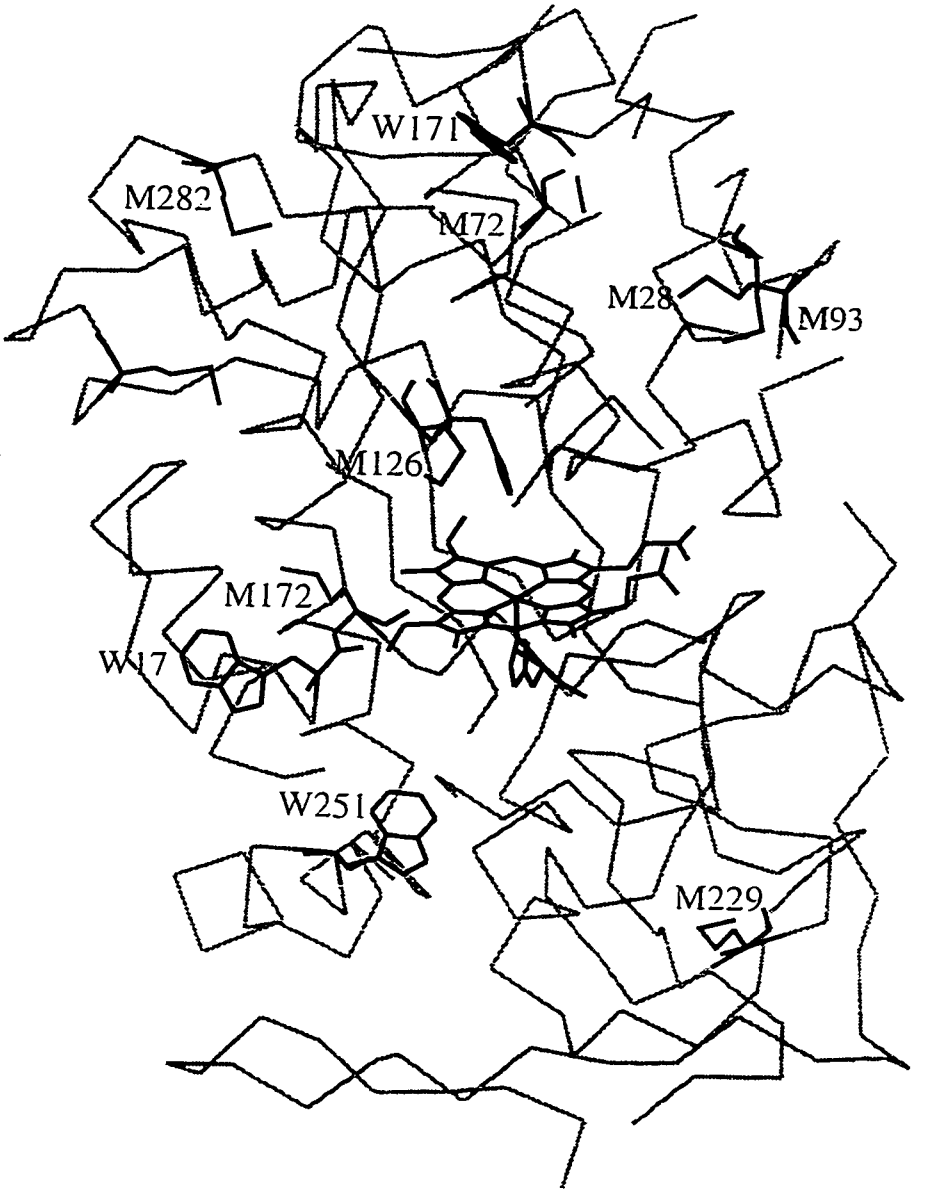

Figure 1.8 The C_α backbone of LIP showing the location of the methionine (M), and tryptophan (W) residues relative to the heme.

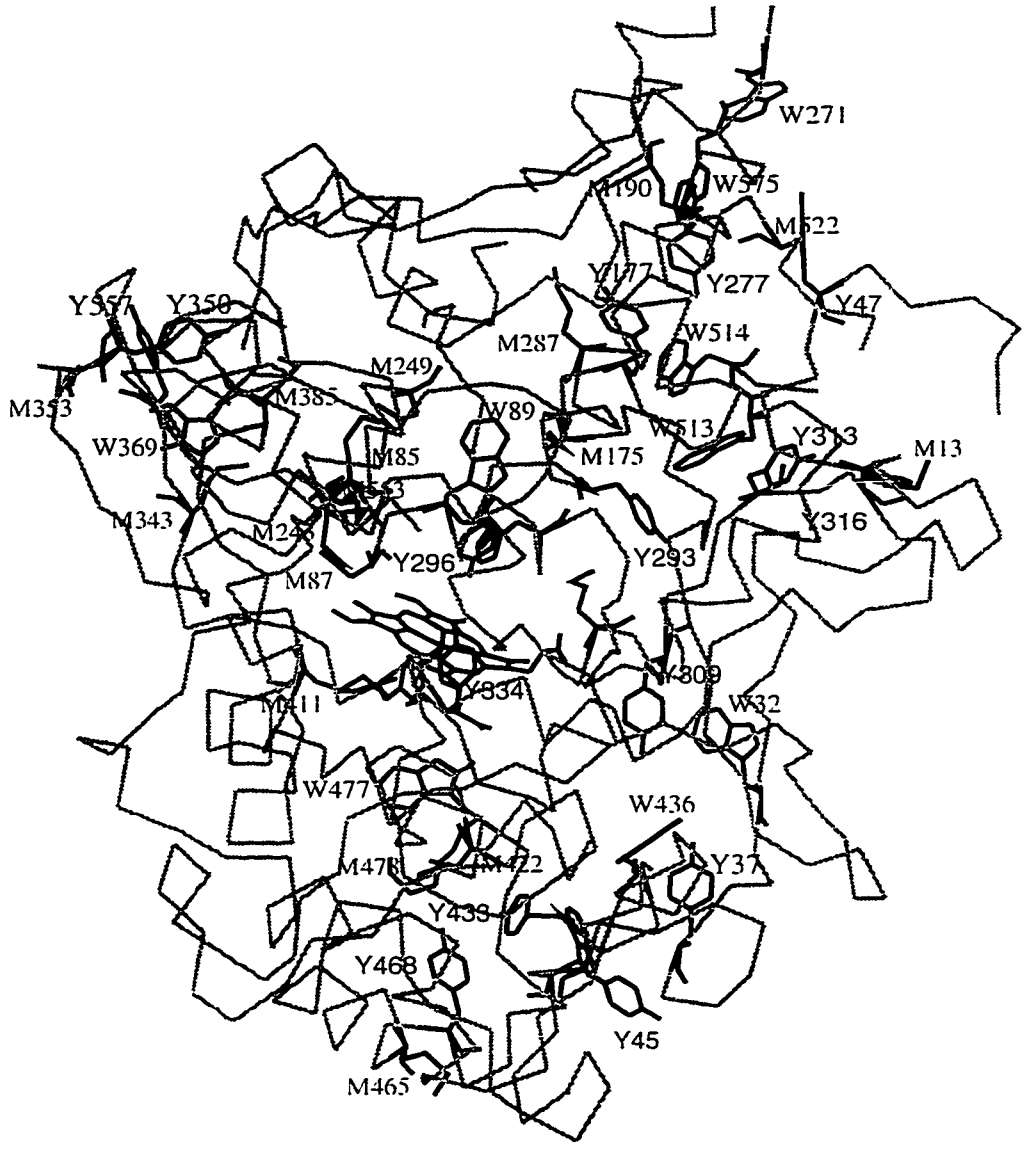

Figure 1.9 The C_α backbone of MPO showing the location of the methionine (M), tryptophan (W) and tyrosine (Y) residues relative to the heme.

in CCP compound I decay slowly to give a product which has an absorption spectrum similar to resting ferric CCP (Figure 1.5).[74] This decay product has lost the two oxidizing equivalents of compound I but retains ~ 75% activity.[90] A loss of 0.2 Trp, 0.5 Tyr and 0.5 Phe was observed on amino acid analysis of the CCP compound I decay product.[91]

1.5 Reaction of CCP With Two or More Molar Equivalents of H_2O_2

CCP can reduce up to a 10-fold molar excess of H_2O_2 without detectable O_2 formation by further oxidation of its amino acid residues.[90] A significant loss of amino acids was seen in the analysis of the decay product of CCP reacted with 20 equivalents of H_2O_2. A total loss of 3.4 Tyrs, 1.5 Phes and 0.6 Trp was observed at pH 7.0.[90]

Met residues, but not aromatic residues, in proteins are readily oxidized by millimolar concentrations of peroxide.[92] This implies that the oxidation of aromatic residues in CCP at micromolar H_2O_2 concentration must be mediated by the heme. The rate of intramolecular oxidation of the polypeptide in compound I will depend on the separation between oxidizable residues and the heme. The most likely electron donors in a protein are the side chains of Trp, Tyr and Met residues,[93] and CCP contains 7 Trps, 14 Tyrs and 5 Mets (Figure 1.10) which could act as endogenous electron donors.

The abundance of oxidizable residues in CCP is consistent with the ability of

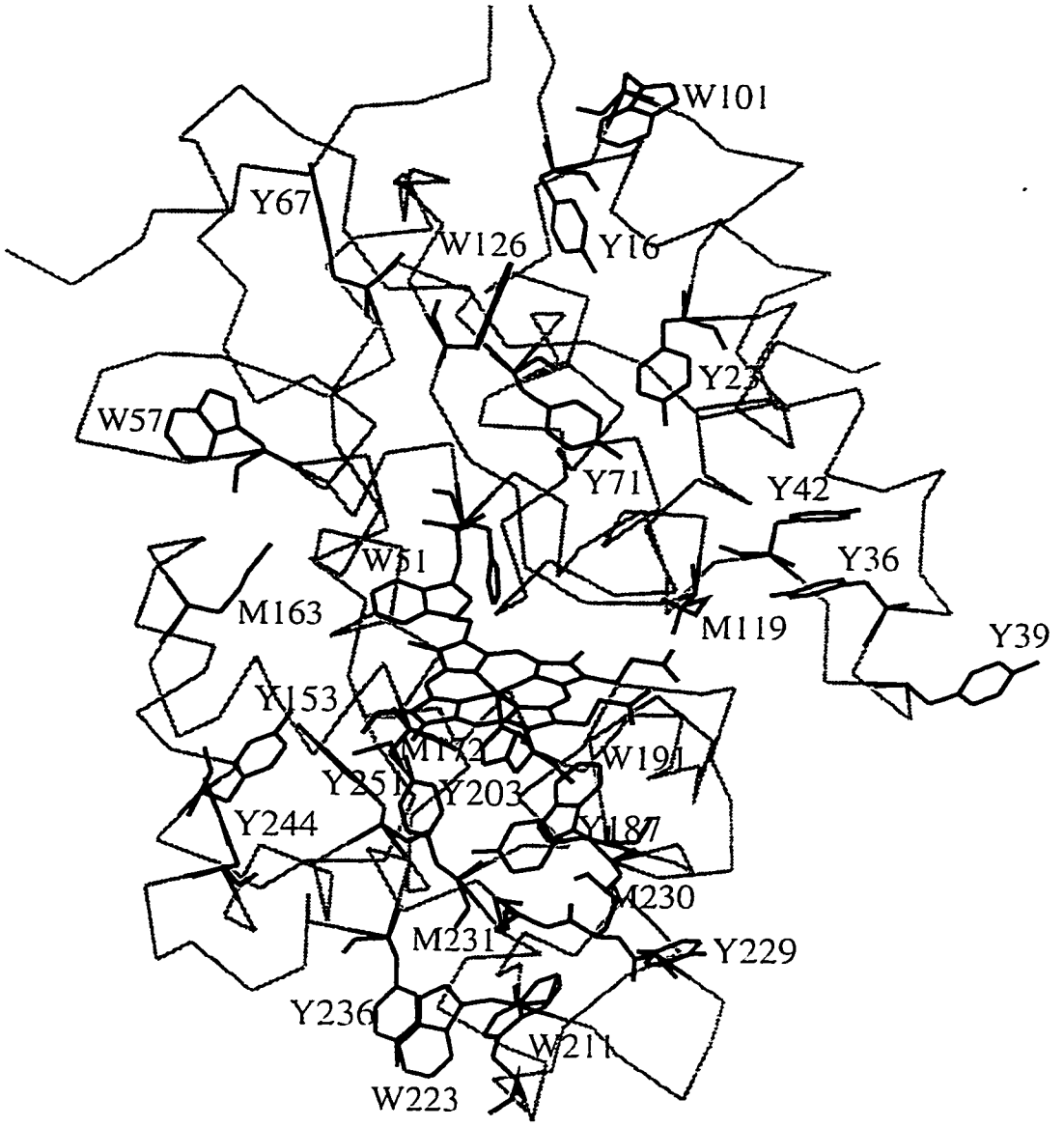

Figure 1.10 The C_α backbone of CCP showing the location of the methionine (M), tryptophan (W) and tyrosine (Y) residues relative to the heme.

the protein to reduce up to 20 equivalents of H_2O_2 in the absence of exogenous electron donors.[90] The ability of CCP to store a large number of oxidizing equivalents on its polypeptide may be related to its biological function as an antioxidant in yeast mitochondria. Yeast presumably undergo oxidative stress when they convert from anaerobic to aerobic metabolism, and the ability of CCP to reduce more than one molar equivalent of H_2O_2 in the absence of its reducing substrate, ferrocyt *c*, may be important under certain physiological conditions.

1.6 Scope and Aims of this Thesis

There is currently much interest in the roles played by amino acid radicals such as tyrosyl radicals in proteins,[94] and many enzymes that use protein-based free radicals as cofactors have been identified.[95] Further examination of the radicals generated in plant and fungal peroxidases should provide important insights into the control of reactivity of protein radicals. CCP in particular provides an ideal system to study the generation, stabilization, storage, translocation and quenching of amino acid radicals in a protein matrix. This is primarily due to the large number of endogenous donors in its polypeptide coupled with the availability of high-resolution X-ray structures of native CCP and many of its engineered mutants.[96]

An extension of previous investigations of protein-based radicals formed in CCP is presented in this thesis. As a means of increasing our understanding of control of heme and polypeptide reactivity in peroxidases, the conformational stabilities of

CCP and HRP (a peroxidase not thought to store lots of oxidizing equivalents), were investigated using a variety of conformational probes. Specifically, the conformational states in denaturants of unligated and cyanide-ligated CCP and HRP were compared using fluorescence, circular dichroism (CD), and UV/VIS absorption spectroscopy and the results are presented in Chapters 2 and 3.

Intrinsic protein steady-state fluorescence was exploited to estimate the loss of Trp residues following the reaction of yeast CCP, its recombinant form, CCP(MI), and active-site mutants (W51F and W191F) with H_2O_2. Amino acid analyses are reported for the H_2O_2-oxidized proteins, as well as their enzymatic activities. The extent of *intermolecular* crosslinking due to radical migration to the surface was also investigated and the combined results are given in Chapters 4 and 5.

Peptide mass mapping by on-line high performance liquid chromatography electrospray ionization mass spectrometry (HPLC-ESI-MS) was used to probe alterations of redox-active residues in CCP(MI) and its W191F mutant following reaction with H_2O_2. Spin-trapping followed by HPLC-ESI-MS analysis of the spin adducts allowed the location of surface-exposed redox-active residues in CCP(MI) as discussed in Chapter 6.

Finally, Chapter 7 gives a brief general conclusion as well as suggestions for future work. The research outlined in Chapters 4 and 5 is presented as the published papers while that in Chapters 2 and 3 represents papers submitted for publication and that in Chapter 6 a manuscript in preparation. The numbering system of the figures and tables, however, has been changed from the original publications for continuity

and clarity, and follows a numerical ordered system. In addition, addenda have been added to Chapters 4 and 6, and a common referencing system has been adopted.

1.7 References

1 Everse, J., Everse, K. E., & Grisham, M. B. (1991) in *Peroxidases in Chemistry and Biology,* Vol. I & II, CRC Press: Boca Raton, FL.

2 Poulos, T. L., Freer, S. T., Alden, R. A., Edwards, S. L., Skogland, U., Takio, K., Eriksson, B., Xuong, N. H., Yonetani, T., & Kraut, J. (1980) *J. Biol. Chem. 255,* 575.

3 Finzel, B. C., Poulos, T. L., & Kraut, J. (1984) *J. Biol. Chem. 259,* 13027.

4 Altschul, A., Abrams, R., & Hogness, T. R. (1940) *J. Biol. Chem. 136,* 777.

5 Daum, G., Böhni, P. C., & Schatz, G. (1982) *J. Biol. Chem. 257,* 13028.

6 Welinder, K. G. (1992) *Curr. Opin. Struc. Biol. 2,* 388.

7 English, A. M., & Tsaprailis, G. (1995) *Adv. Inorg. Chem. 43,* 75.

8 Ellfolk, N., Rönnberg, M., & Österlund, K. (1991) *Biochim. Biophys. Acta 1080,* 68.

9 Paul, J. M., & Barrett, J. (1980) *Int. J. Parasitol. 10,* 121.

10 McKelvey, J. R., & Fioravanti, C. F. (1986) *Comp. Biochem. Physiol. 85B,* 333.

11 Kusel, J. P., Boveris, A., & Storey, B. T. (1973) *Arch. Biochem. Biophys. 158,* 799.

12 Barrett, J. (1980) *J. Parasitol. 66,* 697.

13 Campos, E. G., Smith, J. M., & Prichard, R. G. (1994) *Comp. Biochem. Physiol. 111B,* 371.

14 Campa, A. (1991) in *Peroxidases in Chemistry and Biology* (Everse, J., Everse, K. E., & Grisham, M. B., Eds.,) Vol. II, pp 25-50, CRC Press: Boca Raton, FL.

15 English, A. M. (1994) in *Encyclopedia of Inorganic Chemistry: Iron: Heme Protein, Peroxidases, & Catalases* (King, R. B., Ed.,) Vol. 4, pp 1682-1697, John Wiley & Sons: Chistester, England.

16 Takio, K., Titani, K., Ericsson, L. H., & Yonetani, T. (1980) *Arch. Biochem. Biophys. 203,* 615.

17 Bosshard, H. R., Anni, H., & Yonetani, T. (1991) in *Peroxidases in Chemistry and Biology* (Everse, J., Everse, K. E., & Grisham, M. B., Eds.,) Vol. II, pp 52-84, CRC Press: Boca Raton, FL.

18 Kaput, J., Goltz, S., & Blobel, G. (1982) *J. Biol. Chem. 257,* 11186.

19 Reid, G. A., Yonetani, T., & Schatz, G. (1982) *J. Biol. Chem. 257,* 13068.

20 Poulos, T. L., & Finzel, B. C. (1984) *Pept. Protein Rev. 4,* 115.

21 Yonetani, T. (1967) *J. Biol. Chem. 242,* 5008.

22 Welinder, K. G. (1991) in *Biochemical, Molecular and Physiological Aspects of Plant Peroxidases* (Lobarzewski, J., Creppin, H., Penel, C., & Gaspar, T., Eds.,) pp 3-13, University of Geneva Press: Geneva, Switzerland.

23 Zeng, J., & Fenna, R. E. (1992) *J. Mol. Biol. 226,* 185.

24 Poulos, T. L., & Fenna, R. E. (1994) in *Metal ions in Biological Systems:*

Metalloenzymes Involving Amino Acid-Residue and Related Radicals (Sigel, H. & Sigel, A., Eds.,) Vol. 30, pp 25-75, Marcel Dekker: New York, NY.

25 Picot, D., Loll, P. J., & Garavito, M. (1994) *Nature 367,* 291.

26 Yonetani, T., & Schleyer, H. (1967) *J. Biol. Chem. 242,* 1974.

27 Dawson, J. H. (1989) *Science 240,* 433.

28 Miller, M. A., Shaw, A., & Kraut, J. (1994) *Nature Struc. Biol. 1,* 524.

29 Fox, J. R., Jr., Nicolas, R. A., Ackerman, S. A., & Swift, C. E. (1974) *Biochemistry 13,* 5178.

30 Allentoff, A. J., Bolton, J. L., Wilks, A., Thompson, J. A., & Ortiz de Montellano, P. R. (1992) *J. Am. Chem. Soc. 114,* 9744.

31 Moore, G. R., & Pettigrew, G. W. (1990) in *Cytochrome c: Evolutionary Structural and Physiological Aspects,* Springer-Verlag: Berlin, Germany.

32 Bechtold, R., & Bosshard, H. R. (1985) *J. Biol. Chem. 260,* 5191.

33 Zhang, Q., Hake, R., Billstone, V., Simmons, J., Falvo, J., Holzchu, D., Lu, K., McLendon, G., & Corin, A. (1991) *Mol. Cryst. Liq. Cryst. 194,* 343.

34 McLendon, G. (1991) in *Metal Ions in Biological Systems: Electron transfer Reactions in Metalloproteins* (Sigel, H. & Sigel, A., Eds.,) Vol. 27, pp 183-198, Marcel Dekker: New York, NY.

35 Northrup, S. H. Boles, J. O., & Reynolds, J. C. L. (1988) *Science 241,* 67.

36 Wang, J., Larsen, R. W., Moench, S. J., Satterlee, J. D., Rousseau, D. L., & Ondrias, M. R. (1996) *Biochemistry 35,* 453.

37 Pappa, H. S., Tajbaksh, S., Saunders, A. J., Pielak, G. J., & Poulos, T. L.

(1996) *Biochemistry 35,* 4837.

38 Miller, M. A., Geren, L., Han, G. W., Saunders, A., Beasley, J., Pieak, G. J., Durham, B., Millett, F., & Kraut, J. (1996) *Biochemistry 35,* 667.

39 Erman, J. E., Kresheck, G. C., Vitello, L. B., & Miller, M. A. (1997) *Biochemistry 36,* 4054.

40 Hahm, S., Durham, B., & Millet, F. (1992) *Biochemistry 31,* 3472.

41 Liu, R. Q., Miller, M. A., Han, G. W., Hahm, S., Geren, L., Hibdon, S., Kraut, J., Durham, B., & Millet, F. (1994) *Biochemistry 33,* 8678.

42 Hazzard, J. T., & Tollin, G. J. (1991) *J. Am. Chem. Soc. 113,* 8956.

43 Nuevo, M. R., Chu, H. H., Vitello, L. B., & Erman, J. E. (1993) *J. Am. Chem. Soc. 115,* 5873.

44 Hahm, S., Miller, M. A., Geren, L., Kraut, J., Durham, B., & Millet, F. (1994) *Biochemistry 33,* 1473.

45 Stemp, E. D. A., & Hoffman, B. M. (1993) *Biochemistry 32,* 10848.

46 Zhou, J. S., & Hoffman, B. M (1993) *J. Am. Chem. Soc. 115,* 11008.

47 Pappa, H. S., & Poulos, T. L. (1995) *Biochemistry 34,* 6573.

48 Wang, K., Mei, H., Geren, L., Miller, M. A., Saunders, A., Wang, X., Waldner, J. L., Pielak, G. J., Durham, B., & Millett, F. (1996) *Biochemistry 35,* 15107.

49 Liu, R. Q., Geren, L., Anderson, P., Fairris, J. L., Peffer, N., McKee, A., Durham, B., & Millett, F. (1995) *Biochimie 77,* 549.

50 Pelletier, H., & Kraut, J. (1992) *Science 258,* 1748.

51 Yonetani, T., & Anni, H. (1987) *J. Biol. Chem. 262,* 9547.

52 Yonetani, T. (1965) *J. Biol. Chem. 240,* 4509.

53 Yonetani, T., Schleyer, H., & Ehrenberg, A. (1966) *J. Biol. Chem. 214,* 3240.

54 Iizuka, T., Kotani, M., & Yonetani, T. (1968) *Biochim. Biophys. Acta 167,* 1968.

55 Lang, G., Spartalian, K., & Yonetani, T. (1976) *Biochim. Biophys. Acta 451,* 250.

56 Thomson, A. J., Greenwood, C., Gadsby, P. M. A., & Foote, N. (1987) in *Cytochrome Systems: Molecular Biology and Energetics,* (Papa, S., Chance, B., & Ernster, L., Eds.,) pp. 349-365, Plenum Press: New York, NY.

57 Chance, M., Powers, L., Poulos, T. L., & Chance, B. (1986) *Biochemistry 25,* 1266.

58 Hashimoto, S., Teraoka, J., Inubushi, T., Yonetani, T., & Kitagawa, T. (1986) *J. Biol. Chem. 261,* 11110.

59 Wittenberg, B. A., Kampa, L., Wittenberg, J. B., Blumberg, W. E., & Peisach, J. (1968) *J. Biol. Chem. 243,* 1863.

60 Hoffman, B., Roberts, T. G., Kang, C. H., & Margoliash, E. (1979) *Proc. Natl. Acad. Sci. U.S.A. 76,* 6132.

61 Poulos, T. L., & Kraut, J. (1980) *J. Biol. Chem. 255,* 8199.

62 Hori, H., & Yonetani, T. (1985) *J. Biol. Chem. 260,* 349.

63 Goodin, D. B., Mauk, G. A., & Smith, M. (1987) *J. Biol. Chem. 262,* 7719.

64 Erman, J. E., Vitello, L. B., Mauro, J. M., & Kraut, J. (1989) *Biochemistry 28,* 7992.

65 Scholes, C. P., Liu, Y., Fishel, L. A., Farnum, M. F., Mauro, J. M., & Kraut, J. (1989) *Isr. J. Chem. 29,* 85.

66 Goodin, D. B., Mauk, G. A., & Smith, M. (1986) *Proc. Natl. Acad. Sci. U.S.A. 83,* 1295.

67 Edwards, S., Xuong, N. H., Hamlin, R. C., & Kraut, J. (1987) *Biochemistry 26,* 1503.

68 Sivaraja, M., Goodin, D. B., Smith, M., & Hoffman, B. M. (1989) *Science 245,* 738.

69 Fishel, L. A., Farnum, M. F., Mauro, J. M., Miller, M. A., & Kraut, J. (1991) *Biochemistry 30,* 1986.

70 Huyett, J. E., Doan, P. E., Gurdiel, R., Houseman, A. L. P., Sivaraja, M., Goodin, D. B., & Hoffman, B. H. (1995) *J. Am. Chem. Soc. 117,* 9033.

71 Prince, R. G., & George, G. N. (1990) *Trends Biochem. Sci. 15,* 70.

72 Bollinger, J. M., Jr, Tung, W. H., Ravi, N., Huynh, B. H., Edmondson, D. E., & Stubbe, J. (1994) *J. Am. Chem. Soc. 116,* 8024.

73 Essenmacher, C., Kim, S. -T., Atamian, M., Babcock, G. T., & Sancar, A. (1993) *J. Am. Chem. Soc. 115,* 1602.

74 Erman, J. E., & Yonetani, T. (1975) *Biochim. Biophys. Acta 393,* 350.

75 Fox, T., Tsaprailis, G., & English, A. M. (1994) *Biochemistry 33,* 186.

76 Jovanovic, S. V., Harriman, A., & Simic, M. G. (1986) *J. Phys. Chem. 90,* 1935.

77 Miller, M. A., Han, G. W., & Kraut, J. (1994) *Proc. Natl. Acad. Sci. U.S.A. 91,*

11118.

78 Fenwick, C. W., English, A. M., & Wishart, J. F. (1997) *J. Am. Chem. Soc. 119,* 0000.

79 Andrawis, A., Johnson, K. A., & Tien, M. (1988) *J. Biol. Chem. 263,* 1195.

80 Farhangrazi, Z. S., Copeland, B. R., Nakayama, T., Amachi, T., Yamazaki, I., & Powers, L. S. (1994) *Biochemistry 33,* 5647.

81 Andersen, M. B., Hsuanyu, Y., Welinder, K. G., Scheider, P., & Dunford, H. B. (1991) *Acta Chem. Scand. 45,* 1080.

82 Renganathan, V., & Gold, M. H. (1986) *Biochemistry 25,* 1626.

83 Schonbaum, G. R., & Lo, S. (1972) *J. Biol. Chem. 247,* 3353.

84 Hurst, J. K. (1991) in *Peroxidases in Chemistry and Biology* (Everse, J., Everse, K. E., & Grisham, M. B., Eds.,) Vol. I, pp 37-62, CRC Press: Boca Raton, FL.

85 Kohler, H., Taurog, A., & Dunford, H. B. (1988) *Arch. Biochim. Biophys. 264,* 438.

86 Lambeir, A. M., Markey, C. M., & Dunford, H. B. (1985) *J. Biol. Chem. 260,* 14894.

87 Marnett, L. J., & Maddipati, K. R. (1991) in *Peroxidases in Chemistry and Biology* (Everse, J., Everse, K. E., & Grisham, M. B., Eds.,) Vol. I, pp 293-334, CRC Press: Boca Raton, FL.

88 Tsai, A. L., Back, H., Van Wart, H. E., Palmer, G., & Kulmacz, R. J. (1992) *Biophys. J. 61,* A205.

89 Thomas, E. L., Bozeman, P. M., & Learn, D. B. (1991) in *Peroxidases in Chemistry and Biology* (Everse, J., Everse, K. E., & Grisham, M. B., Eds.,) Vol. I, pp 123-142, CRC Press: Boca Raton, FL.

90 Erman, J. E., & Yonetani, T. (1975) *Biochim. Biophys. Acta 393,* 343.

91 Coulson, A. F. W., & Yonetani, T. (1972) *Biochem. Biophys. Res. Commun. 49,* 391.

92 Neuman, N. P. (1967) *Methods Enzymol. 11,* 485.

93 Isied, S. S. (1991) in *Metal Ions in Biological Systems: Electron transfer Reactions in Metalloproteins* (Sigel, H. & Siegel, A., Eds.,) Vol. 27, pp 1-56, Marcel Dekker: New York, NY.

94 Sigel, H., & Sigel, A. (1994) *Metal Ions in Biological* Systems: *Metalloenzymes Involving Amino Acid-Residue and Related Radicals,* Vol. 30, Marcel Dekker: New York, NY.

95 Pedersen, J. Z., & Finazzi-Agrò, A. (1993) *FEBS Lett. 325,* 53.

96 Mauro, J. T., Miller, M. A., Edwards, S. L., Wang, J., Fishel, L. A., & Kraut, J. (1989) in *Metal Ions in Biological Systems: Exploring Structure-Function Relationships in Yeast Cytochrome c Peroxidase Using Mutagenesis and Crystallography* (Sigel, H. & Sigel, A., Eds.,) Vol. 27, pp 477-503. Marcel Dekker: New York, NY.

CHAPTER 2

CONFORMATIONAL STATES IN DENATURANTS OF CYTOCHROME *c* AND HORSERADISH PEROXIDASES EXAMINED BY FLUORESCENCE AND CIRCULAR DICHROISM

ABSTRACT

Steady-state fluorescence and circular dichroism (CD) were used to examine the unfolding in denaturants of recombinant cytochrome *c* peroxidase [CCP(MI)] and horseradish peroxidase (HRP) in their ferric forms. CCP(MI) unfolds in urea and in guanidine hydrochloride (GdHCl) at pH 7.0, while HRP loses its secondary structure only in the presence of GdHCl. Both peroxidases exhibit <100% fluorescence relative to Trp and Tyr standards in these denaturants, indicative of heme quenching and/or residual tertiary structure in the denatured state. CCP(MI) unfolds in urea by 2 distinct steps as monitored by fluorescence, but the loss of its secondary structure as monitored by UV/CD occurs in a single step between 3.4 - 5 M urea and 1.5 - 2.5 M GdHCl. The localized changes detected by fluorescence involve the CCP(MI) heme cavity since the Soret maximum red shifts from 408 to 416 nm, and the heme CD changes examined in urea are biphasic. The polypeptide of HRP also loses secondary structure in a single step between 1.2 - 2.7 M GdHCl as monitored by UV/CD. A fluorescence intermediate is observed at 3 - 4 M GdHCl and the $I \rightleftharpoons U$ transition, involving conformational change in the Trp117-containing loop of HRP, occurs above 4 M GdHCl. Free energies of denaturation extrapolated to 0 M denaturant ($\Delta G_{d,aq}$) of ~ 6 and ~ 4 kcal/mol were calculated for CCP(MI) and HRP, respectively, from the UV/CD data. The refolding mechanisms of the 2 peroxidases differ since heme capture in CCP(MI) is synchronous with refolding while apoHRP captures heme *after* refolding. Thus, the denatured form of apoHRP does not recognize heme and has to

correctly refold *prior* to heme capture. The half-life for unfolding of native HRP in 6 M GdHCl is slow (519 s) compared to that for CCP(MI) (14.3 s), indicating that HRP is kinetically a lot more stable than CCP(MI). Treatment with EDTA and DTT greatly destabilizes HRP and unfolding in 4 M GdHCl occurs with $t_{½}$ = 0.42 s.

INTRODUCTION

The last decade has seen an explosion in the X-ray structure determination of heme proteins and heme peroxidases in particular. Notable among these are the structures of cytochrome *c* peroxidase (CCP),[1] lignin peroxidase (LIP),[2] *Arthromyces ramosus* peroxidase (ARP),[3] *Coprinus cinereus* peroxidase (CIP),[4] pea ascorbate peroxidase (APX),[5] manganese peroxidase (MnP),[6] and peanut peroxidase (PNP).[7] An inspection of the three-dimensional structures of these peroxidases reveals that they possess similar secondary structure.[8,9] Moreover, they have been grouped into the plant peroxidase superfamily which consists of evolutionary-related heme peroxidases from bacteria, fungi, and plants.[10] Structural elements are also conserved around the prosthetic group in heme peroxidases,[11] emphasizing their evolutionary relationship.

Horseradish peroxidase isoenzyme C (HRP) is the most studied heme peroxidase.[12] Despite this, the X-ray structure has just been solved for this isoenzyme (T.L. Poulos, personal communication). The secondary and tertiary structure of HRP is very similar to those of ARP, CIP, LIP and PNP since they all share a number of

common structural features. These include Ca^{2+} binding sites proximal and distal to the heme, 4 disulfide bridges, and a number of N-glycosylation sites.[8-10,13] The newly solved X-ray structure of HRP shows that its secondary structure is essentially identical to that of PNP with which it shares 50% sequence homology. Moreover, the 4 disulfide bridges, the Ca^{2+} binding sites, and other key residues in the proximal and distal sides of the heme are conserved between HRP and PNP although they differ slightly around the entrance to the heme cavity (T.L. Poulos, personal communication).

The first crystal structure obtained for a heme peroxidase was that of CCP published in 1980[14] and a 1.7-Å resolution structure appeared in 1984.[1] Since then CCP has served in large part as the archetypical heme peroxidase but, despite its similar tertiary and secondary structure to other enzymes in the plant peroxidase superfamily, CCP does not possess disulfide bridges, bound Ca^{2+} nor glycosylation sites.[15] A need for an examination of the effects of these structural elements on the conformational stabilities of related heme peroxidases was noted by Holzbaur et al.[16] Heme capture on folding of peroxidases is also anticipated to depend on the presence of stabilizing structural elements since, for example, recombinant HRP has been isolated in inclusion bodies largely as the apoprotein and peroxidase activity could only be restored on refolding the protein in the presence of added Ca^{2+} as well as heme.[17]

Heme peroxidases oxidize a wide variety of organic and inorganic substrates by H_2O_2 according to:

$$H_2O_2 + 2AH \rightarrow 2H_2O + 2A \quad (1)$$

Heme reactivity is an important aspect of peroxidase catalysis since the first step involves the donation of 2 electrons to H_2O_2 to form compound I which is 2 oxidizing equivalents above the resting Fe^{III} enzyme. In most peroxidases the 2 oxidizing equivalents of peroxide are stored at the heme in the form of oxyferryl iron (Fe^{IV}=O) and a porphyrin π-cation radical.[18] CCP is the first known peroxidase to use a stable amino acid radical instead of a porphyrin π-cation radical in compound I, and the redox-active residue has been identified as Trp191 which lies within 5 Å of the heme.[19] The X-ray structure of APX shows that Trp179 is in an analogous position to Trp191 in CCP,[5] but APX forms a porphyrin π-cation radical[20] on reaction with peroxide, underscoring the special structural environment surrounding the heme and the redox-active Trp in CCP.

In this study, steady-state fluorescence and circular dichroism have been used to compare the conformational stability in denaturants of recombinant cytochrome *c* peroxidase from *E. coli* [CCP(MI)] and HRP. The unfolding intermediates of CCP(MI) and HRP were investigated in urea and guanidine hydrochloride (GdHCl) at pH 7.0 by monitoring protein fluorescence, Soret absorption, as well as changes in backbone and heme CD. Heme capture by CCP(MI) and HRP on refolding of the denatured peroxidases was also investigated by steady-state fluorescence, Soret absorption, and CD.

EXPERIMENTAL PROCEDURES

Materials. Grade I, salt-free, lyophilized horseradish peroxidase isoenzyme C (HRP) (EC 1.11.1.7) was obtained from Boehringer Mannheim and used without further purification. Recombinant cytochrome *c* peroxidase from *E. coli* [CCP(MI)] (EC 1.11.1.5) was isolated following a previously described procedure.[21] Ultra pure grade urea was purchased from Anachemia and guanidine hydrochloride 99+% (GdHCl) from Sigma. *N*-acetyltryptophanamide (NATA) and *N*-acetyltyrosinamide (NAYA) standards were also purchased from Sigma, and DTT and EDTA from ICN. All solutions were prepared using distilled water (specific resistance 18 MΩ) from a Barnstead Nanopure system. Absorption spectra were recorded on a Hewlett Packard 8451A diode array spectrophotomer, fluorescence spectra on a Shimadzu Model RF-5000 spectrofluorophotometer, and CD spectra on a JASCO J-710 spectropolarimeter purged with N_2 at a flow rate of 5 L/min.

Methods

Denaturation of CCP(MI) and HRP as Monitored by Steady-State Fluorescence. Stock protein solutions were prepared in 100 mM sodium phosphate buffer (pH 7.0) using ε_{408}= 102 $mM^{-1}cm^{-1}$,[21] and ε_{403} = 102 $mM^{-1}cm^{-1}$,[22] for CCP(MI) and HRP, respectively. The concentrations of NATA (ε_{280} = 5.69 $mM^{-1}cm^{-1}$) and NAYA (ε_{276} = 1.49 $mM^{-1}cm^{-1}$) were also determined spectrophotometrically.[23] GdHCl

(0 - 6.4 M) and urea (0 - 8 M) solutions of known concentration were prepared by weight in 100 mM sodium phosphate buffer (pH 7.0). The proteins were allowed to denature over 20 - 24 h at ambient temperature prior to recording the fluorescence spectra, and the concentrations used in the fluorescence measurements were 1 μM CCP(MI) and 2 μM HRP. The emission of the blank (denaturant in buffer) was subtracted from that of the protein samples prior to integration. The steady-state fluorescence intensities of CCP(MI) were standardized to 7 μM NATA and those of HRP to a solution containing 2 μM NATA and 10 μM NAYA since the fluorescence intensity (λ_{ex} 280 nm) of fully denatured 1 μM CCP(MI) is equal to that of 7 μM free Trp[24] while that of 2 μM HRP is equal to 2 μM Trp and 10 μM Tyr.[25,26] The integrated intensity obtained for the standards under identical conditions was taken to be 100%.

To test the reversibility of denaturation, ~ 30 μM solutions of CCP(MI) and HRP were incubated for 20 - 24 h in 8 M urea (pH 7.0) and 6 M GdHCl (pH 7.0), respectively. Following incubation, the samples were diluted to give the desired final concentrations of denaturant and then incubated for another 20 - 24 h before the fluorescence spectra were recorded as described above.

Denaturation of CCP(MI) and HRP as Monitored by CD Spectroscopy. Stock protein solutions (~ 30 μM) prepared in 100 mM sodium phosphate buffer (pH 7.0) were diluted to ~ 5 μM for backbone CD-monitored denaturation measurements. Backbone refolding of HRP and CCP(MI) was examined following denaturation over

20 - 24 h of ~ 100 μM stock HRP and ~ 80 μM CCP(MI) in 6 M GdHCl (pH 7.0) and 8 M urea (pH 7.0), respectively. All CD spectra in the backbone region (210 - 240 nm; UV/CD) were recorded in a 0.05-cm pathlength cell (~ 150 μL) using a scan speed of 100 nm/min with a response time of 0.25 s. The UV/CD spectra reported here are the average of 5 scans at 0.2-nm resolution and a bandwidth of 1 nm. The observed ellipticity θ (mdeg) was divided by (10 x C x l) to convert to molar ellipticity [θ], where C is the concentration (mol/L) and l the pathlength (cm).[27] For the CD spectra in the aromatic and Soret regions (240 - 480 nm), a 0.5-cm pathlength cell was used and a protein concentration of ~ 10 μM. All other parameters were the same as those used in the UV/CD measurements.

Analysis of the UV/CD Transition Curves. As discussed below, the unfolding of the CCP(MI) and HRP backbones as monitored by UV/CD appears to follow a two-state transition and hence was analyzed according to the method of Pace et al.:[28]

$$N \rightleftharpoons U \qquad (2)$$

where N is the native protein and U the unfolded protein. The equilibrium constant between the unfolded and native states is given by:

$$K = [U] / [N] \qquad (3)$$

K is related to the fraction of unfolded protein (F_U), and the standard Gibbs free energy of denaturation (ΔG_d) by:

$$\Delta G_d = - RT \ln K = - RT \ln \ (F_U / 1- F_U) \qquad (4)$$

where R is the universal gas constant and T the absolute temperature. F_U and hence K may be calculated by recording the change in molar ellipticity [θ] as follows:

$$F_U = ([\theta]_N - [\theta]_{obs})/([\theta]_N - [\theta]_U) \qquad (5a)$$

$$K = ([\theta]_N - [\theta]_{obs})/([\theta]_{obs} - [\theta]_U) \qquad (5b)$$

where $[\theta]_{obs}$ is the observed molar ellipticity, and $[\theta]_N$ and $[\theta]_U$ are the values of $[\theta]$ characteristic of the native and unfolded conformations, respectively. ΔG_d and K depend on the denaturant concentration according to the linear extrapolation method:[29]

$$\Delta G_d = \Delta G_{d,aq} - m[\text{Denaturant}] \qquad (6)$$

where $\Delta G_{d,aq}$ is the value of ΔG_d at zero concentration of denaturant and m is a measure of the dependence of ΔG_d on denaturant concentration. A nonlinear least-squares fit[30,31] to the UV/CD data yielded the thermodynamic parameters $\Delta G_{d,aq}$ and m which are listed in Table 2.1. $\Delta G_{d,aq}$ represents the free energy under normal

conditions (aqueous solutions in the absence of denaturant at room temperature), and hence defines the conformational stability of a protein that undergoes a single $N \rightleftharpoons U$ transition.[32]

Steady-State Fluorescence-Monitored Denaturation of EDTA- and DTT-Treated HRP. Solutions of 10 μM HRP were incubated with (1) 3 mM DTT, (2) 30 mM DTT, (3) 2 mM EDTA and (4) 3 mM DTT + 2 mM EDTA for 18 h at 4° C before aliquots of the protein were unfolded in 0 - 6 M GdHCl (pH 7.0) over 20 - 24 h at ambient temperature. The integrated fluorescence intensities (300 - 450 nm) were normalized relative to 2 μM NATA/10 μM NAYA solutions that had been similarly treated with DTT and EDTA.

Kinetics of Unfolding of CCP(MI) and HRP in Denaturants. The time-dependent unfolding of both peroxidases was investigated at pH 7.0 by diluting 5 μM CCP(MI) into 8 M urea and 10 μM HRP into 6 M GdHCl. Following rapid manual mixing, quartz cuvettes containing 1 μM CCP(MI) or 2 μM HRP in denaturant were quickly placed in the spectrofluorophotometer and the fluorescence intensity at 350 nm monitored vs time. The excitation wavelength was 280 nm and the emission and excitation slits were 5 nm. The time-dependent fluorescence increase was fitted by a single exponential. The time courses of unfolding of EDTA- and DTT- treated HRP were also examined. The kinetics of HRP unfolding following incubation with *both* EDTA and DTT was investigated by stopped-flow in 4 M GdHCl. Equal volumes of

8 M GdHCl and 10 μM HRP in 3 mM DTT/2 mM EDTA were mixed and the fluorescence was measured using an Applied Photophysics SX17MV stopped-flow spectrofluorophotometer. The growth of the fluorescence intensity at 350 nm (λ_{ex} 280 nm; 5 nm excitation and emission slits) was also fitted by a single exponential.

RESULTS

Denaturation of CCP(MI) and HRP as Monitored by Steady-State Fluorescence. Quenching of peroxidase fluorescence emission is caused by the presence of the heme prosthetic group.[33] Relief of heme quenching, as well as a red shift in the steady-state fluorescence of CCP(MI), is observed when the protein is incubated in increasing concentrations of urea at pH 7.0. Both of these observations are indicative of protein unfolding and Trp exposure to the aqueous environment.[34] The fluorescence intensities of CCP(MI) in varying concentrations of urea at pH 7.0 are shown in Figure 2.1A. The emission maximum gradually shifts from 325 ± 2 nm in 0 M urea to 350 ± 2 nm in ≥ 5.5 M urea. The same fluorescence behavior is seen when CCP(MI) is incubated with increasing concentrations of GdHCl at pH 7.0 (data not shown), but since GdHCl is a stronger denaturant than urea,[35] the emission maximum occurs at 350 nm in ≥ 2.2 M GdHCl. Relief of heme quenching is also observed when HRP is incubated with GdHCl at pH 7.0 (Figure 2.1B). A red shift from the 326 ± 2-nm emission maximum in buffer occurs at ≥ 0.2 M GdHCl, and the maximum has fully red shifted to 348 ± 2 nm in 2.6 M GdHCl.

Figure 2.1 Fluorescence spectra at pH 7.0 of (**A**) 1 μM CCP(MI) in 0 M(●), 1 M (○), 3 M (■), 4 M (□), 5 M (◆), 5.5 M (▲), 6 M (◊) and 8 M (△) urea; (**B**) 2 μM HRP in 0 M (●),1 M (○), 1.6 M (■), 2 M (□), 4.4 M (▲) and 6 M (△) GdHCl; (C) 2 μM HRP (◊) , 2 μM L-NATA/10 μM L-NAYA (▲), and 2 μM L-NATA (◆) in 6.4 M GdHCl. Excitation 280 nm; slits 5 nm; scan rate 102 nm/min.

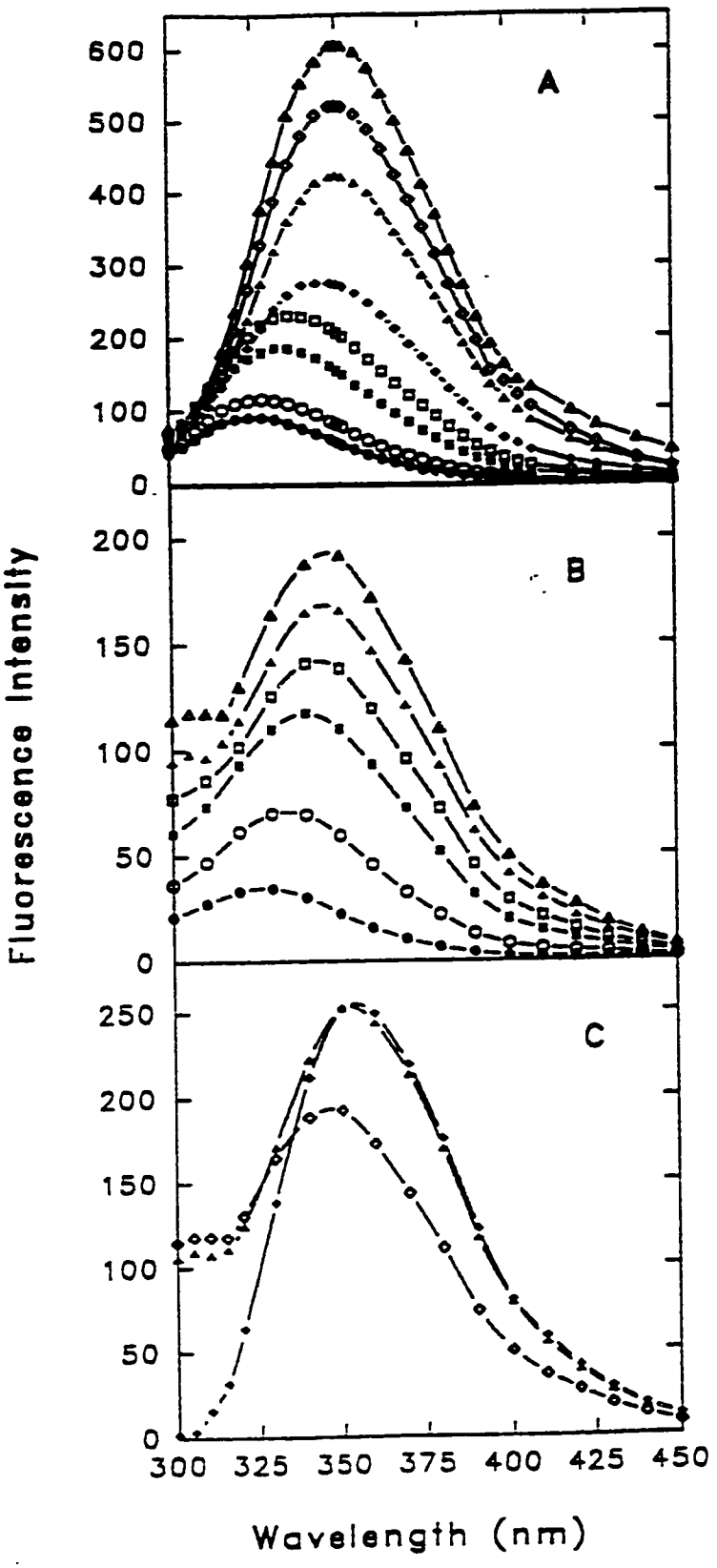
A
B
C
600
500
400
300
200
100
0
200
150
100
50
0
250
200
150
100
50
0
300 325 350 375 400 425 450
Wavelength (nm)
Fluorescence Intensity

HRP denaturation in urea was not monitored since our observations and those of Pappa and Cass[25] reveal that HRP retains significant secondary structure in the presence of 8 M urea as monitored by UV/CD.

Excitation wavelength-dependent fluorescence is observed for HRP but not for CCP(MI). Figure 2.1C, which shows the fluorescence intensity of HRP, a NATA/NAYA mixture and NATA in 6.4 M GdHCl (pH 7.0), clearly indicates that Tyr residues contribute to the fluorescence profile of HRP on excitation at 280 nm. A distinct maximum due to Tyr fluorescence[36] is observed at 303 nm in the HRP spectra and this disappears on 295-nm excitation (data not shown). The emission spectrum of CCP(MI) in both urea and GdHCl resembles that in Figure 2.1C of the Trp standard (NATA) on excitation at 280 or 295 nm.

Figure 2.2A summarizes the integrated fluorescence intensity of CCP(MI) relative to NATA as a function of urea concentration. It can be seen that CCP(MI) does not unfold in urea by a simple two-state process. Rather, a stable intermediate appears at 3 - 4 M urea, followed by a sharp rise in the relative fluorescence intensity above 4 M urea which levels off at ~ 60 ± 4 % at 8 M urea. A plot of the observed fluorescence intensity at 350 nm (data not shown) is coincident with the relative integrated intensity (300 - 450 nm) of CCP(MI) (Figure 2.2A), consistent with Trp emission dominating CCP(MI) fluorescence. A two-step unfolding process is also seen when CCP(MI) is incubated with GdHCl (Figure 2.2B). A stable intermediate appears at 1.3 - 1.8 M GdHCl which is converted to the denatured state (~ 65% relative fluorescence) above 2.5 M GdHCl. Thus, the denaturation of CCP(MI) as monitored

Figure 2.2 Relative integrated fluorescence (300 - 450 nm) intensities at pH 7.0 of **(A)** 1 μM CCP(MI) vs urea concentration; **(B)** 1 μM CCP(MI) vs GdHCl concentration; **(C)** 2 μM HRP vs GdHCl concentration. The points represent the average of 2-8 measurements for CCP(MI) and 2 - 3 measurements for HRP. The intensities are plotted relative to 7 μM NATA for CCP(MI) and 2 μM NATA/10 μM NAYA for HRP under the same conditions. Excitation 280 nm; slits 5 nm; scan rate 102 nm/min. **(D)** Fluorescence intensity at 350 nm of 2 μM HRP vs GdHCl concentration on excitation at 295 nm. Slits 5 nm; scan rate 402 nm/min.

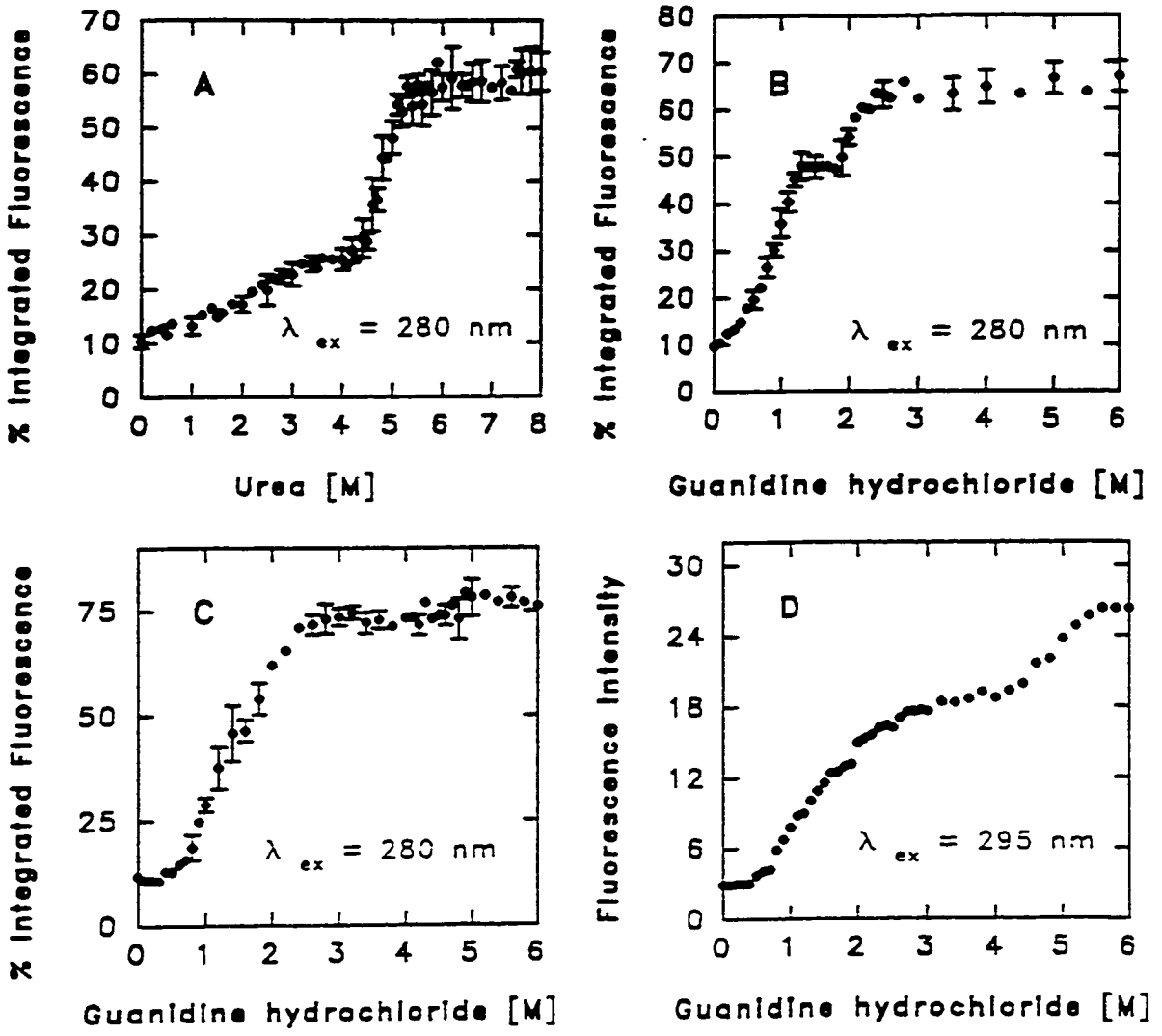
A
% Integrated Fluorescence
Urea [M]
λ ex = 280 nm
B
% Integrated Fluorescence
Guanidine hydrochloride [M]
λ ex = 280 nm
C
% Integrated Fluorescence
Guanidine hydrochloride [M]
λ ex = 280 nm
D
Fluorescence Intensity
Guanidine hydrochloride [M]
λ ex = 295 nm

by steady-state fluorescence is best described by:

$$N \rightleftharpoons I \rightleftharpoons U \qquad (7)$$

where I represents an intermediate state in the equilibrium unfolding process. The relative fluorescence of the intermediate I is ~ 25% in urea and ~ 50% in GdHCl, revealing that the CCP(MI) intermediate has looser structure in GdHCl compared to urea, unlike the final denatured forms which possess similar relative fluorescence in both denaturants.

The fluorescence-monitored unfolding behavior of HRP in GdHCl is presented in Figure 2.2C. A stable intermediate accumulates at higher GdHCl concentrations than in CCP(MI), and the increase in protein fluorescence observed above 4 M GdHCl due to an $I \rightleftharpoons U$ transition is a lot less pronounced on excitation at 280 nm (Figure 2.2C) than at 295 nm, the wavelength which preferentially excites the single Trp117 in HRP[26] (Figure 2.2D). Hence, the $I \rightleftharpoons U$ transition in HRP is associated with a relaxation of the Trp117-containing extended chain which occurs *after* loss of secondary structure and heme (see discussion below).

Renaturation of CCP(MI) and HRP as Monitored by Steady-State Fluorescence. CCP(MI) renaturation likely occurs by the same mechanism as denaturation since both curves are similar (Figure 2.3A, B). HRP denaturation and renaturation, on the other hand, must occur by different mechanisms since, as can be

seen from Figure 2.3C, renaturation involves refolding of the polypeptide prior to heme capture below 1 M GdHCl. Both renatured peroxidases exhibit higher fluorescence intensities due to incomplete heme capture during renaturation, but addition of exogenous heme quenched the fluorescence to the levels seen before denaturation.

Heme Soret Absorption and CD of Denatured CCP(MI) and HRP. The Soret absorption of the peroxidases was recorded in various concentrations of denaturants following the fluorescence measurements. At low denaturant concentration (1 M urea, 0.3 M GdHCl) the intensity of the Soret band of CCP(MI) at 408 nm is diminished (Figure 2.4A, B). A sharpening and red shifting of the Soret to 416 nm is observed in 3.8 M urea and 1.3 M GdHCl, denaturant concentrations corresponding to those at which the unfolding intermediates of CCP(MI) have reached their maximum concentrations (Figure 2.2A, B). Since the GdHCl intermediate has a less intense 416-nm band, it must have lower affinity for heme than the urea intermediate, consistent with the higher relative fluorescence of the former (~ 50%) compared to the latter (~ 25%). At denaturant concentrations above the transition regions, the Soret bands broaden again and blue shift, and the resultant spectra in 8 M urea and 6 M GdHCl are nearly identical to those of free hemin under the same conditions (Figure 2.4C). The heme CD absorption of CCP(MI) at 410 nm as a function of urea is plotted in Figure 2.4D. The stable intermediate seen in the fluorescence-monitored

Figure 2.3 Integrated fluorescence intensity (300 - 450 nm) at pH 7.0 of (**A**) 1 μM CCP(MI) during unfolding (—Δ—) and refolding (····●····) in urea; (**B**) 1 μM CCP(MI) during unfolding (—Δ—) and refolding (····●····) in GdHCl, and (**C**) 1 μM HRP during unfolding (—Δ—) and refolding (····●····) in GdHCl. Excitation 280 nm; slits 5 nm; scan rate 102 nm/min.

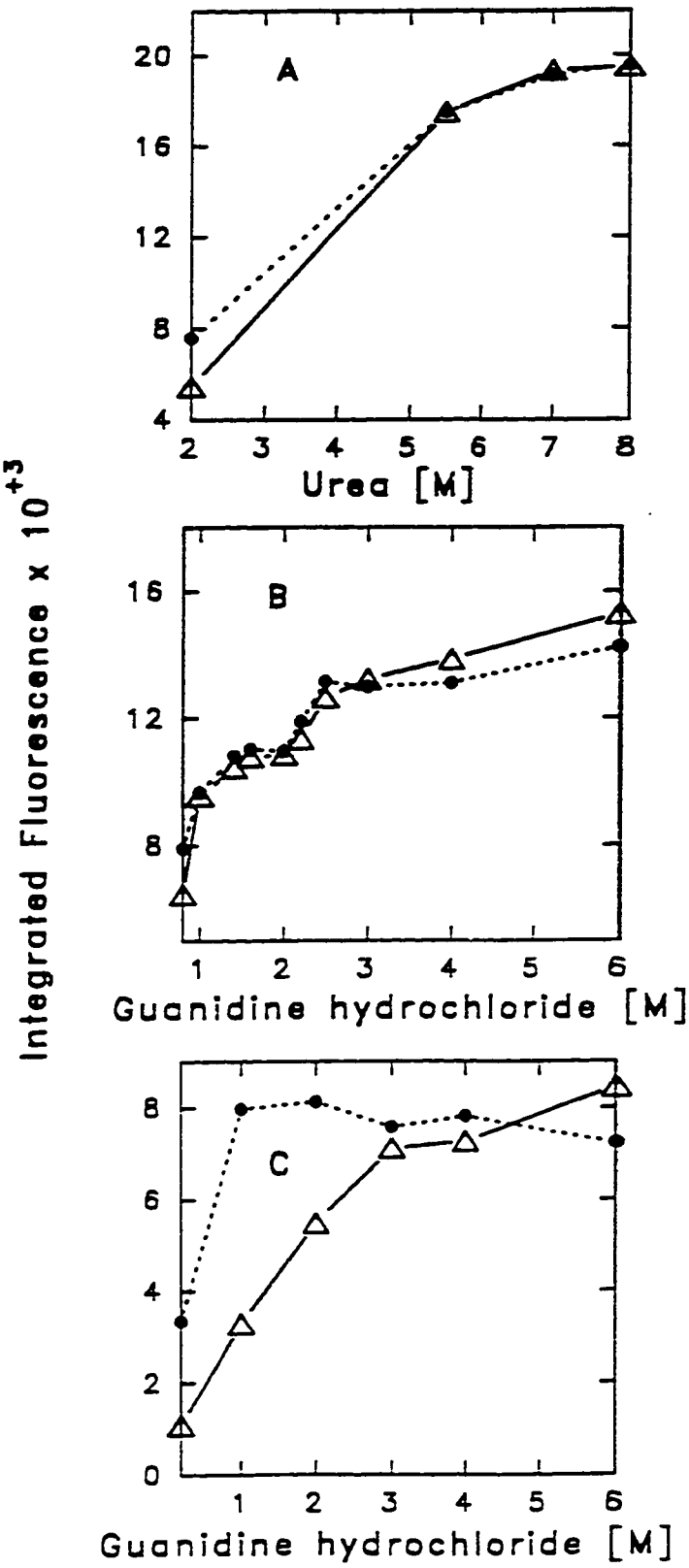
A
B
C
Integrated Fluorescence x 10+3
Urea [M]
Guanidine hydrochloride [M]
Guanidine hydrochloride [M]

Figure 2.4 Soret absorption at pH 7.0 of **(A)** 1 μM CCP(MI) in 0 M (—), 1 M (·····), 3.8 M (— · —), and 8 M (— —) urea; **(B)** 1 μM CCP(MI) in 0 M (—), 0.3 M (·····),1.3 M (— · —), 2 M (— —), and 6 M (— · · —) GdHCl; **(C)** 0.44 μM hemin in 8 M (—) urea and 6 M (·····) GdHCl. Pathlength 1 cm. **(D)** The molar CD absorption ($\Delta\varepsilon$) at 410 nm of CCP(MI) vs urea at pH 7.0, where $\Delta\varepsilon = [\theta] / 3298$.[80] The effective concentration of CCP(MI) in urea was 9.39 μM for the CCP(MI) heme CD measurements. Pathlength 0.5 cm.

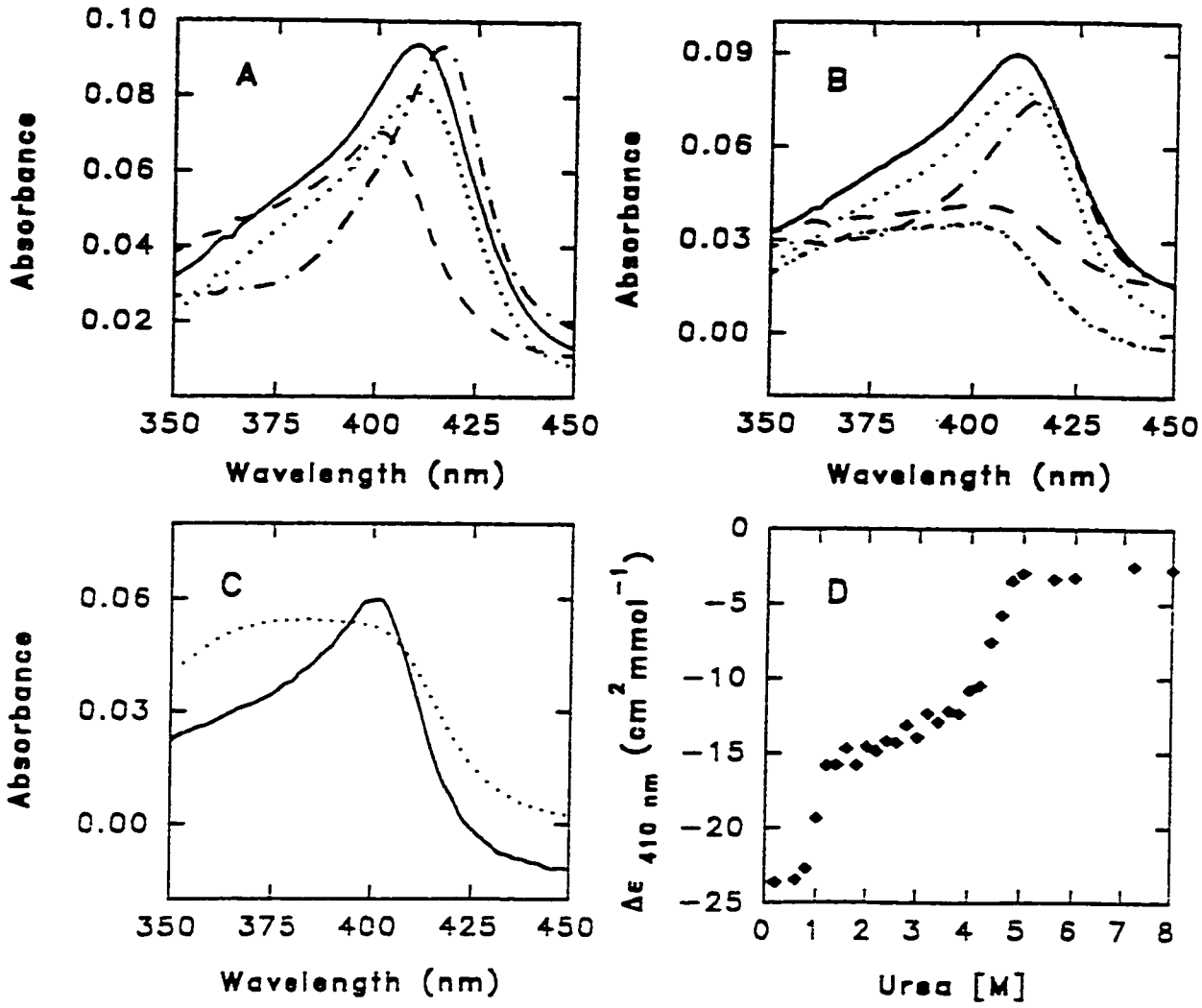
A
B
C
D
Absorbance
Wavelength (nm)
Urea [M]
0.10
0.08
0.06
0.04
0.02
0.09
0.03
0.00
350
375
400
425
450
0
−5
−10
−15
−20
−25
1
2
3
4
5
6
7
8

unfolding of CCP(MI) and in the Soret spectra is also clearly observed in heme-CD-monitored denaturation which is a more sensitive probe of the $N \rightleftharpoons I$ transition than fluorescence.

The Soret absorption of HRP at different concentrations of GdHCl is shown in Figure 2.5A. No red shift is observed in the Soret of HRP as the protein unfolds. Rather, a dramatic change is observed between 1 and 2 M GdHCl, and the Soret absorption in 3 M GdHCl resembles that of free hemin in 6 M GdHCl (Figure 2.4C). The smoothed heme CD spectra of HRP are shown in Figure 2.5B, and reveal that in 2.6 M GdHCl the heme has dissociated from the polypeptide and lost the asymmetric character necessary for optical activity. This mirrors the heme absorption data shown in Figure 2.5A.

The Soret absorption of CCP(MI) and HRP was also recorded during renaturation (spectra not shown). The Soret spectra of CCP(MI) undergoing renaturation were similar to those observed during denaturation (Figure 2.4A, B); specifically, the CCP(MI) intermediates at 416 nm were observed over the same denaturant concentrations on refolding. The Soret spectra of HRP showed that refolding of the polypeptide was necessary for capture of the heme since no increase in Soret intensity was observed on renaturation until the GdHCl concentration was reduced to $\leq$ 1 M. Due to incomplete heme capture during refolding, the Soret intensity was only ~ 60% that of the native protein in 0.2 M GdHCl. However, addition of excess hemin during renaturation resulted in 100% heme loading of HRP (data not shown).

Figure 2.5 (A) Soret absorption of 2 μM HRP at pH 7.0 in 0 M (—), 1 M (·····), 1.8 M (— · —), 2 M (— —), and 3 M (— · · —) GdHCl. Pathlength 1 cm. (B) Smoothed CD spectra of 11 μM HRP in the aromatic and heme region (240 - 480 nm) at different GdHCl concentrations at pH 7.0; 0 M (—), 1 M (·····), 1.8 M (— · —), and 2.6 M (— —). Pathlength 0.5 cm.

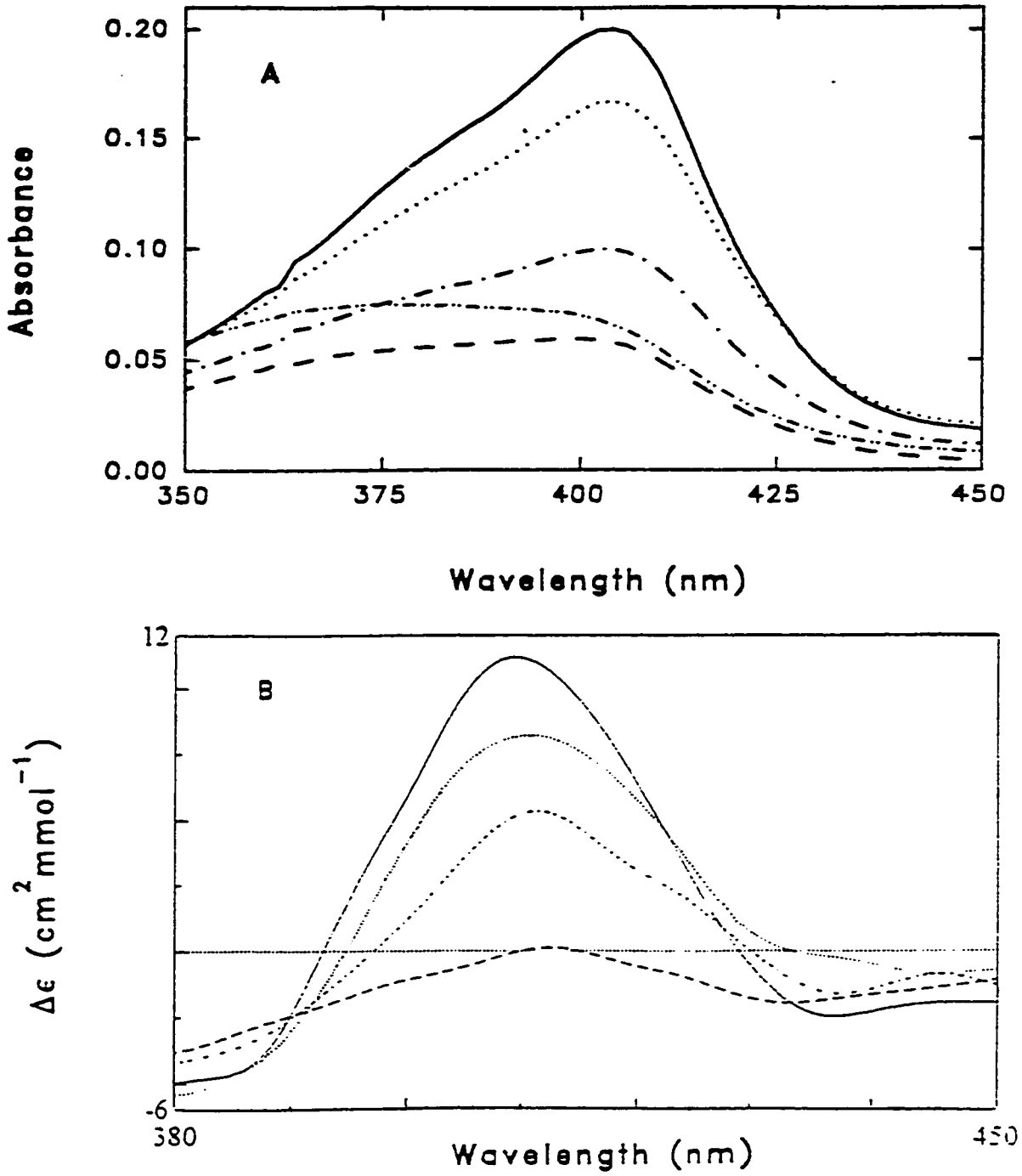
A
0.20
0.15
0.10
0.05
0.00
Absorbance
350
375
400
425
450
Wavelength (nm)
B
12
-6
Δε (cm² mmol⁻¹)
380
450
Wavelength (nm)

Denaturation of CCP(MI) and HRP as Monitored by UV/CD. The loss in ellipticity of the backbone absorption at 222 nm of CCP(MI) and HRP vs urea or GdHCl concentration is shown in Figure 2.6. Unlike the fluorescence measurements (which are mainly sensitive to and report on localized changes with respect to the heme), the $[\theta]_{222}$ measurements indicate that the backbone of CCP(MI) unfolds in a single step with no accumulation of stable intermediates. The backbone of HRP also unfolds in a single step (Figure 2.6C), and loss of secondary structure is almost complete before the fluorescence-detected intermediate appears above 2.5 M GdHCl (Figure 2.2C).

The refolding of the CCP(MI) and HRP backbones as monitored by $[\theta]_{222}$ is shown in Figure 2.7. The results indicate that the backbone unfolding and refolding pathways of CCP(MI) are essentially the same. However, there is a loss in backbone ellipticity as HRP refolds over 24 h. Allowing the protein to refold over a period > 24 h slightly increased the ellipticity of the *refolded* protein (data not shown), but on duplicate experiments it was observed that a fraction of HRP had precipitated and a decrease in heme absorbance was also observed in these samples. Precipitation of HRP in 6 M GdHCl is concentration dependent since it was observed at the high concentrations of stock HRP (~ 100 μM) required for the UV/CD refolding experiments, but not in the ~ 30-μM stock used in the fluorescence-monitored refolding experiments. A competition between folding and aggregation has also been reported for multidomain and multisubunit proteins on refolding. For example, the yield of refolded lactate dehydrogenase was protein concentration dependent with

Figure 2.6 Molar ellipticity at 222 nm at pH 7.0 of **(A)** 4.7 μM CCP(MI) in urea; **(B)** 5.7 μM CCP(MI) in GdHCl, and (C) 5.9 μM HRP in GdHCl. The solid lines show the fit of the data by nonlinear least-squares analysis.[30,31] The CD conditions are described in the text.

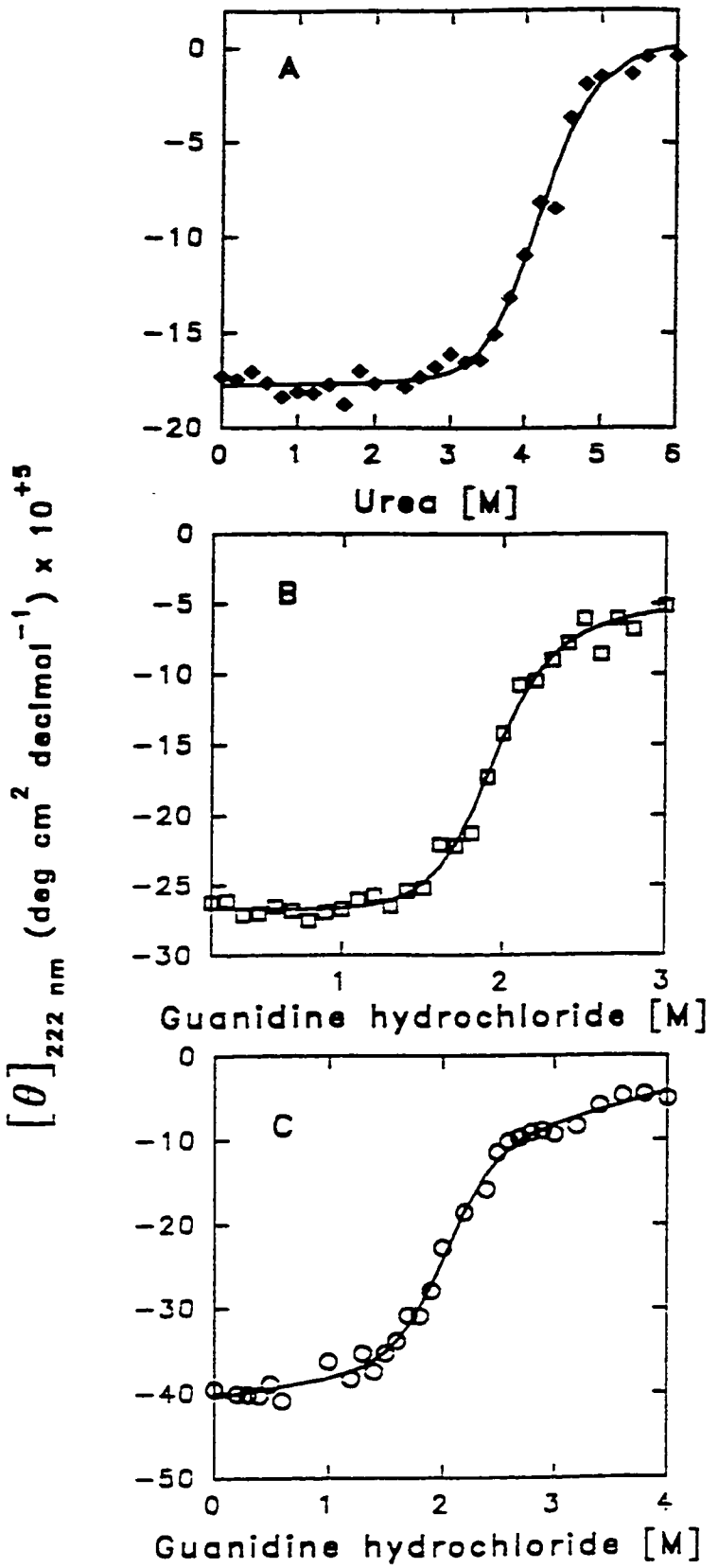
A
B
C
0
−5
−10
−15
−20
−25
−30
−40
−50
0 1 2 3 4 5 6
Urea [M]
1 2 3
Guanidine hydrochloride [M]
0 1 2 3 4
Guanidine hydrochloride [M]
$[\theta]_{222\ nm}$ (deg cm^2 decimol^{-1}) x 10^{+5}

Figure 2.7 Molar ellipticity at 222 nm at pH 7.0 of (**A**) 5.2 μM CCP(MI) during unfolding (—●—) and refolding (···· ▽ ····) in urea, and (**B**) 6.5 μM HRP during unfolding (—●—) and refolding (···· ▽ ····) in GdHCl. The CD conditions are described in the text.

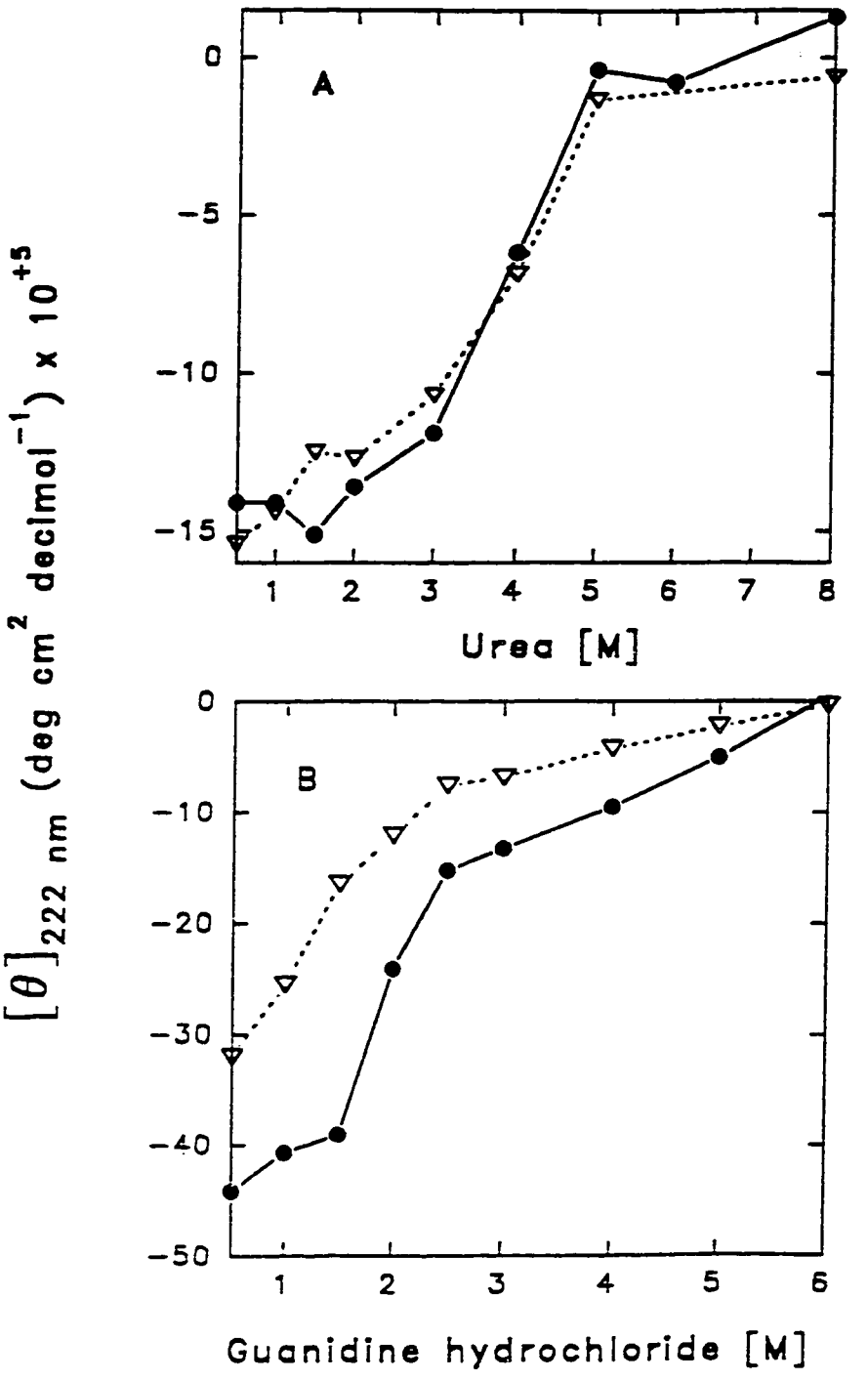
A
B
0
−5
−10
−15
−20
−30
−40
−50
1
2
3
4
5
6
7
8
Urea [M]
Guanidine hydrochloride [M]
$[\theta]_{222\ nm}$ (deg cm^2 decimol^{-1}) x 10^{+5}

concentrations above ~ 0.1 μg/mL producing > 25% aggregation.[37]

Denaturation of EDTA- and DTT-treated HRP as Monitored by Steady-State Fluorescence. The fluorescence intensity vs denaturant concentration of HRP following incubation with EDTA or DTT is shown in Figure 2.8. Incubation with 2 mM EDTA makes HRP more sensitive to denaturation since the GdHCl concentration at half-maximum fluorescence ($[GdHCl]_{½}$) decreases from 2 to 0.45 M (Figure 2.2C vs 2.8A). Incubation of HRP with 3 and 30 mM DTT results in $[GdHCl]_{½}$ values of 1.3 M and 0.9 M, respectively (Figure 2.8B), indicating that the Ca^{2+} ions have a greater effect on the overall sensitivity of the protein to denaturant than the disulfide bridges. It should be noted that the number of free cysteines following 18 h incubation with DTT were not determined because of the difficulty in carrying out such experiments in the presence of excess free thiol. However, since incubation of HRP with DTT results in decreased $[GdHCl]_{½}$ values, it can be assumed that reduction of 1 or more disulfides occurs in 3 mM DTT, and a higher number in 30 mM DTT. Consistent with this speculation, the relative integrated fluorescence (λ_{ex} 280 nm) of HRP treated with 30 mM DTT is ~ 20% higher than that of 3-mM-DTT-treated HRP (Figure 2.8B), and the fluorescence maximum of the former has red shifted from 326 to 342 nm in buffer only (data not shown). Figure 2.8C shows the fluorescence intensity at 350 nm in 0 - 6 M GdHCl following 295-nm excitation of untreated HRP and HRP incubated with 3 mM DTT. It is clearly evident from these denaturation curves that the sharp increase in fluorescence above 4 M GdHCl observed in untreated HRP is absent in DTT-treated

HRP. This reveals that disulfide reduction affects the fluorescence behavior of Trp117 which is preferentially excited at 295 nm.[26] It is of interest that after 18 h incubation of HRP with *both* 2 mM EDTA and 3 mM DTT, Trp117 is largely solvent exposed as revealed by the red-shifted fluorescence maximum at 350 nm in the *absence* of denaturant.

Kinetics of Unfolding of CCP(MI) and HRP in Denaturants. Exponential growth of the fluorescence intensity at 350 nm was observed on rapidly mixing the proteins with high concentrations of denaturants (data not shown). The intensity vs time data for CCP(MI) in 8 M urea and HRP in 6 M GdHCl at pH 7.0 were fit by single exponentials and the half-lives ($t_{½}$) are listed in Table 2.2. CCP(MI) and HRP unfold in denaturant with $t_{½}$ values of 14.3 and 519 s, respectively. HRP treated with 3 mM DTT or 2 mM EDTA unfolds only slightly faster than untreated HRP, but denaturation in 4 M GdHCl of HRP treated with *both* DTT and EDTA occurs with $t_{½}$= 0.42 s (Table 2.2). The large decrease in kinetic stability of HRP indicates that both types of stabilizing elements are removed on incubation with DTT *and* EDTA together.

DISCUSSION

Both steady-state fluorescence and circular dichroism are very useful

Figure 2.8 (A) Relative integrated fluorescence intensities (300 - 450 nm) vs GdHCl concentration at pH 7.0 of 2 μM EDTA-treated HRP. HRP (10 μM) was incubated for 18 h with 2 mM EDTA prior to dilution in GdHCl. Intensities are plotted relative to 2 μM NATA/10 μM NAYA treated with 2 mM EDTA, and the data points represent the average of 2 measurements. Excitation 280 nm; slits 5 nm; scan rate 102 nm/min. (B) Relative integrated fluorescence intensities (300 - 450 nm) vs GdHCl concentration at pH 7.0 of 2 μM HRP treated with 3 mM DTT (■) and 30 mM DTT (□). HRP (10 μM) was incubated for 18 h with DTT prior to dilution in GdHCl. Intensities are plotted relative to 2 μM NATA/10 μM NAYA treated with 3 mM DTT and 30 mM DTT and the data points represent the average of 2 measurements. Excitation 280 nm; slits 5 nm; scan rate 102 nm/min. (C) Fluorescence intensity at 350 nm of untreated HRP (●) and 3-mM-DTT-treated HRP (○). Excitation 295 nm; slits 5 nm; scan rate 402 nm/min. The fluorescence intensity curves of the 2 samples have been offset for clarity.

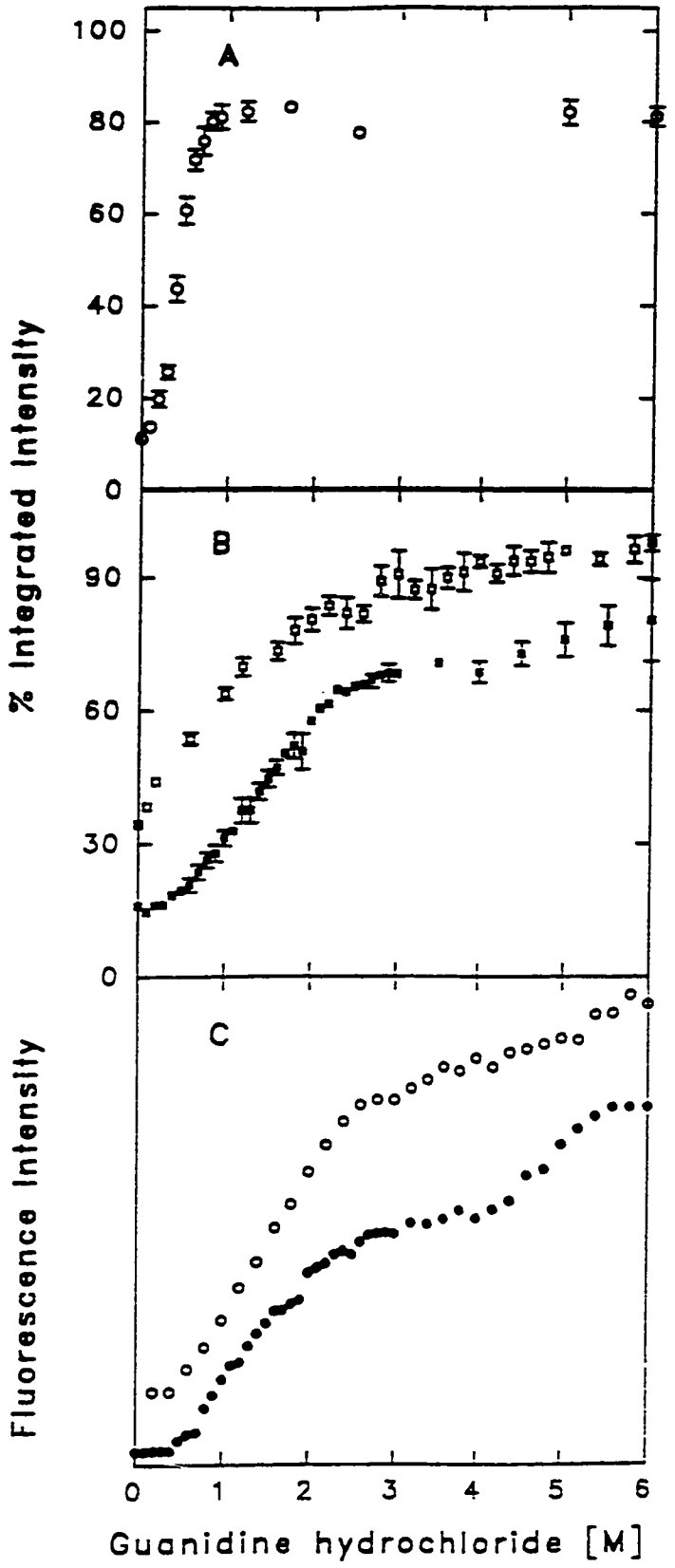
A
B
C
100
80
60
40
20
0
90
60
30
0
% Integrated Intensity
Fluorescence Intensity
0
1
2
3
4
5
6
Guanidine hydrochloride [M]

Table 2.1 Thermodynamic parameters for the unfolding of CCP(MI) and HRP as monitored by UV/CD

Protein samples	$\Delta G_{d,aq}$ (kcal/mol)[a]	*m* (kcal/mol/M)[a]	$[D]_{½}$[b] (M)
CCP(MI) in urea	6.2 ± 0.3 (3)[c]	1.5	4.2
CCP(MI) in GdHCl	6.4 ± 0.5 (2)[c]	3.4	1.9
HRP in GdHCl	4.0 ± 0.6 (2)[c]	2.0	2.0

[a] Calculated using the nonlinear least-squares analysis method of Hughson and Baldwin[30] where T = 298 K. $\Delta G_{d,aq}$ represents the free energy in 0 M denaturant and *m* the slope of the linear dependence of ΔG_d on denaturant concentration (eq 6). The UV/CD data are from Figure 2.6.

[b] Denaturant concentration at half maximum ellipticity.

[c] Number of separate determinations of $\Delta G_{d,aq}$.

Table 2.2 Half-lives ($t_{½}$) for CCP(MI) and HRP unfolding in denaturants

Protein samples	$t_{½}$ (s)[a]	n[b]
CCP(MI)[c]	14.3 ± 3.4	9
HRP[d]	519 ± 36	4
HRP+DTT[d,e]	450 ± 23	3
HRP+EDTA[d,e]	395 ± 37	4
HRP+DTT+EDTA[f]	0.42 ± 0.006	2

[a] Half-lives were obtained by fitting the fluorescence intensities at 350 nm vs time by first-order kinetics.

[b] Number of observations.

[c] 1 μM protein was rapidly mixed with 8 M urea at pH 7.0.

[d] 2 μM protein was rapidly mixed with 6 M GdHCl at pH 7.0.

[e] HRP was incubated for 18 h with 3 mM DTT or 2 mM EDTA prior to unfolding.

[f] 5 μM HRP was rapidly mixed with 4 M GdHCl at pH 7.0 after 18 h incubation with 3 mM DTT *and* 2 mM EDTA.

techniques for studying the structure and dynamics of proteins.[29,37] The intrinsic fluorescence of proteins from residues such as Trp, Tyr, and Phe[36] is an excellent built-in reporter. For example, the microenvironment surrounding Trp residues can be probed since these exhibit emission maxima that red shift from ~ 320 to 350 nm as their environment changes from nonpolar to polar.[34] A fluorescence red shift also occurs when Trps buried in a protein interior become solvent exposed as a result of denaturation. Unfolding of heme proteins generally results in a dramatic increase in steady-state protein fluorescence due to relief of heme quenching in the denatured state.[24,25,39,40] In addition to fluorescence and CD, heme absorption is yet another useful conformational probe[41] for the study of heme proteins.

Denaturation of CCP(MI). CCP(MI), like the yeast form of the enzyme, contains 7 Trps[42] which dominate the steady-state fluorescence of the protein.[24] A low quantum yield due to efficient energy transfer to the heme is seen in the native protein (Figure 2.1A); however, the fluorescence exhibits a shift to longer wavelengths and increases in intensity when CCP(MI) is denatured in urea. The fluorescence emission of native CCP(MI) is independent of the excitation wavelength, and the protein exhibits a spectrum in 8 M urea (pH 7.0) similar to the Trp standard, NATA (Figure 2.1A and 2.1C), revealing that there is no fluorescence contribution from the 14 Tyr or 18 Phe residues,[42] which as free amino acids in solution also have fluorescent properties.[36] Denaturation of CCP(MI) is observed on incubation with increasing concentrations of both urea and GdHCl. The unfolding of CCP(MI) as examined by

intrinsic fluorescence is not a simple two-state ($N \rightleftharpoons U$) process since stable thermodynamic intermediates are observed at 3 - 4 M urea and 1 - 2 M GdHCl (Figure 2.2A, B). Thermodynamically-stable unfolding intermediates have been observed with apo- and holoMb,[30,41] the α-subunit of tryptophan synthase,[43] α-lactalbumins,[44,45] and porphyrin cytochrome *c* (Hu & English, unpublished results). Since Trp fluorescence in heme proteins is indirectly a measure of the Trp → heme energy transfer, formation of the unfolding intermediates in CCP(MI) most likely involves localized changes around the heme cavity that alter the energy-transfer efficiency. In support of this speculation, the heme CD absorption vs urea profile of CCP(MI) is also biphasic (Figure 2.4D), and the Soret absorption spectra recorded in 3.8 M urea and 1.3 M GdHCl reveal that the heme undergoes a transition from five-coordinate high-spin to six-coordinate low-spin prior to loss of secondary structure (Figure 2.4A, B).

Loss of CCP(MI) secondary structure appears to be a cooperative two-state process in both urea and GdHCl as monitored by backbone CD absorbance (Figure 2.6A, B). A comparison of the fluorescence and backbone CD curves (Figures 2.2A, B vs 2.6A, B) indicates that the fluorescence-sensitive intermediates are formed before the UV/CD-monitored loss of secondary structure occurs. In fact, the loss in secondary structure essentially coincides with the major fluorescence-detected $I \rightleftharpoons U$ transition in CCP(MI) in both urea and GdHCl (Figure 2.2A, B). Furthermore, the Soret absorption spectra of CCP(MI) (Figure 2.4) reveal heme loss from the polypeptide occurs mainly during the $I \rightleftharpoons U$ transition, and the resultant heme spectra

at high denaturant concentrations resemble those of free hemin shown in Figure 2.4C.

Calorimetry studies[46] have shown 2 mid-point transition temperatures (44 °C and 63 °C) in the thermal denaturation of yeast CCP at pH 7.0. However, the amide I' bands in the FTIR spectrum of CCP(MI) show no changes between 25 and 50 °C,[16] indicating a single transition as the protein loses its secondary structure. These results suggest that the second transition (but not the first transition) in the thermal unfolding of CCP(MI) involves loss of secondary structure. The temperature dependence of the FTIR ν(CO) bands of CCP(MI) also reveals that CCP-CO undergoes a conformational transition which affects the heme pocket prior to loss of secondary structure.[16] Additionally, the decrease in the FTIR amide II' intensity of CCP(MI) as a function of temperature indicates loosening of the tertiary structure before unfolding of the secondary structure.[16] Formation of an intermediate with partially collapsed tertiary structure and intact secondary structure[47] would account for the $N \rightleftharpoons I$ transition in the denaturant-induced unfolding of CCP(MI). A temperature-induced shift in the Soret maximum from 408 to 414 nm at pH 7.0 has been observed previously in yeast CCP and was attributed to binding of a distal amino acid residue to the heme at 36 °C.[48] Similarly, at low urea and GdHCl concentrations a denaturant-induced conformational change results in the coordination of a sixth ligand to the heme (Figure 2.4A, B), most likely the distal His52. It is of interest that a single endotherm was observed for heme-free apoCCP[46] with a mid-point transition temperature (T_m ~ 60 °C) corresponding to the higher T_m transition observed for holoCCP.

Denaturation of HRP. Isoenzyme C of HRP has a single Trp residue (Trp117)[49] which contributes to the fluorescence of the protein.[25] Denaturation of HRP also results in red shifting of the fluorescence maximum as well as an increase in fluorescence intensity. Previous time-resolved fluorescence studies have shown that pH-induced conformational changes in HRP result in an increase in the fluorescence lifetime observed on the picosecond timescale.[26] Unlike CCP(MI), excitation-wavelength-dependent fluorescence is observed in HRP. There is a definite contribution to the intrinsic fluorescence of HRP from its 5 Tyr residues when 280-nm excitation is used[26] and the fluorescence spectra of HRP in > 2 M GdHCl resemble that of a mixture of Trp and Tyr standards (Figure 2.1B, C).

It has been previously reported that HRP retains some activity and 50% secondary structure following incubation in 8 M urea.[25] Our observations also show that in 8 M urea at pH 7.0 HRP exhibits < 50% relative fluorescence. Increased interaction of GdHCl with the peptide groups of HRP was noted in a previous study on urea and GdHCl denaturation of HRP,[40] so given the relatively weak effects of urea on HRP conformation, our present study focuses on GdHCl denaturation only.

Denaturation of HRP in GdHCl results in an intermediate with ~ 70% relative fluorescence between 2.5 and 4 M. No "heme-cavity" intermediate is detected by heme absorption or heme CD (Figure 2.5), which suggests that the heme pocket in HRP is more stable compared to CCP(MI). A further examination of the fluorescence-detected intermediate (Figure 2.2C) shows that its relative fluorescence and that of the denatured state differ by ~ 5%. Trp117 in HRP is located in an extended chain

between helix D and D' based on the X-ray structure of PNP[7] (T.L. Poulos, personal communication). A *local* relaxation of this chain rather than a gross protein conformation change could account for the ~ 5% increase in relative fluorescence above 4 M GdHCl. Trp117 in HRP is preferentially excited at 295 nm[26] and no contribution to protein fluorescence at 350 nm is observed from Tyr on 295-nm excitation.[36] Movement of the Trp117-containing extended chain in HRP above 4 M GdHCl is supported by the dramatic increase in fluorescence intensity at 350 nm on 295-nm excitation compared to that observed on 280-nm excitation (Figure 2.2C, D).

The GdHCl-induced changes in the UV/CD spectra of HRP (Figure 2.6C) support a two-state backbone unfolding process. Secondary structure in HRP is lost by 3 M GdHCl and no UV/CD-detectable intermediate accumulates at the GdHCl concentrations (0 - 6 M) investigated. The Soret absorbance of HRP shows a large decrease over 1 - 3 M GdHCl at pH 7.0 (Figure 2.6B), the denaturant concentration range where significant changes in fluorescence and backbone CD spectra are also observed (Figure 2.2C and 2.6C, respectively). Unlike CCP(MI), there is no shift of the Soret absorption maximum of HRP at 403 nm; rather, a sharp crossover to solvent-exposed heme absorption is seen in denatured HRP at ≥ 2 M GdHCl (Figure 2.5A) and the heme CD spectra are also those of free heme at ≥ 2 M GdHCl (Figure 2.5B). Together, these observations indicate that heme loss in HRP is coincident with secondary structure loss, whereas the fluorescence-detected $I \rightleftharpoons U$ transition occurs *after* secondary structure loss.

A recent FTIR investigation showed that HRP is thermally more stable than

CCP(MI) since it loses its secondary structure at 90 °C while that of CCP(MI) is lost at 50-55 °C.[16] A single T_m (~ 79°C) was found for HRP using differential scanning calorimetry[50] and along with the FTIR studies of Holzbaur et al.,[16] a two-state thermal denaturation process of HRP is suggested. The FTIR spectra in the ν(CO) region also indicated that denaturation of the heme cavity coincides with the global thermal denaturation of HRP-CO,[16] reinforcing the view of a more stable heme pocket in HRP compared to CCP(MI).

Denaturation of EDTA- and DTT-Treated HRP. Enhanced conformational stability in native HRP is conferred by the presence of the bound Ca^{2+} ions and the 4 disulfide bridges.[17,25,51] Incubation with EDTA and DTT, which presumably chelates the bound ions[17,52] and reduces the disulfide bonds,[17,53] respectively, results in a dramatic decrease in the kinetic stability of HRP as judged by the half-life of unfolding of the treated vs untreated protein in 4 M GdHCl ($t_{½}$ ~ 0.4 vs 519 s). The X-ray structure of PNP (Figure 2.9) shows that a disulfide bridge (Cys44-Cys49) forms a loop encompassing several of the distal Ca^{2+} ligand residues[7] and this same disulfide bridge is also seen in the X-ray structure of HRP (T.L. Poulos, personal communication). The half-life of unfolding of 2-mM-EDTA-treated HRP is 26% lower than that of untreated HRP (Table 2.2). However, the significantly increased sensitivity of EDTA-treated HRP to denaturant ($[GdHCl]_{½}$ ~ 0.45 M; Figure 2.8A) suggests that thermodynamic stability is reduced more than kinetic stability on Ca^{2+} removal. Furthermore, the work of Pappa and Cass[25] also demonstrated that apoHRP

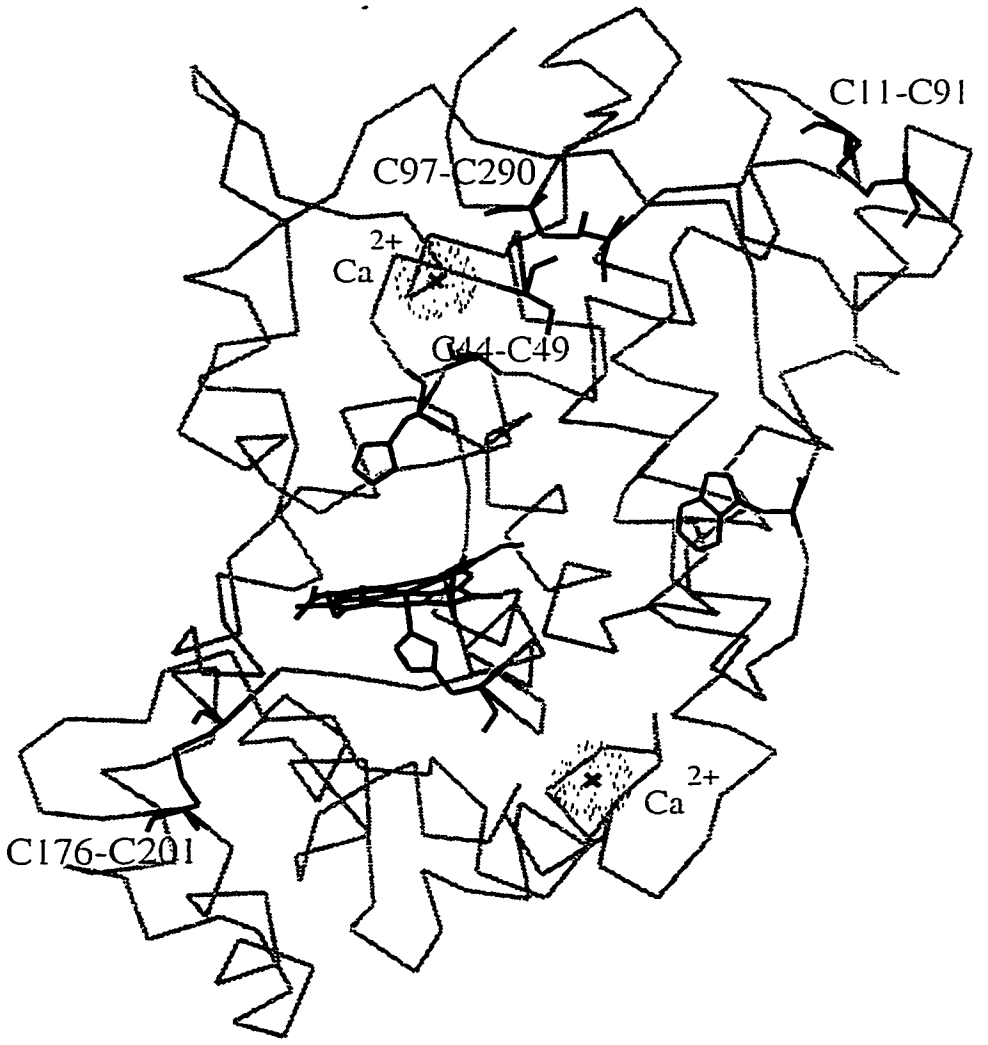

Figure 2.9 The C_α backbone of PNP generated from the X-ray coordinates.[7] The heme, distal His42, proximal His169, Trp117, 4 disulfide bridges, and van der Waals radii of the 2 Ca^{2+} ions are shown in bold.

is more resistant to denaturation in the presence of Ca^{2+}, reinforcing a structural role for this cation in stabilizing the native conformation.[17,52] Of the 2 Ca^{2+} ions,[51] only 1 appears to be important for maintaining the structure and function of HRP.[54-56]

Calcium also seems to play an important role in PNP,[57] LIP[58] and CIP.[59] While CCP does not bind cations, a proximal cation binding site has been engineered into the protein, and was found to decrease the stability of the Trp191 radical in CCP compound I.[60] Electrostatic calculations have shown that the proximal pocket in CCP is uniquely suited to stabilize the Trp191 radical.[61] Thus, although a proximal cation might increase the conformational stability of CCP, it would be counter productive with respect to stabilization of protein-based radicals. APX, which contains a proximal cation (probably K^+) binding site and has Trp179 in an analogous position to Trp191 in CCP, does not form an amino acid radical during normal turnover.[20] Class II and III peroxidases,[10] which include HRP, PNP, CIP and LIP, all contain both distal and proximal Ca^{2+} ions (Figure 2.9) for enhanced structural stability, but these peroxidases possess few oxidizable residues,[9] suggesting that formation of protein-based radicals may not be important in these enzymes. It would be of interest to compare the thermodynamic and kinetic stabilities of APX and CCP(MI) (Class I peroxidases) since, except for a proximal cation, APX does not possess other stabilizing elements.[20]

HRP treated with 3 and 30 mM DTT has intermediate GdHCl sensitivity ($[GdHCl]_{½}$= 1.3 and 0.9 M, respectively) compared to HRP ($[GdHCl]_{½}$= 2.0 M) and EDTA-treated HRP ($[GdHCl]_{½}$= 0.45 M). This suggests that the disulfide bridges

contribute less than the bound Ca^{2+} ions to the thermodynamic stability of the native conformation of HRP. An inspection of the solvent accessibility of the 4 disulfide bridges in PNP (and presumably in HRP) shows that they are all solvent exposed (Figure 2.9). Cys11-Cys91 is the most solvent accessible followed by Cys97-Cys290, while Cys44-Cys49, which forms a loop encompassing several of the distal Ca^{2+} ligand residues in HRP, is the closest disulfide bridge to Trp117 at a distance of ~ 11.4 Å (T.L. Poulos, personal communication). Pace and coworkers found that of the 2 disulfides in RNase T_1, the most solvent accessible is reduced first in the presence of 100 mM DTT.[62] Hence, we speculate that Cys11-Cys91 is reduced first in folded HRP on incubation with 3 mM DTT, but since 30-mM-DTT-treated HRP has ~ 20% higher fluorescence than 3-mM-DTT-treated HRP (Figure 2.2C and 2.8B), reduction of Cys97-Cys290 by the 10-fold extra free thiol is also likely. Furthermore, the protein fluorescence vs [GdHCl] profiles on excitation at 280 and 295 nm of DTT-treated HRP are similar in shape (Figure 2.8B, C), revealing that the $I \rightleftharpoons U$ transition in the absence of DTT is due to conformational change around 1 or more disulfides. Given the dramatic change in the fluorescence profiles of untreated and DTT-treated HRP above 4 M GdHCl on 295-nm excitation, Trp117 alone must be reporting on the $I \rightleftharpoons U$ transition.

Comparison of CCP(MI) and HRP Heme Capture and Thermodynamic Parameters. The denaturant-induced unfolding behavior of CCP(MI) and HRP is clearly different despite their similar secondary and tertiary structures. Although the

CD unfolding curves at 222 nm (Figure 2.7) suggest a simple $N \rightleftharpoons U$ transition in both CCP(MI) and HRP, heme capture by the denatured peroxidases on refolding is remarkably different. The refolding data for CCP(MI) (CD, heme Soret absorption and fluorescence) reveal heme capture at high denaturant concentrations, indicating that a non-native form of CCP(MI) recognizes heme. While heme incorporation in CCP(MI) coincides with refolding of the polypeptide, heme capture by HRP occurs *after* polypeptide refolding. This is supported by the observation that the secondary structure of HRP must be largely reformed before heme capture occurs (Figure 2.3C and 2.7B). The heme CD spectra also indicate that heme capture only occurs below 1 M GdHCl since no heme CD signal on refolding was observed between 6 and 1 M GdHCl and the heme CD spectra (not shown) over this GdHCl concentration range were similar to those of the denatured samples at ≥ 2 M GdHCl (Figure 2.5B). The Soret absorption measurements confirm that heme capture by the polypeptide occurs below 1 M GdHCl and gives rise to the heme spectrum of native HRP.

Recently, proton NMR spectroscopy on a sperm whale Mb mutant[63] revealed the existence of well-folded regions in the apoprotein that are remarkably similar to the corresponding regions in the native holoprotein. A compact subdomain made up of the A-B-G-H helix interface in sperm whale apoMb[64] is speculated to represent the region of the folding intermediate responsible for heme capture. Formation of this compact subdomain, however, is not heme-dependent since addition of free heme to folded apoMb results in a reconstituted Mb which has identical secondary structure and properties to native Mb.[25] In HRP, in addition to the requirement that the

secondary structure be formed for heme capture *in vitro*, the distal His42 and proximal His170 also contribute to heme recognition since His → Phe single-point mutants (H42F and H170F) show altered kinetics of heme entrapment.[65]

The conformational stability of a protein that undergoes a reversible two-state $N \rightleftharpoons U$ transition (eq 2) is given by its $\Delta G_{d,aq}$.[32] The UV/CD-monitored unfolding of CCP(MI) and HRP (Figure 2.6) and refolding (Figure 2.7) curves suggest that secondary structure formation in the peroxidases follows a two-state reversible transition when allowance is made for the fraction of heme and polypeptide that undergoes precipitation. Thus, from the UV/CD data, $\Delta G_{d,aq}$ values of ~ 6 and ~ 4 kcal/mol are calculated (eq 6) for CCP(MI) and HRP, respectively. These are at the low end of the range of values reported for globular proteins where the native state appears to be stabilized by 4 - 20 kcal/mol.[36,66-68] A $\Delta G_{d,aq}$ ~ 6 kcal/mol was calculated for HRP at 25 °C and pH 6.4 in denaturants as studied by UV difference spectrophotometry.[40] The lower $\Delta G_{d,aq}$ for HRP compared to CCP(MI) is surprising since the 2 bound Ca^{2+} ions and the 4 disulfide bridges in HRP are expected to yield a compact denatured state, which is inherently higher in energy than a fully extended polypeptide. Previous studies have shown that engineering artificial disulfide bonds into a protein enhances conformational stability by lowering the entropy of the unfolded state.[62,69-73] Nonetheless, the introduction of a single disulfide bond in yeast cytochrome *c* lowers $\Delta G_{d,aq}$ by ~ 1 kcal/mol despite the fact that the crosslink creates a compact denatured state.[31] It is of interest that DTT- and EDTA-treated HRP must possess a $\Delta G_{d,aq} < 0$ since it exhibits high fluorescence intensity and an emission

maximum at 350 nm in buffer only.

The *m* values calculated for the unfolding of CCP(MI) in urea and GdHCl are typical (~ 1.5 - 2 kcal/mol/M in urea; ~ 3 - 5 kcal/mol/M in GdHCl) of those seen in the denaturant-induced unfolding of heme proteins.[74] The 1.7-fold larger *m* value in GdHCl for CCP(MI) compared to HRP (Table 2.1) is an indication of increased cooperativity of unfolding in the former peroxidase. Cooperative unfolding is often observed with small (< 20 kDa) single domain proteins[75] but it is also not uncommon to find multidomain proteins where the domains unfold cooperatively in a single transition.[76,77] Multidomain proteins unfold with cooperativity in the presence of strong domain interactions which cause mutual domain stabilization. The crystal structure of CCP shows that the protein is folded into 2 clearly defined domains (I and II) and that the heme occupies a crevice between them.[14] Hence, the highly cooperative unfolding of the secondary structure of CCP(MI) in GdHCl indicates strong interactions between domains I and II. The presence of disulfides in HRP might be responsible for the lower cooperativity of its secondary structure unfolding in GdHCl (Table 2.1) since, based on the sequence alignment of PNP, HRP, and CCP,[7] domains I and II of HRP are covalently bonded by the Cys97-Cys290 disulfide bridge. Furthermore, the work of Betz and Pielak[31] has shown that a smaller *m* value is calculated for the cytochrome *c* Cys20-Cys102 crosslinked variant than for the non-crosslinked variant (2.7 vs 4.6 kcal/mol/M). Interestingly, the GdHCl concentration (~ 2 M) at half maximal backbone ellipticity ($[D]_{½}$) is almost the same for CCP(MI) and HRP. The $[D]_{½}$ was also reported to be approximately the same in non-crosslinked

and crosslinked cytochrome *c*.[31]

The unfolding rates of CCP(MI) and HRP (Table 2.2) show that the native form of CCP(MI) unfolds significantly faster in high denaturant concentrations ($t_{½}$ ~ 14 s) than HRP ($t_{½}$ ~ 519 s), which reveals the higher kinetic stability of HRP. This is due to the presence of its stabilizing structural elements (2 Ca^{2+} ions and 4 disulfide bridges), since removal of these elements gives rise to a protein which is both kinetically (Table 2.2) and thermodynamically highly unstable.

Conclusions. Despite the similar tertiary structures of CCP(MI) and HRP, their denaturation/renaturation and heme capture mechanisms in denaturants differ. Furthermore, the unfolding rates of the 2 peroxidases indicate that HRP is kinetically more stable than CCP(MI). The kinetic stability of HRP is associated with its bound Ca^{2+} ions and disulfides since their removal *greatly* destabilizes the protein. The kinetic stability of native HRP makes it an ideal protein for use in biotechnology,[78] while the greater conformational flexibility of CCP presumably facilitates radical generation, stabilization and translocation within its polypeptide matrix.[9] Also, such flexibility should facilitate heme capture by the apoprotein, which is the dominant form *in vivo* when yeast are grown under unaerobic conditions.[79]

ACKNOWLEDGEMENTS

We wish to thank Dr. Mark Miller (UCSD) for providing the *E. coli* transformed with recombinant cytochrome *c* peroxidase used to isolate the CCP(MI) for this study. Professor Oswald Tee and Dr. Timothy Gadosy are thanked for their assistance with the stopped-flow experiments. Craig Fenwick is thanked for many helpful discussions and Yazhen Hu for her technical assistance. We would also like to thank Professor Joanne Turnbull for critically reading this manuscript. This work was funded by a grant from the Natural Sciences and Engineering Research Council of Canada (NSERC) to A.M.E.

REFERENCES

1 Finzel, B. C., Poulos, T. L., & Kraut, J. (1984) *J. Biol. Chem. 259,* 13027.

2 Poulos, T. L., Edwards, S. L., Wariishi, H., & Gold, M. H. (1993) *J. Biol. Chem. 268,* 4429.

3 Kunishima, N., Fukuyama, K., Matsubara, H., Hatanakana, H., Shibano, Y., & Amalhi, T. (1994) *J. Mol. Biol. 235,* 331.

4 Petersen, J. F. W., Kadziola, A., & Larsen, S. (1994) *FEBS Lett. 339,* 291.

5 Patterson, W. R., & Poulos, T. L. (1995) *Biochemistry 34,* 4331.

6 Sundaramoorthy, M., Kishi, K., Gold, M. H. & Poulos, T. L. (1994) *J. Biol. Chem. 269,* 32759.

7 Schuller, D. J., Ban, N., van Huystee, R. B., McPherson, A., & Poulos, T. L.

(1996) *Structure 4*, 311.

8 Poulos, T. L., & Fenna, R. E. (1994) in *Metal Ions in Biological Systems: Metalloenzymes Involving Amino Acid-Residue and Related Radicals* (Siegel, H. & Sigel, A., Eds.,) Vol. 30, pp 25-75, Marcel Dekker: New York, NY.

9 English, A. M., & Tsaprailis, G. (1995) *Adv. Inorg. Chem. 43*, 79.

10 Welinder, K. G. (1992) *Curr. Opin. Struct. Biol. 2*, 388.

11 Garavito, R. M., Picot, D., & Loll, P. J. (1994) *Curr. Opin. Struct. Biol. 4*, 529.

12 Dunford, H. B. (1991) in *Peroxidases in Chemistry and Biology* (Everse, J., Everse, K. E., & Grisham, M. B., Eds.,) Vol. II, pp 1-24, CRC Press: Boca Raton, FL.

13 Poulos, T. L. (1993) *Curr. Opin. Biotech. 4*, 484.

14 Poulos, T. L., Freer, S. T., Alden, R. A., Edwards, S. L., Skogland, U., Takio, K., Eriksson, B., Xuong, N. H., Yonetani, T., & Kraut, J. (1980) *J. Biol. Chem. 255*, 575.

15 Bosshard, R. H., Anni, H., & Yonetani, T. (1991) in *Peroxidases in Chemistry and Biology* (Everse, J., Everse, K. E., & Grisham, M. B., Eds.,) Vol. II, pp 51-84, CRC Press: Boca Raton, FL.

16 Holzbaur, I. E., English, A. M., & Ismail, A. A. (1996) *Biochemistry 35*, 5488.

17 Smith, A. T., Santama, N., Dacey, S., Edwards, M., Bray, R. C., Thorneley, R. N. F., & Burke, J. F. (1990) *J. Biol. Chem. 265*, 13335.

18 Dawson, J. E. (1988) *Science 240*, 433.

19 Sivaraja, M., Goodin, D. B., Smith, M., & Hoffman, B. M. (1989) *Science 245*,

738.

20 Patterson, W. R., Poulos, T. L., & Goodin, D. B. (1995) *Biochemistry 34,* 4342.

21 Fishel, L. A., Villafranca, J. E., Mauro, J. M., & Kraut, J. (1987) *Biochemistry 26,* 351.

22 Veitch, N. C. & Williams, R. J. P. (1990) *Eur. J. Biochem. 189,* 351.

23 Edelhoch, H. (1967) *Biochemistry 6,* 1948.

24 Fox, T., Tsaprailis, G., & English, A. M. (1994) *Biochemistry 33,* 186.

25 Pappa, H. S., & Cass, A. E. G. (1993) *Eur. J. Biochem. 212,* 227.

26 Das, T. K., & Mazumdar, S. (1995) *Eur. J. Biochem. 227,* 823.

27 Sievers, G. (1978) *Biochim. Biophys. Acta 536,* 212.

28 Pace, C. N., Shirley, B. R., & Thomson, J. A. (1990) in *Protein Structure. A Practical Approach* (Creighton, T. E., Ed.,) pp 311-330, IRL Press at Oxford University: Oxford, England.

29 Pace, C. N. (1986) *Methods Enzymol. 131,* 266.

30 Hughson, F. M., & Baldwin, R. L. (1989) *Biochemistry 28,* 4415.

31 Betz, S. F., & Pielak, G. J. (1992) *Biochemistry 31,* 12337.

32 Pace, C. N. (1990) *Trends Biotechnol. 8,* 93.

33 Willis, K. J., Szabo, A. G., Zuker, M., Ridgeway, J. M., & Alpert, B. (1990) *Biochemistry 29,* 5270.

34 Burnstein, E. A., Vedenkina, N. S., & Ivkova, M. N. (1973) *Photochem. Photobiol. 18,* 263.

35 Rainer, J., & Rainer, R. (1990) in *Protein Structure: A Practical Approach* (Creighton, T. E., Ed.,) pp 191-223, IRL Press at Oxford University: Oxford, England.

36 Creighton, T. E. (1990) in *Protein Structure: A Practical Approach* (Creighton, T. E., Ed.,) pp 155-167, IRL Press at Oxford University: Oxford, England.

36 Creighton, T. E. (1993) in *Proteins: Structure and Molecular Properties,* W.H. Freeman and Company: New York, NY.

37 Garel, J. -R. (1992) in *Protein Folding* (Creighton, T. E., Ed.,) pp 405-454, Freeman: New York, NY.

38 Beechem, J. M., & Brand, L. (1985) *Annu. Rev. Biochem. 54,* 43.

39 Ugarova, N. N., Savitski, A. P., & Berezin, I. V. (1981) *Biochim. Biophys. Acta 662,* 210.

40 Moosavi-Movahedi, A. A., & Nazari, K. (1995) *Int. J. Biol. Macromol. 17,* 43.

41 Irace, G., Bismuto, E., Savy, F., & Colonna, G. (1986) *Arch. Biochem. Biophys. 244,* 459.

42 Takio, K., & Yonetani, T. (1980) *Arch. Biochem. Biophys. 203,* 605.

43 Matthews, C. R., & Crisanti, M. M. (1981) *Biochemistry 20,* 784.

44 Murphy, K. P., & Freire, E. (1992) *Adv. Protein Chem. 41,* 313.

45 Hayne, D. T., & Freire, E. (1993) *Proteins: Struct., Funct., Genet. 16,* 115.

46 Kresheck, G. C., & Erman, J. E. (1988) *Biochemistry 27,* 2490.

47 van Stokkum, I. H. M., Linsdell, H., Hadden, J. M., Haris, P. I., Chapman, D., & Bloemendal, M. (1995) *Biochemistry 34,* 10518.

48 Gross, T. M., & Erman, J. E. (1985) *Biochim. Biophys. Acta 830,* 140.

49 Welinder, K. G. (1979) *Eur. J. Biochem. 96,* 483.

50 Huddleston, S., Robertson, S., Dobson, C., Kwong, F. Y. P., & Charalmbous, B. M. (1995) *Biochem. Soc. Trans. 23,* 108S.

51 Haschke, R. H., & Friedhoff, J. M. (1978) *Biochem. Biophys. Res. Commun. 80,* 1039.

52 Pahari, D., Patel, A. B., & Behere, D. V. (1995) *J. Inorg. Biochem. 60,* 245.

54 Ogawa, S., Shiro, Y., & Morishima, I. (1979) *Biochem. Biophys. Res. Commun. 90,* 674.

55 Morishima, I., Kurono, M., & Shiro, Y. (1986) *J. Biol. Chem. 261,* 9391.

56 Shiro, Y., Nurono, M., & Morishima, I. (1986) *J. Biol. Chem. 261,* 9382.

57 Rodríguez Marañón, M. J., Stillman, M. J., & van Huystee, R. B. (1993) *Biochem. Biophys. Res. Commun. 194,* 326.

58 Doyle, W. A., & Smith, A. T. (1995) *Biochem. J. 315,* 15.

59 Tams, J. W., & Welinder, K. G. (1996) *Biochemistry 35,* 7573.

60 Bonagura, C. A., Sundaramoorthy, M., Pappa, H. S., Patterson, W. R., & Poulos, T. L. (1996) *Biochemistry 35,* 6107.

61 Miller, M. A., Shaw, A., & Kraut, J. (1994) *Nature Struct. Biol. 1,* 524.

62 Pace, C. N., Grimsley, G. R., Thomson, J. A., & Barnett, B. J. (1988) *J. Biol. Chem. 263,* 11820.

63 Lecomte, J. T. J., Kao, Y., & Cocco, M. J. (1996) *Proteins: Struct., Funct., Genet. 25,* 267.

64 Takano, T. (1977) *J. Mol. Biol. 110,* 537.

65 Gazaryan, I. G., Doseeva, V. V., Galkin, A. G., & Tishkov, V. I. (1994) *FEBS Lett. 354,* 248.

66 Tanford, C. (1964) *J. Am. Chem. Soc. 86,* 2050.

67 Rowe, E. S., & Tanford, C. (1973) *Biochemistry 12,* 4822.

68 Pace, C. N., & Vanderburg, K. E. (1979) *Biochemistry 18,* 288.

69 Perry, L. J., & Wetzel, R. (1984) *Science 226,* 555.

70 Pantoliano, M. W., Landner, R. C., Bryan, P. N., Rollence, M. L., Wood, J. F., & Poulos, T. L. (1987) *Biochemistry 26,* 2077.

71 Matsamura, M., Becktel, W. J., Levitt, M., & Matthews, B. W., (1989) *Proc. Natl. Acad. Sci. U.S.A. 86,* 6562.

72 Gusev, N. B., Grabarek, Z., & Gergely, J. (1991) *J. Biol. Chem. 266,* 16622.

73 Kanaya, S., Katsuda, C., Kimura, S., Nakai, T., Kitakuni, E., Nakamura, H., Katayamagi, K., Morikawa, K., & Ikehara, M.(1991) *J. Biol. Chem. 266,* 6038.

74 Alonso, D. O. V, & Dill, K. A. (1991) *Biochemistry 30,* 5974.

75 Privalov, P. L. (1992) in *Protein Folding* (Creighton, T. E., Ed.,) pp 243-300, Freeman: New York, NY.

76 Griko, Y. V., Venyaminov, S. Y., & Privalov, P. L. (1989) *FEBS Lett. 244,* 276.

77 Pakula, A. A., & Sauer, R. T. (1989) *Proteins: Struct., Funct., Genet. 5,* 202.

78 Ryan, O., Smyth, M. R., & Ó Fágáin, C. (1994) *Enzyme Microb. Technol. 16,* 501.

79 Djavadi-Ohaniance, L., Rudin, Y., & Schatz, G. (1978) *J. Biol. Chem. 253,* 4402.

80 Kahn, P. C. (1979) *Methods Enzymol. 61,* 339.

CHAPTER 3

EFFECTS OF CYANIDE LIGATION ON THE CONFORMATIONAL STATES OF CYTOCHROME *c* AND HORSERADISH PEROXIDASES IN DENATURANTS

ABSTRACT

The effects of cyanide ligation on the conformational states of cytochrome *c* and horseradish peroxidases in denaturants were examined using fluorescence and UV circular dichroism (UV/CD). The denaturant-induced unfolding curves of cyanide-ligated recombinant ferric cytochrome *c* peroxidase (CCP-CN) in urea and cyanide-ligated horseradish peroxidase (HRP-CN) in guanidine hydrochloride (GdHCl) as monitored by UV/CD are sigmoidal and similar to those obtained for the unligated ferric forms, CCP(MI) and HRP (Chapter 2), revealing that cyanide ligation leads to little change in secondary structure stabilization. However, in contrast to the steady-state fluorescence monitored unfolding of CCP(MI) and HRP, no intermediates were observed in the CCP-CN and HRP-CN unfolding curves, but the Soret absorption spectra of CCP-CN reveal the presence of an unfolding intermediate with a blue-shifted Soret maximum. Under refolding conditions, denatured CCP(MI) captures hemindicyanide as the polypeptide refolds, but secondary structure reformation appears to be less cooperative than the unfolding transition. Only ~ 30% HRP-CN reforms in the presence of ~ 1 mM KCN, presumably because free CN^- breaks the disulfide bonds which are essential structural elements in the folding of HRP. Also, hemindicyanide appears to non-specifically bind to the denatured HRP polypeptide which, combined with the effects of CN^-, alters the mechanism of holoenzyme formation from that observed for unligated HRP.

Cyanide ligation confers kinetic stability to CCP-CN which unfolds ~ 7-fold

more slowly in 8 M urea/1 mM KCN at pH 7.0 ($t_{½}$ = 107 s) compared to unligated [CCP(MI)]. In contrast, HRP-CN unfolds 5-fold faster ($t_{½}$ = 93.9 s) in 6 M GdHCl/1 mM KCN at pH 7.0 than unligated HRP. The folded form of HRP-CN appears to be thermodynamically stabilized in the presence of ~ 1 mM KCN but excess CN^- causes the unfolded form to aggregate, presumably as a result of cyanide-induced disulfide cleavage

INTRODUCTION

As with other heme peroxidases, small inorganic ligands such as HF and HCN bind reversibly to the ferric iron of cytochrome *c* peroxidase (CCP) and HRP.[1,2] The binding kinetics and properties of HRP-CN and yeast CCP-CN have been studied using a variety of spectroscopic probes.[1-12] It is generally accepted that HCN binds to HRP and CCP to form the CN^- adduct and a proton simultaneously binds to the distal His to form the imidazolium side chain which H-bonds strongly to the CN^- ligand.[2,4,13-15] The structure of yeast CCP-CN has been determined,[16] and reveals 0.3-Å movement of the distal Arg48 away from the CN^- ligand plus rearrangement of water molecules in the distal cavity. More recently, the structure of ARP-CN shows that cyanide binding also causes movement of the protonated distal His56 to within H-bonding distance of the CN^- ligand.[17]

The recent X-ray structure of peanut peroxidase (PNP)[18] serves as an excellent

model for HRP until its structure becomes available. Nonetheless, in the absence of a published X-ray structure of HRP to date,[19] investigators have focused on the use of techniques such as FTIR,[20] NMR[10,21] and RR[22-24] to provide information on the structure of HRP, as well as on key residues near the distal and proximal sides of the heme. For example, RR studies have been very useful in showing that the heme of HRP coexists in a five- and six-coordinate high-spin state.[23,25] Furthermore, combined RR data from recombinant HRP and CCP(MI) distal-heme-cavity mutants [F41V, F41W, R38K in HRP and R48L, R48K, W51F, H52L in CCP(MI)], have demonstrated that the distal heme pocket architecture of the 2 peroxidases is not identical since differences are observed in the porphyrin skeletal vibrational modes above 1450 cm^{-1}.[23,25,26] However, the distal- and proximal-heme H-bonding network appears to be similar in both proteins.[27,28]

Knowledge of the conformational properties of a protein is important in understanding its function. In this study, the effects of cyanide ligation on the conformational stability in denaturants of CCP(MI) and HRP were examined. The unfolding mechanisms of CCP-CN in urea and HRP-CN in GdHCl were investigated at pH 7.0 by monitoring protein steady-state fluorescence and backbone UV/CD changes. Furthermore, the rates of unfolding in denaturants were determined by fluorescence, and the equilibrium and kinetic data are compared to those obtained for the unligated peroxidases.[29]

EXPERIMENTAL PROCEDURES

Denaturation of CCP-CN and HRP-CN as Monitored by Steady-State Fluorescence. Fluorescence was carried our as described previously.[29] KCN (~ 1 mM) was added to 5 μM CCP(MI) and 10 μM HRP stock solutions to yield the cyanide-bound forms (CCP-CN and HRP-CN). Following dilution into urea and GdHCl, respectively, CCP-CN and HRP-CN were allowed to denature over 20 - 24 h at ambient temperature prior to recording the fluorescence spectra. The protein concentrations used in the fluorescence measurements were 1 μM CCP-CN and 2 μM HRP-CN. The emission of the blank (denaturant in buffer) was subtracted from that of the protein samples prior to integration. The steady-state fluorescence intensities of CCP-CN were standardized to 7 μM NATA and those of HRP-CN to a solution containing 2 μM NATA and 10 μM NAYA.[29] KCN was also added to the Trp (NATA) and Tyr (NAYA) standard solutions and the integrated intensity obtained for the standards under identical conditions was taken to be 100%.

To investigate renaturation, stock solutions of ~ 15 μM CCP-CN and 30 μM HRP-CN were incubated for 20 - 24 h in 8 M urea with ~ 1 mM KCN (urea/KCN) and 6 M GdHCl with ~ 1 mM KCN (GdHCl/KCN), respectively. Following incubation, the samples were diluted to give the desired final concentration of denaturant and protein, and incubated for another 20 - 24 h before the fluorescence spectra were recorded as described above.

Steady-state fluorescence was also used to study the time-dependent unfolding

of the cyanide-ligated peroxidases. CCP-CN (5 μM) and HRP-CN (10 μM) were diluted 5-fold into 8 M urea and 6 M GdHCl (pH 7.0), respectively, and the fluorescence intensity at 350 nm was monitored following rapid manual mixing. The excitation wavelength was 280 nm and the emission and excitation slits were 5 nm. The fluorescence intensity vs time data were fitted by a single exponential.

Denaturation of CCP-CN and HRP-CN as Monitored by UV/CD. Stock protein solutions of ~ 30 μM CCP-CN and HRP-CN were prepared in 100 mM sodium phosphate buffer (pH 7.0) with ~ 1 mM KCN. The final protein concentration in denaturant was ~ 6 μM for the UV/CD measurements which were performed as previously described.[29] The reversibility of denaturation was also probed by UV/CD. Stock solutions of ~ 90 μM CCP-CN and 30 - 160 μM HRP-CN were denatured in 8 M urea/KCN (pH 7.0) and 6 M GdHCl/KCN (pH 7.0), respectively, and after 20 - 24 h the solutions were diluted to ~ 5 μM protein and the desired denaturant concentration.

Analysis of the Transition Curves. The transition curves were analyzed by the same methods that have been outlined previously.[29] Briefly, the unfolding curves of CCP-CN and HRP-CN were analyzed according to the method of Pace et al.[30] based on a two-state transition,

$$N \rightleftharpoons U$$

where N and U are the native and unfolded forms of the protein, respectively. $\Delta G_{d,aq}$, which represents the free energy in aqueous solutions in the absence of denaturant and defines the conformational stability of a protein,[31] was obtained from nonlinear least-squares analysis of the raw data,[32,33] as was the m value.[34]

RESULTS

Denaturation of CCP-CN and HRP-CN as Monitored by Steady-State Fluorescence. Relief of heme quenching of Trp fluorescence[35] occurs on protein unfolding. As well as an increase in the steady-state fluorescence intensity, the emission maximum red shifts in the denatured state.[36] We have shown that on excitation at 280 nm, the steady-state fluorescence of denatured CCP(MI) is due to its 7 Trps[37] while that of denatured HRP is attributed to its 1 Trp and 5 Tyrs.[29] The CN-ligated peroxidases also exhibit an increase in steady-state fluorescence and a red shift in emission maximum to ~ 350 nm when incubated in denaturants.

Figure 3.1A summarizes the integrated fluorescence intensity of CCP-CN relative to NATA as a function of urea concentration. It can be seen that CCP-CN exhibits cooperative unfolding between 5 and 6 M urea, but relief of fluorescence quenching also occurs at low urea concentrations. The relative fluorescence in 8 M urea at pH 7.0 is ~ 70 % which is similar to that reported for unligated CCP(MI).[29] Figure 3.1B shows the relative fluorescence of HRP-CN in 0 - 6 M GdHCl at pH 7.0.

Figure 3.1 Relative integrated fluorescence (300 - 450 nm) intensities at pH 7.0 of **(A)** 1 μM CCP-CN vs urea concentration; **(B)** 2 μM HRP-CN vs GdHCl concentration. The intensities are plotted relative to 7 μM NATA for CCP-CN and 2 μM NATA/10 μM NAYA for HRP-CN. KCN (~ 1 mM) was added to the samples and standards prior to the fluorescence measurements. Excitation wavelength 280 nm; slits 5 nm; scan rate 102 nm/min. The solid lines show the fit of the data by non linear least-squares analysis.[32,33]

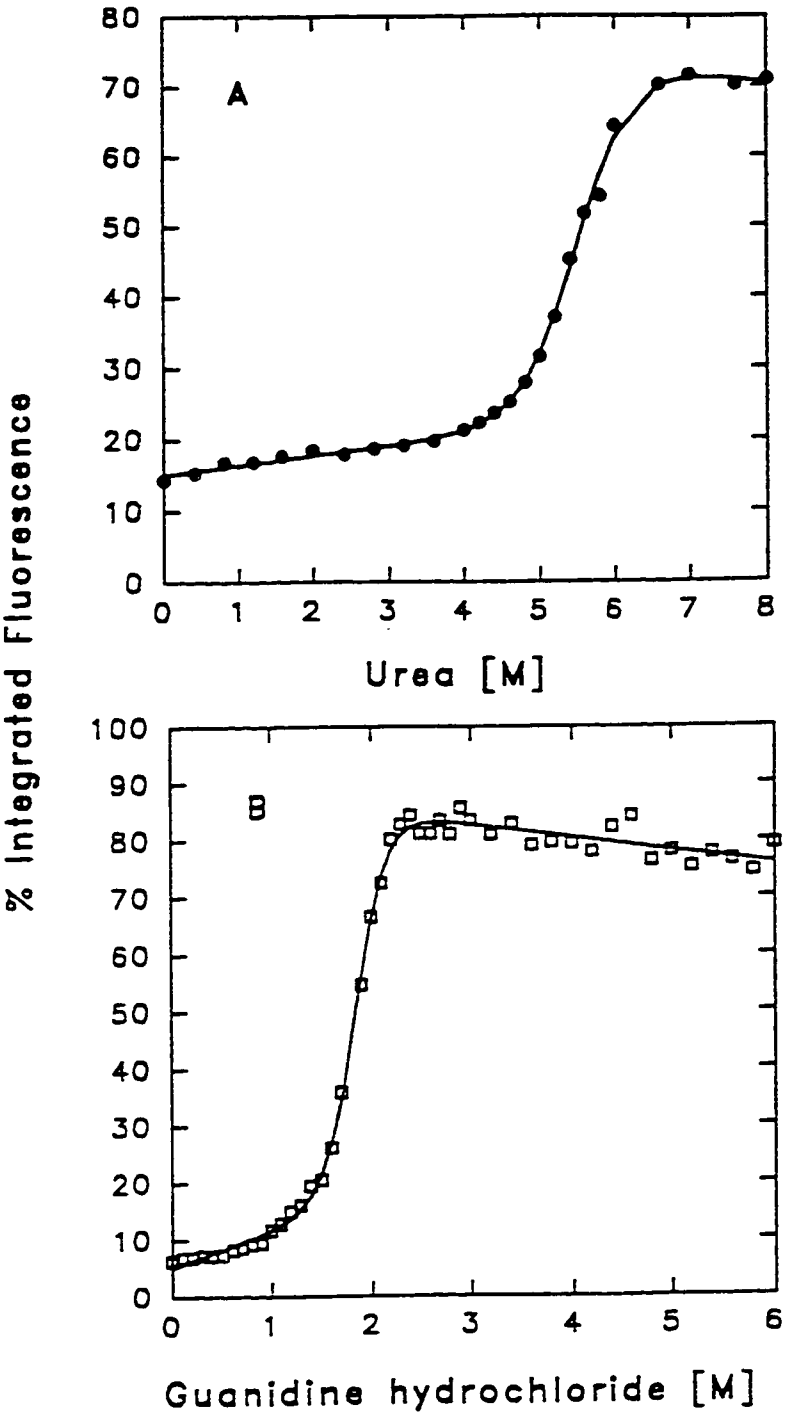
A
B
% Integrated Fluorescence
Urea [M]
Guanidine hydrochloride [M]

Unlike HRP, where relief of heme fluorescence quenching begins above 0.3 M GdHCl,[29] HRP-CN exhibits essentially constant fluorescence between 0 - 1 M GdHCl. The denatured form in 6 M GdHCl has ~ 80 % relative fluorescence compared to ~ 75% for unligated HRP.[29]

Uptake of Hemindicyanide as Monitored by Steady-State Fluorescence. Changes in fluorescence intensities due to the uptake of hemindicyanide on refolding of the peroxidases are shown in Figure 3.2. Previously, we have shown by steady-state fluorescence and UV/CD that heme uptake by CCP(MI) occurs simultaneously with secondary and tertiary structure formation.[29] The refolding of the apoprotein in the presence of ~ 1 mM KCN as probed by fluorescence suggests that different denaturation and renaturation mechanisms exist since the shapes of the curves are clearly different (Figure 3.1A and 3.2A). This is not surprising since renaturation most likely involves uptake of hemindicyanide (see below).

The steady-state fluorescence-monitored renaturation profile of HRP-CN is also different from that of unligated HRP. Previously, we have shown that in the absence of KCN the polypeptide of apoHRP refolds prior to heme capture.[29] From Figure 3.2B, which shows the integrated fluorescence intensity during refolding of denatured HRP-CN in the presence of ~ 1 mM KCN, it is evident that hemindicyanide entrapment by the apoprotein in GdHCl/KCN is inefficient since the fluorescence intensity remains high even in 0.2 M GdHCl.

The Soret absorption of CCP-CN and HRP-CN in buffer, and after unfolding

Figure 3.2 Integrated fluorescence (300 - 450 nm) intensity at pH 7.0 during refolding in the presence of ~ 1 mM KCN of (**A**) 1 μM CCP-CN and (**B**) 1 μM HRP-CN. Excitation 280 nm; slits 5 nm; scan rate 102 nm/min.

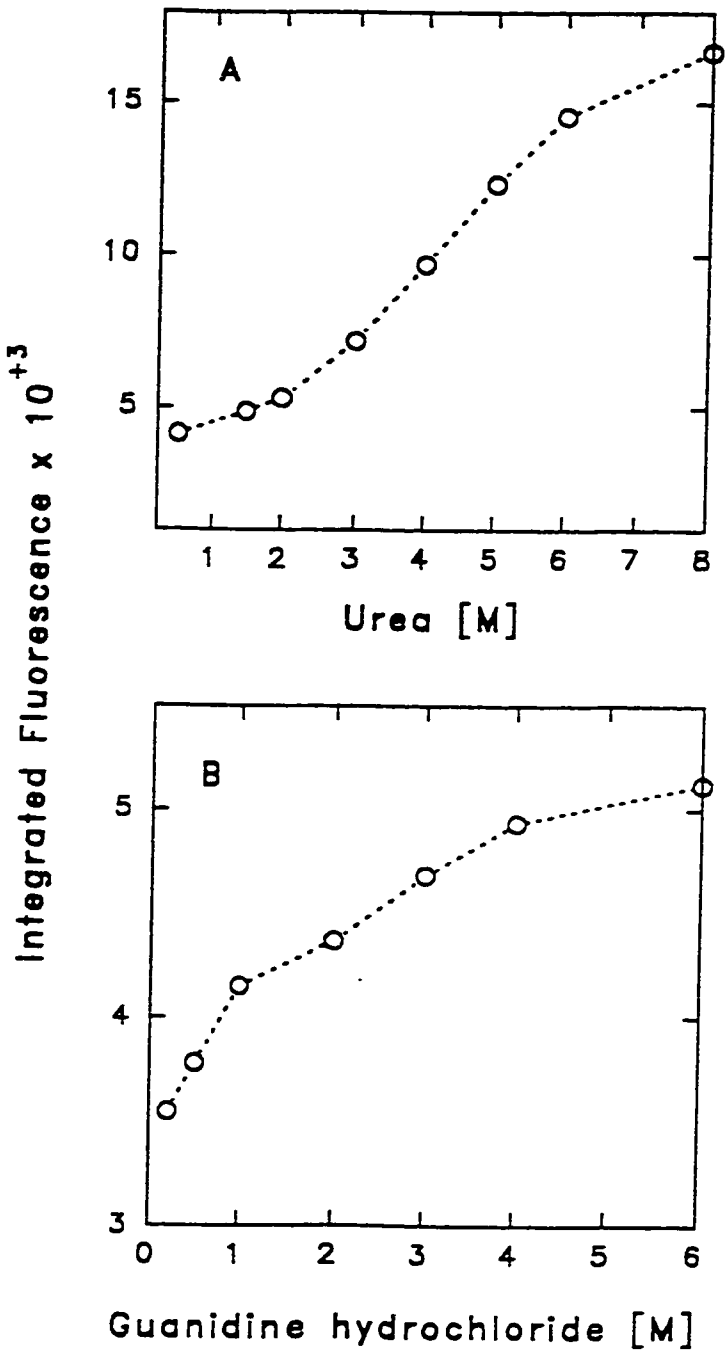
A
15
10
5
1
2
3
4
5
6
7
8
Urea [M]
Integrated Fluorescence x 10+3
B
5
4
3
0
1
2
3
4
5
6
Guanidine hydrochloride [M]

and refolding are compared in Figure 3.3. The spectrum of CCP-CN in 8 M urea/KCN is similar to that of the free prosthetic group (Figure 3.3A, C), indicating hemindicyanide formation upon CCP-CN denaturation. However, the spectrum of the refolded protein in 0.5 M urea is not identical to that of CCP-CN in buffer, suggesting that different forms of the enzyme-cyanide complex exist in low urea and buffer. CCP-CN samples undergoing denaturation also show a blue shift of the Soret maximum to 420 nm between 3 and 5.5 M urea while above 5.5 M urea, the Soret maximum returns to 424 nm. The variation in the Soret band reveals the existence of an unfolding intermediate which resembles the alkaline form of CCP-CN since a heme-linked pH-dependent isomerization of yeast CCP-CN results in a shifting of the Soret maximum from 426 at pH 6.0 to 421 nm at pH 9.0.[2]

Hemindicyanide formation upon HRP-CN denaturation in 6 M GdHCl/KCN is also suggested from a comparison of the Soret spectra in Figures 3.3B and C. However, a red shift of the Soret maximum to 426 nm is observed in 6 M GdHCl/KCN, suggesting that hemindicyanide may be associated non-specifically with hydrophobic regions of the HRP polypeptide (Figure 3.3B) since a Soret maximum at $\geq$ 426 nm is observed when hemindicyanide is incorporated into liposomes.[38,39] Figure 3.3B shows the Soret absorption of HRP in 0.2 M GdHCl after refolding and, although the spectrum is the same as that of HRP-CN in buffer, the intensity is significantly reduced. This is attributed to the fact that only ~ 30% of the apoprotein correctly refolds in the presence of ~ 1 mM KCN, consistent with the fluorescence data which

Figure 3.3 Soret absorption at pH 7.0 of **(A)** 5.8 μM CCP-CN (——) in 100 mM sodium phosphate buffer, 5.2 μM refolded CCP-CN (– – – –) in 0.5 M urea, and 5.2 μM unfolded CCP-CN (— ·· —) in 8 M urea; **(B)** 7.0 μM HRP-CN (——) in 100 mM sodium phosphate buffer, 6.0 μM refolded HRP-CN (– – – –) in 0.5 M GdHCl, and 6.0 μM HRP-CN unfolded HRP-CN (— ·· —) in 6 M GdHCl, and **(C)** 1.2 μM hemindicyanide in 100 mM sodium phosphate buffer (——), 0.56 μM hemindicyanide in 6 M GdHCl (— ·· —) and 1.1 μM hemindicyanide in 8 M urea (– – – –). Pathlength 1 cm.

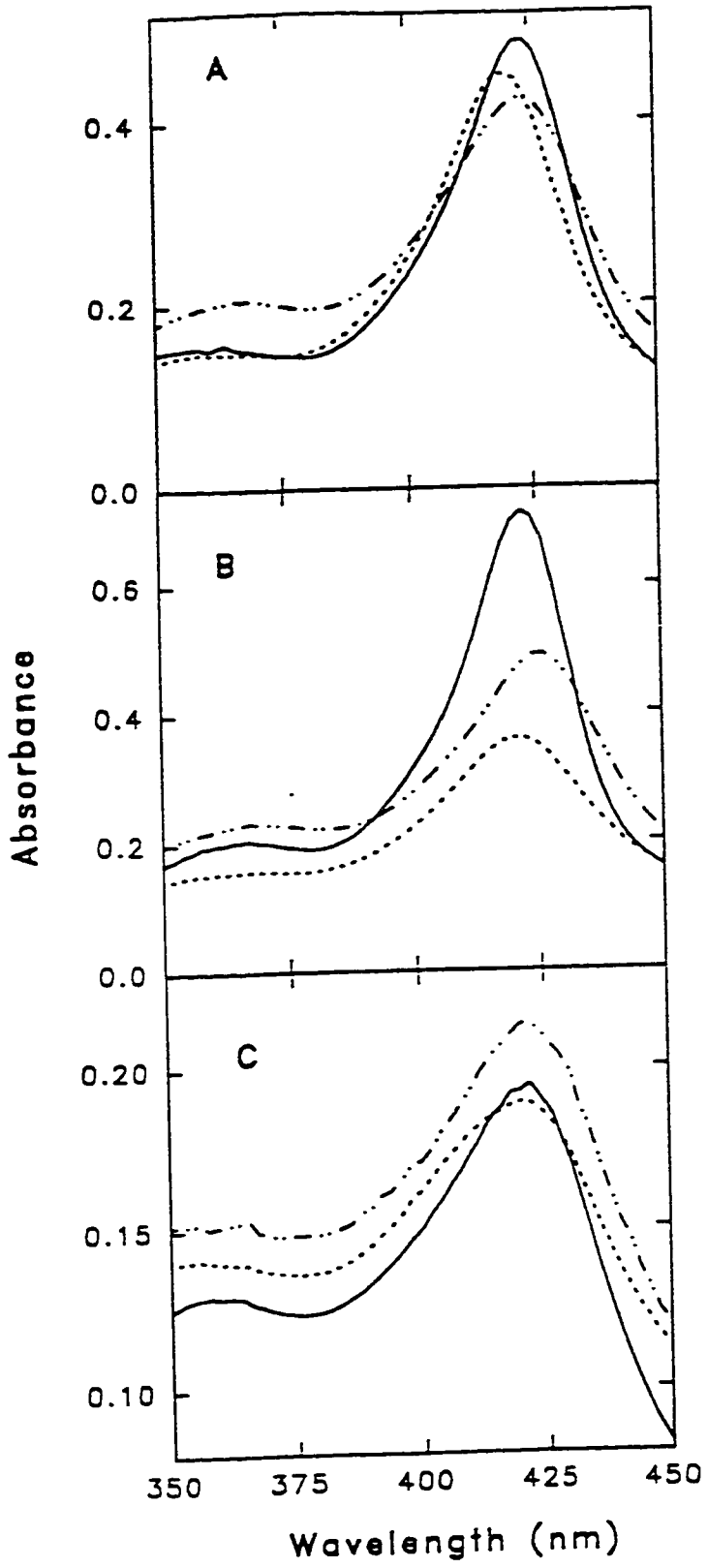
A
B
C
0.4
0.2
0.0
0.6
0.4
0.2
0.0
0.20
0.15
0.10
Absorbance
350
375
400
425
450
Wavelength (nm)

reveal only ~ 30% heme quenching on refolding (Figure 3.2B).

Denaturation of CCP-CN and HRP-CN as Monitored by UV/CD. The loss in ellipticity of the backbone absorption of CCP-CN in urea and HRP-CN in GdHCl at pH 7.0 is shown in Figure 3.4. Both cyanide-ligated peroxidases unfold in an apparent two-state process. Loss of secondary structure in CCP-CN occurs between ~ 4 and 6 M urea (Figure 3.4A), and between ~ 1.5 and 2.2 M GdHCl in HRP-CN (Figure 3.4B). These denaturant concentrations bracket the regions of cooperative unfolding detected by steady-state fluorescence (Figure 3.1).

Backbone refolding of CCP-CN and HRP-CN was also monitored by the change in ellipticity at 222 nm and is shown in Figure 3.5. Like the fluorescence unfolding (Figure 3.1A) and refolding (Figure 3.2A) curves of CCP-CN, the UV/CD-monitored curves are also not superimposable. Previously, we have shown that refolding of the CCP(MI) backbone is coincident with heme capture, resulting in essentially superimposable fluorescence and UV/CD unfolding and refolding curves.[29] Refolding of CCP-CN from 8 M urea/KCN requires cleavage of 1 of the axial Fe^{III}-CN bonds in hemindicyanide to reform holoCCP-CN with a proximal His175 ligand. Since the polypeptide-unfolding and refolding curves of CCP-CN are non-coincidental, heme-ligand exchange must *succeed* secondary structure formation as discussed below. The backbone UV/CD denaturation and renaturation curves of HRP-CN (Figure 3.5B) indicate that ~ 30% of the ellipticity is regained on transferring denatured HRP-CN from 6 to 1 M GdHCl. This suggests that either the protein possesses 30% secondary

Figure 3.4 Molar ellipticity at 222 nm at pH 7.0 in the presence of ~ 1 mM KCN of (**A**) 5.8 μM CCP-CN in urea; (**B**) 6.5 μM HRP-CN in GdHCl. The solid lines show the fit of the data by nonlinear least-squares analysis.[32,33] The UV/CD conditions are described in the text.

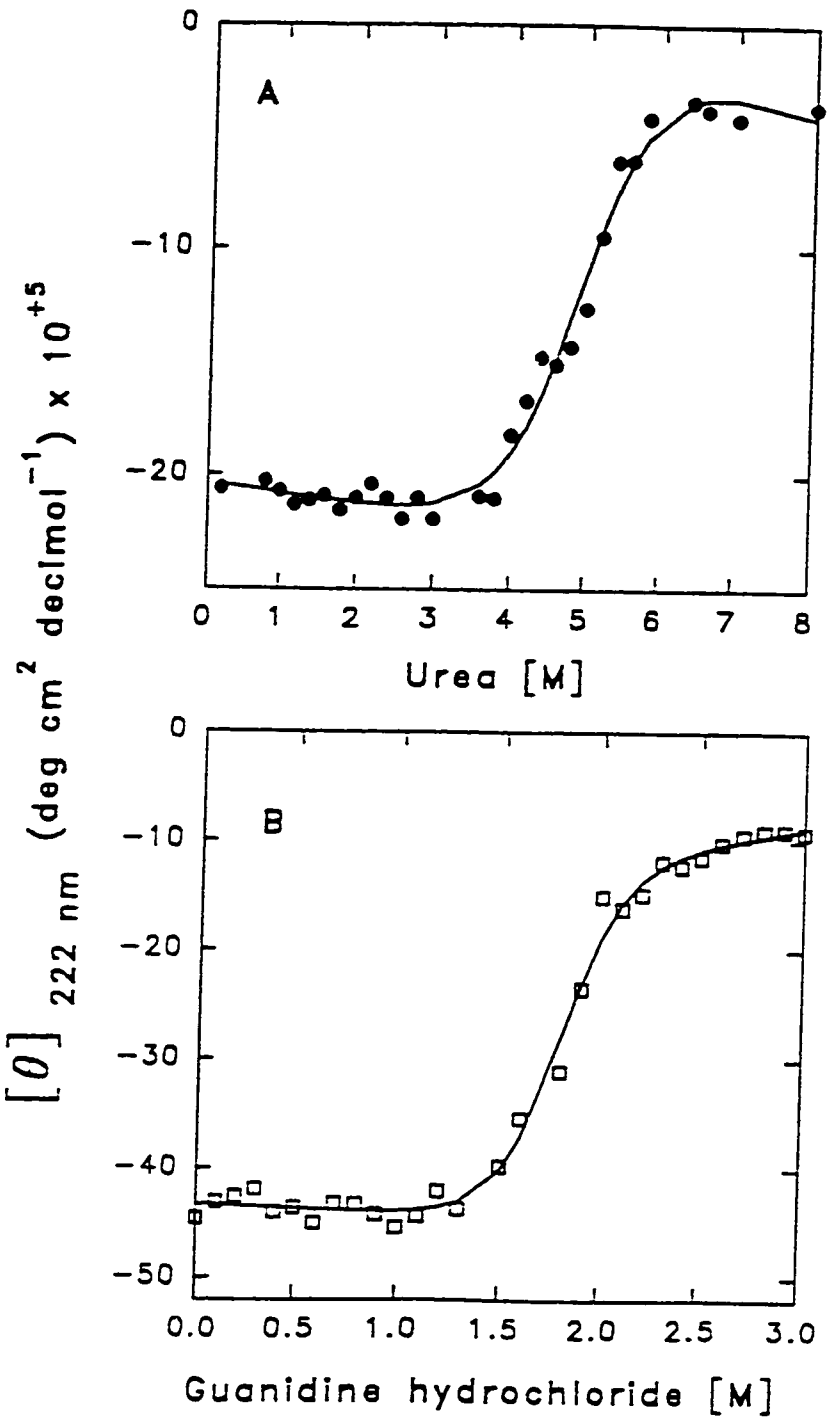
A
B
0
−10
−20
−30
−40
−50
0 1 2 3 4 5 6 7 8
Urea [M]
0.0 0.5 1.0 1.5 2.0 2.5 3.0
Guanidine hydrochloride [M]
[θ] 222 nm (deg cm² declmol⁻¹) x 10⁺⁵

Figure 3.5 Molar ellipticity at 222 nm at pH 7.0 of (A) 5.2 μM CCP-CN during refolding in urea and (B) 2.1 μM HRP-CN during refolding in GdHCl. The UV/CD conditions are described in the text with the exception that in (B), a 0.1-cm cell was used.

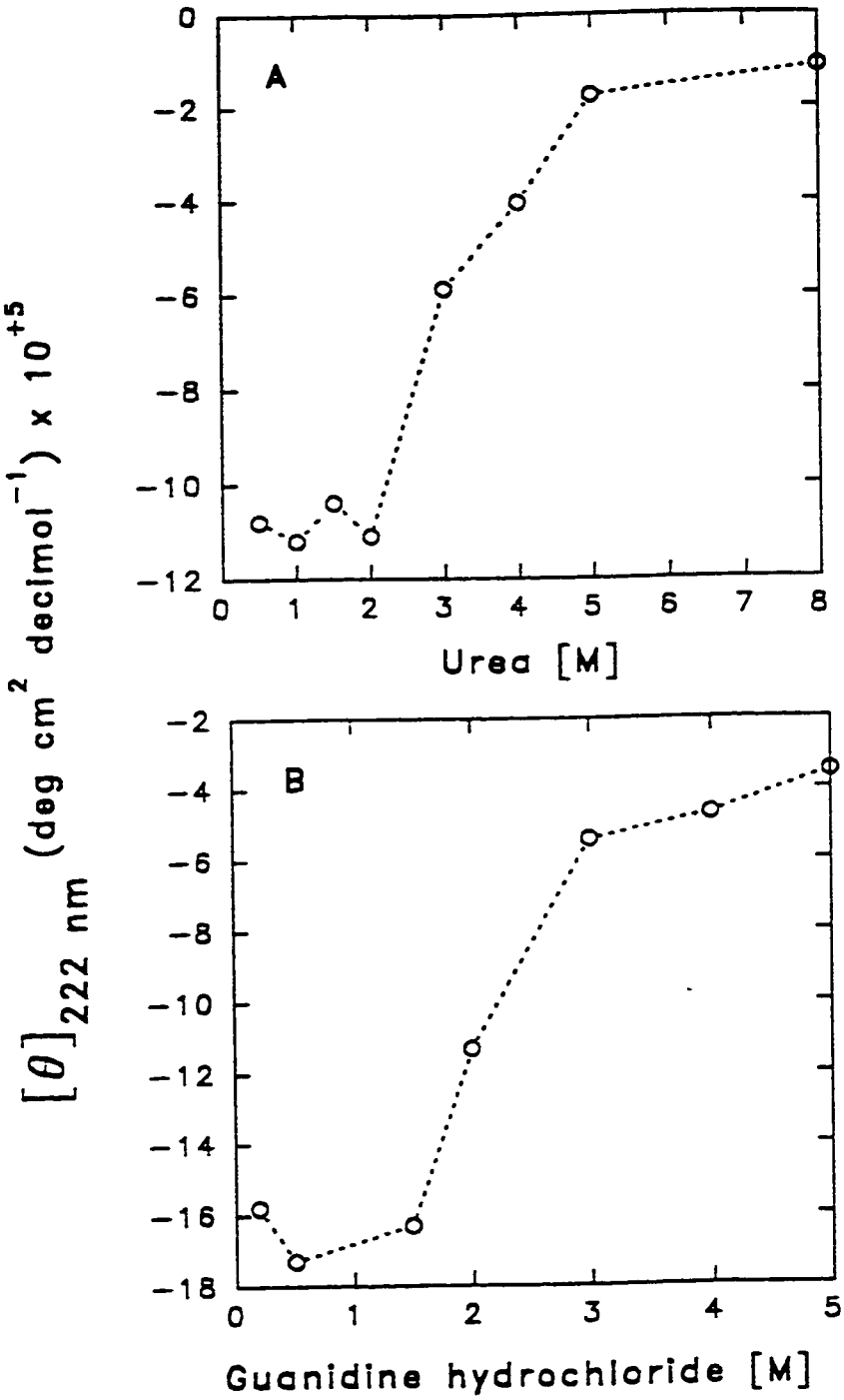
A
B
$[\theta]_{222\ nm}$ (deg cm^2 decimol^{-1}) x 10^{+5}
Urea [M]
Guanidine hydrochloride [M]

structure in the presence of KCN or that 30% of the molecules refold completely. The latter, however, is more likely based on the identical Soret absorption spectra (Figure 3.3B) of HRP-CN in buffer and refolded HRP-CN in 0.2 M GdHCl, except that the intensity of the latter is ~ 30% that of the former. Also, only ~ 30% quenching is observed in 0.2 M GdHCl after refolding (Figure 3.2B), relative to that observed during unfolding (Figure 3.1B). The high concentration of HRP-CN stock solutions (≥ 30 μM) required for the UV/CD experiments resulted in protein precipitation in 6 M GdCHl/KCN. Following centrifugation and removal of GdHCl on a C_{18} HPLC column, a total protein assay[40] was performed, which revealed that 31 ± 5% of HRP-CN remained in solution. This is in agreement with the estimate of the renatured HRP-CN from both UV/CD (Figure 3.5B) and fluorescence (Figure 3.2B).

Thermodynamic and Kinetic Parameters for CCP-CN and HRP-CN Unfolding. The fluorescence and UV/CD unfolding curves were analyzed based on a two-state ($N \rightleftharpoons U$) transition and the thermodynamic parameters are presented in Table 3.1. The binding of cyanide to HRP results in a $\Delta G_{d,aq}$ = 6.5 kcal/mol as determined by UV/CD, and the value from the fluorescence data is the same within experimental error. Furthermore, similar m and $[D]_{½}$ values are obtained using both conformational probes. The $\Delta G_{d,aq}$ and the m values for HRP-CN are larger than those calculated for unligated HRP (6.5 vs 4.0 kcal/mol and 3.8 vs 2.0 kcal/mol/M), but the denaturant concentrations at half maximum ellipticity/fluorescence ($[D]_{½}$) are approximately the same (~ 1.9 M) for both HRP-CN and HRP (Table 3.1).

Unlike CCP(MI), CCP-CN exhibits a two-state denaturation process as monitored by fluorescence. Hence, the thermodynamic parameters were estimated using both spectroscopic probes, and yielded $\Delta G_{d,aq}$ values of 8.8 and 5.4 kcal/mol for CCP(MI) for the fluorescence and UV/CD data, respectively (Table 3.1). The UV/CD value for CCP-CN is close to that obtained from UV/CD-monitored denaturation of CCP(MI) (6.2 kcal/mol),[29] as is the $[urea]_{½}$ value (4.9 vs 4.2 M) (Table 3.1).

Relative to their unligated forms, kinetic stability and kinetic instability is conferred on CCP(MI) and HRP, respectively, on cyanide binding at pH 7.0. The half-life ($t_{½}$) of CCP-CN unfolding in 8 M urea/KCN (107 s; Table 3.1) is almost an order of magnitude longer than that of CCP(MI), while $t_{½}$ for HRP-CN unfolding in 6 M GdHCl/KCN (93.9 s) is 5.5-fold smaller than that observed for unligated HRP (Table 3.1).

DISCUSSION

Denaturation of CCP-CN. The Soret absorption spectrum of CCP in its resting ferric state is characteristic of a five-coordinate high-spin heme.[41] Cyanide binding to CCP results in a heme which is six-coordinate low-spin with a red-shifted Soret absorption maximum at 421 - 426 nm[2] and characteristic UV/CD absorption.[3] Formation of oxyferryl iron (Fe^{IV}=O) on reaction of resting CCP with H_2O_2 is also accompanied by red shifting of the Soret maximum to 420 nm.[41] The heme UV/CD

Table 3.1 Thermodynamic and Kinetic Parameters for Unfolding of CCP-CN and HRP-CN and their Unligated Forms

Protein	Probe	$\Delta G_{d,aq}$[a] (kcal/mol)	m[a] (kcal/mol/M)	$[D]_{½}$[a] (M)	$t_{½}$[b] (s)
CCP-CN in Urea	UV/CD	5.4 ± 0.3[c] (2)[d]	1.1	4.9	
	F	8.8 ± 0.2[e] (2)[d]	1.6	5.5	107 ± 25[f] (4)[g]
CCP(MI)[h] in Urea	UV/CD	6.2 ± 0.3	1.5	4.2	14.3 ±3.4
HRP-CN in GdHCl	UV/CD	6.5 ± 0.3[c] (4)[d]	3.8	1.7	
	F	6.9 ± 1.3[e] (4)[d]	3.7	1.9	93.9 ± 6.3[i] (3)[g]
HRP[h] in GdHCl	UV/CD	4.0 ± 0.6	2.0	2.0	519 ± 36

[a] Calculated using the nonlinear least-squares analysis method of Hughson and Baldwin[32,33] where T = 298 K. $\Delta G_{d,aq}$ represents the free energy in 0 M denaturant, m the slope of the linear dependence of ΔG_d on denaturant concentration[34], and $[D]_{½}$ the denaturant concentration at the half maximum observed ellipticity or fluorescence. [b] Half-lives were obtained by fitting the fluorescence intensities at 350 nm vs time by first-order kinetics. [c] Calculated using the UV/CD data in Figure 3.4. [d] Number of separate determinations. [e] Calculated using the fluorescence data in Figure 3.1. [f] 1 μM protein in 8 M urea at pH 7.0. [g] Number of observations. [h] From Chapter 2.[29] [i] 2 μM protein in 6 M GdHCl at pH 7.0.

absorption spectra of CCP(MI) and CCP-CN (data not shown) obtained in this study were identical to those previously recorded for the yeast form of the enzyme, reinforcing the accepted view that CCP(MI)[42,43] has similar absorption properties to CCP.

Previously, we have shown that on 280-nm excitation the steady-state fluorescence of denatured CCP(MI) is due to its 7 Trps,[37] and that the protein denatures on incubation with increasing concentrations of urea.[29] The latter results in relief of heme quenching, and the same general effects are observed when CCP-CN is incubated with increasing concentrations of urea at pH 7.0. The unfolding of CCP-CN as examined by intrinsic fluorescence appears to be a simple two-state ($N \rightleftharpoons U$) process with no detectable equilibrium intermediates (Figure 3.1A). This is in sharp contrast to the fluorescence-monitored unfolding of CCP(MI) where a thermodynamically-stable intermediate was observed between 3 and 4 M urea before loss of secondary structure.[29] The $N \rightleftharpoons I$ transition of CCP(MI), which presumably results in coordination of the distal His52 (Figure 3.6) to the heme,[29,44] gives rise to a red shift and sharpening of the Soret absorption. However, Figure 3.3A shows little change in the Soret absorption of CCP-CN under native and denaturing conditions compared to unligated CCP(MI) (Figure 2.4; Chapter 2). Since heme quenching efficiency is determined by the overlap integral of the Trp emission and heme absorption spectra,[45] fluorescence is likely a poor probe of the $N \rightleftharpoons I$ transition in CCP-CN because of little variation in the spectral overlap integral.

As mentioned previously, the Soret absorption of the CCP-CN intermediate

resembles that of the alkaline form since both exhibit Soret maxima at 420 nm. The alkaline form ($pK_a = 7.70$)[46] and the urea-induced intermediate of CCP(MI) also have overlapping Soret maxima at ~ 416 nm. Thus, we speculate that the urea-induced $N \rightleftharpoons I$ transitions resemble the acid $\rightleftharpoons$ alkaline transitions in both CCP(MI) and CCP-CN, and that these transitions arise from partial tertiary structure collapse as proposed previously for the urea-induced $N \rightleftharpoons I$ transition in CCP(MI).[29]

Calorimetry studies[47] revealed 2 mid-point temperatures (T_m) (39 °C and 65 °C) in the thermal denaturation of yeast CCP-CN at pH 8.0. Two T_m values (40 °C and 60 °C) were also observed for unligated yeast CCP, while only 1 T_m (~ 60 °C) was observed for apoCCP.[47] These results indicate that a $N \rightleftharpoons I$ transition occurs in the *thermal* denaturation of *both* yeast CCP and yeast CCP-CN; however, removal of the heme eliminates the thermally-induced $N \rightleftharpoons I$ transition at ~ 40 °C. The amide II' region of the FTIR spectra of CCP(MI) shows that the thermally-induced $N \rightleftharpoons I$ transition involves partial collapse of the tertiary structure prior to secondary structure loss.[20] Since we speculate that the denaturant-induced $N \rightleftharpoons I$ transitions in both CCP(MI) and CCP-CN also arise from partial tertiary structure collapse (which in the former results in a change in heme ligation), a FTIR study of CCP-CN and apoCCP(MI) is warranted to determine the effects of CN^- ligation and heme removal on the polypeptide.

Denaturation of HRP-CN. Binding of cyanide to HRP results in a similar Soret absorption spectrum (Figure 3.2B) to that of yeast CCP-CN.[48] The UV/CD

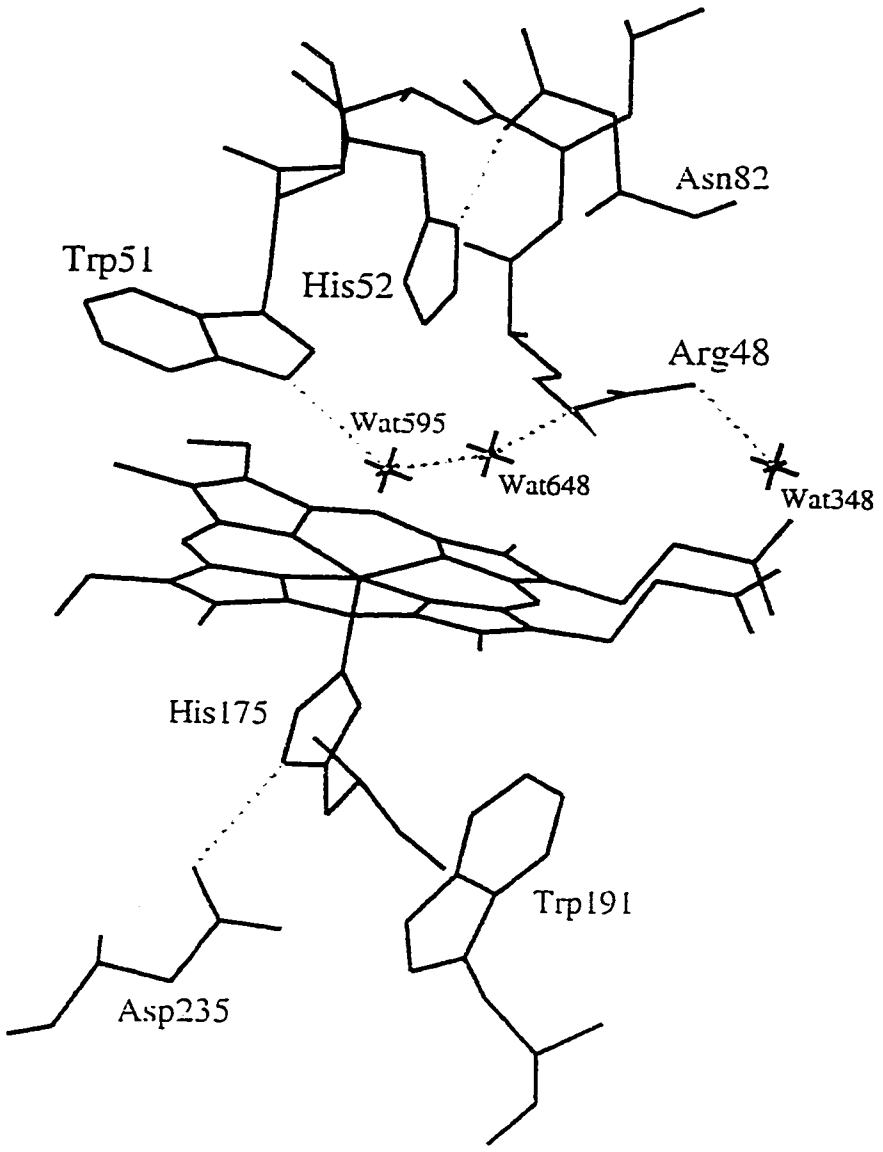

Figure 3.6 Active site of CCP(MI). The dashed lines represent H-bonds between N1 of the distal His52 and the side-chain carbonyl of Asn82, and the N1 of the proximal His175 and the side-chain carboxylate of Asp235. The H-bonds between the distal Arg48 and Trp51 and active-site waters are also shown. This diagram was generated using the X-ray coordinates for the 2.2-Å structure of CCP(MI).[43]

absorption spectrum (250 - 500 nm; not shown) of HRP-CN is identical to that reported,[12] and its steady-state fluorescence spectrum (not shown) is similar to that reported for unligated HRP.[29] The fluorescence-decay characteristics of the single Trp117[49] have been studied for both HRP-CN and unligated HRP by time-resolved fluorescence.[11] Cyanide ligation to HRP increases the picosecond component of the Trp117 fluorescence lifetime from ~ 45 to ~ 60 ps at neutral pH.[11] This significant increase can be accounted for on the basis of changes in Förster energy transfer between the Trp117 donor and the ligated/unligated heme acceptor, which as mentioned above is determined by the overlap integral of the Trp emission and the heme absorption spectra.[45] A study of Trp fluorescence lifetimes in unligated (~ 20 ps) and CN-ligated (~ 28 ps) sperm whale Mb shows that spectral differences also account for most of the observed changes in the Trp-lifetimes.[35]

Both HRP-CN and HRP possess similar (75 - 80%) relative fluorescence in 6 M GdHCl. However, cyanide binding appears to have a stabilizing effect on the protein below 1 M GdHCl (pH 7.0) since unligated HRP exhibits emission increases above 0.3 M GdHCl,[29] which are not observed in Figure 3.1B. Trp fluorescence in heme proteins reports on changes in the fluorophores relative to the heme. Thus, a more stable heme cavity as a result of the extended distal H-bonding network on cyanide binding could explain the decreased sensitivity of HRP-CN to low GdHCl concentrations relative to unligated HRP. Based on the results of recent studies,[23,50] the heme cavity H-bonding network in HRP is expected to be similar to that of CCP (Figure 3.6). On HCN binding, the proton retained in the enzyme-ligand complex is

taken up by the distal His42 which forms a strong H-bond to the CN^- ligand.[21] Recent RR studies of HRP-CN, however, reveal the presence of 2 FeCN conformers and H-bonding of CN^- to both the distal Arg38 and His42 is proposed.[9] A detailed heme-UV/CD analysis of HRP-CN and HRP in 0 - 6 M GdHCl would be of interest since changes around the heme and in its interaction with aromatic residues should be reflected in the CD spectra.[51,52]

Unlike the unligated protein, which undergoes a fluorescence-detectable $I \rightleftharpoons U$ transition following loss of heme and secondary structure above 4 M GdHCl,[29] HRP-CN exhibits a cooperative two-state unfolding process with no accumulation of stable intermediates (Figure 3.1B). Previously, we have shown that the $I \rightleftharpoons U$ transition is absent in DTT-treated HRP as a result of reduction of 1 or more disulfides.[29] Since disulfides are also cleaved by nucleophiles such as cyanide, sulfite, or hydroxide,[53] the absence of an $I \rightleftharpoons U$ transition in HRP-CN in the presence of ~ 1 mM KCN (Figure 3.1B), is not surprising.

Unfolding of the HRP-CN backbone in GdHCl also appears to be a cooperative two-state ($N \rightleftharpoons U$) process as monitored by backbone UV/CD absorbance (Figure 3.4B). A two-state transition is supported by the similarities in the thermodynamic parameters derived from the fluorescence and UV/CD data (Table 3.1). It is suspected that disulfide cleavage by excess free CN^- is responsible for the similarity in the unfolding curves since such similarity was not observed for unligated HRP.[29]

Unlike the backbone of unligated HRP which completely refolds,[29] the backbone of HRP-CN regains only ~ 30% ellipticity under refolding conditions (Figure

3.5B). We speculate this is also due to disulfide cleavage and that the non-crosslinked protein precipitates in 6 M GdHCl/KCN at the high concentrations (30 - 160 μM) used in the UV/CD experiments. Not all the HRP-CN molecules, however, are equally affected by free CN^-, since 31 ± 5% of the total protein remains in solution and must be responsible for the observed increase in 222-nm ellipticity under refolding conditions (Figure 3.5B). Therefore, any apoprotein remaining in solution refolds to yield a Soret spectrum (Figure 3.3B) similar to that of HRP-CN in buffer at pH 7.0.

Uptake of Hemindicyanide by CCP(MI) and HRP. Uptake of heme by denatured CCP(MI) occurs simultaneously with secondary and tertiary structure formation on refolding, while heme capture in HRP occurs only after folding of the polypeptide backbone.[29] In order to reform CCP-CN with a proximal His175 ligand (Figure 3.6), hemindicyanide must be captured by the apoprotein, and ligand-exchange must take place, as discussed above. The kinetics of refolding of horse Mb-CN induced by a urea concentration jump exhibit 3 phases as monitored by fluorescence, 422-nm absorption, far- , near- , and heme-UV/CD absorption.[54] The first phase ($t_{½}$ ~ 7 x 10^{-3} s) involves capture of hemindicyanide by a heme pocket precursor which is ~ 40% helical, followed by secondary and tertiary structure formation around the captured hemindicyanide in the second phase ($t_{½}$ ≈ 0.07 - 0.2 s), and finally a minor structural rearrangement along with heme ligand-exchange in the third phase ($t_{½}$ ≈ 139 - 347 s).[54] A similar mechanism for CCP-CN refolding would be consistent with the non-superimposable fluorescence (Figure 3.1A and 3.2A) and UV/CD (Figure 3.4A

and 3.5A) denaturation and renaturation curves reported here. The data recorded on renaturation, while not extensive, are sufficient to indicate that secondary and tertiary structure formation around the captured hemindicyanide is less cooperative than around hemin. Ligand-exchange after the secondary structure has reformed yields refolded CCP-CN with a Soret maximum at 420 nm in 0.5 M urea (Figure 3.3A).

The fluorescence-monitored entrapment of hemindicyanide by ~ 30% apoHRP (Figure 3.2B) appears to occur over a wide range of GdHCl. This is attributed to partial disulfide cleavage in the fraction of apoHRP which refolds, and also non-specific interactions of hemindicyanide with hydrophobic regions of the polypeptide would result in fluorescence quenching prior to correct heme insertion to reform holoHRP-CN.

Thermodynamic and Kinetic Parameters of CCP-CN and HRP-CN. The conformational stability of a protein that undergoes a reversible two-state $N \rightleftharpoons U$ transition is given by its $\Delta G_{d,aq}$.[31] In the presence of excess free CN^-, neither HRP-CN nor CCP-CN can undergo a two-state ($N \rightleftharpoons U$) transition since conversion of the released heme to hemindicyanide prevents a two-state transition. However, secondary structure unfolding in both ligated peroxidases is reversible and the estimated $\Delta G_{d,aq}$ values are comparable to those estimated for the unligated enzymes CCP(MI) (Table 3.1), suggesting that cyanide binding has little effect on secondary structure stability. Nonetheless, $\Delta G_{d,aq}$ for CCP-CN calculated from the fluorescence data (8.8 kcal/mol) is significantly larger than the UV/CD value and may be a reflection of the increased

thermodynamic stability of the cyanide-ligated heme pocket. The 1.7-Å resolution X-ray structure of CCP[27] reveals a distal H-bonding network involving residues Arg48, Trp51, His52 and active-site waters (Figure 3.6). In addition, His52 in CCP H-bonds to the carboxamide side chain of neighboring Asn82, and this particular H-bond is conserved in all the published peroxidase structures.[18,55-59] In CCP-CN the distal network is extended to include a H-bond between the protonated His52 and the heme-bound cyanide.[8,16,60] NMR studies of the N82D mutant[60] show no H-bonding between His52 and the heme-bound cyanide nor between Asp82 and His52, reinforcing the extent of the distal H-bonding network in unmutated CCP-CN.

The *m* values calculated for the unfolding of CCP-CN in urea and HRP-CN in GdHCl are shown in Table 3.1 and are typical of those seen in the denaturant-induced unfolding of heme proteins.[61] The *m* value of HRP-CN (3.8 kcal/mol/M) is ~ 2-fold larger than unligated HRP (Table 3.1), indicating increased cooperativity of unfolding in HRP-CN. A *m* value of 3.4 kcal/mol/M has also been calculated for CCP(MI) in GdHCl.[29] The available structural data show that the small heme peroxidases are folded into 2 clearly defined domains,[18] and previously we argued that the disulfides might be responsible for a smaller *m* value in HRP compared to CCP(MI).[29] We now speculate that the high cooperativity of unfolding of HRP-CN is due to cyanide-induced cleavage of the *highly* solvent-exposed Cys11-Cys91 disulfide and/or the solvent-exposed Cys97-Cys290 disulfide which covalently links the 2 domains in HRP (see Figure 2.9 of Chapter 2). Although cleavage of former is more likely to occur based on its higher solvent accessibility,[62] cleavage of the latter would likely allow the

2 domains in HRP-CN to unfold in a more cooperative manner.

The unfolding half-lives of CCP-CN in urea and HRP-CN in GdHCl are listed in Table 3.1. The data reveal that cyanide ligation in CCP(MI) confers considerable kinetic stability to the protein, perhaps by stabilizing the conformational flexibility of the heme cavity. Kinetic instability is demonstrated in HRP-CN in the presence of ~ 1 mM KCN, consistent with the proposed loss of disulfide bridges in *folded* HRP-CN. It is of interest that the kinetic stability of DTT-treated-HRP is only marginally decreased ($t_{½}$ ~ 450 s)[29] relative to HRP (Table 3.1), suggesting that disulfide cleavage in HRP-CN by free CN^- is more efficient than DTT reduction, or that DTT and CN^- gain access to different disulfides. In any event, the effects of excess CN^- on crosslinking should be taken into consideration in any spectroscopic or kinetic study on HRP-CN.

ACKNOWLEDGEMENTS

We wish to thank Dr. Mark Miller (UCSD) for providing the *E. coli* transformed with recombinant cytochrome *c* peroxidase used to isolate the CCP(MI) for this study. Craig Fenwick is thanked for many useful discussions. This work was funded by a grant from the Natural Science and Engineering Research Council of Canada (NSERC) to A.M.E.

REFERENCES

1 Ellis, W. D., & Dunford, H. B. (1968) *Biochemistry 7,* 2054.

2 Erman, J. E. (1974) *Biochemistry 13,* 39.

3 Sievers, G. (1978) *Biochim. Biophys. Acta 536,* 212.

4 de Ropp, J. S., La Mar, G. N., Smith, K. M., Langry, K. C. (1984) *J. Am. Chem. Soc. 106,* 4438.

5 Satterlee, J. D., Erman, J. E., & de Ropp, J. S. (1987) *J. Biol Chem. 262,* 11578

6 Thanabal, V., de Ropp, J. S., & La Mar, G. N. (1987) *J. Am. Chem. Soc. 109,* 265.

7 de Ropp, J. S., Yu, L. P., & La Mar, G. N. (1991) *J. Biomol. NMR 1,* 175.

8 Satterlee, J. D., & Erman, J. E. (1991) *Biochemistry 30,* 4398.

9 Al-Mustafa, J., & Kincaid, J. R. (1994) *Biochemistry 33,* 2191.

10 Chen, Z., de Ropp, J. S., Hernández, G., & La Mar, G. N. (1994) *J. Am. Chem. Soc. 116,* 8772.

11 Das, T. K., & Mazumdar, S. (1995) *Eur. J. Biochem. 227,* 823.

12 Pahari, D., Patel, A. B., & Behere, D. V. (1995) *J. Inorg. Biochem. 60,* 245.

13 Lent, B., Conroy, C. W., & Erman, J. E. (1976) *Arch. Biochem. Biophys. 177,* 56.

14 Edwards, S. L., Poulos, T. L., & Erman, J. (1984) *J. Biol. Chem. 259,* 12984.

15 Dunford, H. B. (1991) in *Peroxidases in Chemistry and Biology* (Everse, J. &

Everse, K. E., Eds.,) Vol. II, pp 1-24, CRC Press: Boca Raton, FL.

16 Edwards, S. L., & Poulos, T. L. (1990) *J. Biol. Chem. 265,* 2588.

17 Fukuyama, K., Kunishima, N., Amada, F., Kubota, T., & Matsubara, H. (1995) *J. Biol. Chem. 270,* 21884.

18 Schuller, D. J., Ban, N., van Huystee, R. B., McPherson, A., & Poulos, T. L. (1996) *Structure 4,* 311.

19 Henriksen, A., Gajhede, M., Baker, P., Smith, A. T., & Burke, J. (1995) *J. Am. Chem. Soc. 118,* 3354.

20 Holzbaur, I. E., English, A. M., & Ismail, A. A. (1996) *Biochemistry 35,* 5488.

21 Thanabal, V., de Ropp, J. S., & La Mar, G. N. (1988) *J. Am. Chem. Soc. 110,* 3027.

22 Smulevich, G., Miller, M. A., Kraut, J., & Spiro, T. G. (1991) *Biochemistry 30,* 9546.

23 Smulevich, G., Paoli, M., Burke, J. F., Sanders, S. A., Thorneley, R. N. F., & Smith, A. T. (1994) *Biochemistry 33,* 7398.

24 Howes, B. D., Rodriguez-Lopez, J. N., Smith, A. T., & Smulevich, G. (1997) *Biochemistry 36,* 1532.

25 Smulevich, G., English, A. M., Mantini, A. R., & Marzocchi, M. P. (1991) *Biochemistry 30,* 772.

26 Smulevich, G., Mauro, J. M., Fishel., L. A., English, A. M., Kraut, J., & Spiro, T. G. (1988) *Biochemistry 27,* 5477.

27 Finzel, B. C., Poulos, T. L., & Kraut, J. (1984) *J. Biol. Chem. 259,* 13027.

28 de Ropp, J. S., Thanabal, V., & La Mar, G. N. (1985) *J. Am. Chem. Soc. 107,* 8268.

29 Tsaprailis, G., Chan, D. W. -S, & English, A. M. submitted.

30 Pace, C. N., Shirley, B. R. & Thomson, J. A. (1990) in *Protein Structure. A Practical Approach* (Creighton, T. E., Ed.,) pp 311-330, IRL Press at Oxford University: Oxford, England.

31 Pace, C. N. (1990) *Trends Biotechnol. 8,* 93.

32 Hughson, F. M., & Baldwin, R. L. (1989) *Biochemistry 28,* 4415.

33 Betz, S. F., & Pielak, G. J. (1992) *Biochemistry 31,* 12337.

34 Pace, C. N. (1986) *Methods Enzymol. 131,* 266.

35 Willis, K. J., Szabo, A. G., Zuker, M., Ridgeway, J. M., & Alpert, B. (1990) *Biochemistry 29,* 5270.

36 Burnstein, E. A., Vedenkina, N. S., & Ivkova, M. N. (1973) *Photochem. Photobiol. 18,* 263.

37 Fox, T., Tsaprailis, G., & English, A. M. (1994) *Biochemistry 33,* 186.

38 Rose, M. Y., & Olson, J. S. (1983) *J. Biol. Chem. 258,* 4298.

39 Cannon, J. B., Kuo, F. -S., Pasternack, R. F., Wrong, N. M., & Muller-Eberhard, U. (1984) *Biochemistry 23,* 3715.

40 Bradford, M. (1976) *Anal. Biochem. 72,* 248.

41 Yonetani, T., & Anni, H. (1987) *J. Biol. Chem. 262,* 9547.

42 Fishel, L. A., Villafranca, J. E., Mauro, J. M., & Kraut, J. (1987) *Biochemistry 26,* 351.

43 Wang, J., Mauro, J. M., Edwards, S. L., Oatley, S. J., Fishel, L. A., Ashford, V. A., Xuong, N. -H., & Kraut, J. (1990) *Biochemistry 29,* 7160.

44 Gross, T. M., & Erman, J. E. (1985) *Biochim. Biophys. Acta 830,* 140.

45 Lakowicz, J. R. (1983) in *Principles of Fluorescence Spectroscopy,* Plenum, New York, NY.

46 Wang, J., Zhu, H., & Ondrias, M. R. (1992) *Biochemistry 31,* 12847.

47 Kresheck, G. C., & Erman, J.E. (1988) *Biochemistry 27,* 2490.

48 Dunford, H. B., Hewson, W. D., & Steiner, H. (1978) *Can. J. Chem. 56,* 2844.

49 Welinder, K. G. (1979) *Eur. J. Biochem. 96,* 483.

50 Veitch, N. C., Tams, J. W., Vind, J., Dalbøge, J., & Welinder, K. G. (1994) *Eur. J. Biochem. 222,* 209.

51 Geraci, G., & Parkhurst, L. J. (1981) *Methods Enzymol. 76,* 262.

52 Das, T. K., Mazumdar, S., & Mitra, S. (1995) *Proc. Indian Acad. Sci. 107,* 497.

53 Creighton, T. E. (1993) in *Proteins: Structure and Molecular Properties,* W.H. Freeman and Company, New York, NY.

54 Chiba, K., Ikai, A., Kawamura-Konishi, Y., & Kihara, H. (1994) *Proteins: Struct. Funct. Genet. 19,* 110.

55 Poulos, T. L., Edwards, S. L., Wariishi, H., & Gold, M. H. (1993) *J. Biol. Chem. 268,* 4429.

56 Sundaramoorthy, M., Kishi, K., Gold, M. H. & Poulos, T .L. (1994) *J. Biol. Chem. 269,* 32759.

57 Petersen, J. F. W., Kadziola, A., & Larsen, S. (1994) *FEBS Lett. 339,* 291.

58 Kunishima, N., Fukuyama, K., Matsubara, H., Hatanakana, H., Shibano, Y., & Amalhi, Y. (1994) *J. Mol. Biol. 235,* 331.

59 Patterson, W. R., & Poulos, T. L. (1995) *Biochemistry 34,* 4331.

60 Satterlee, J. D., Alam, S. L., Mauro, J. M., Erman, J. E., & Poulos, T. L. (1994) *Eur. J. Biochem. 224,* 81.

61 Alonso, D. O. V., & Dill, K. A., (1991) *Biochemistry 30,* 5974.

62 Pace, C. N., Grimsley, G. R., Thomson, J. A., & Barnett, B. J. (1988) *J. Biol. Chem. 263,* 11820.

CHAPTER 4

FLUORESCENCE INVESTIGATION OF YEAST CYTOCHROME *c* PEROXIDASE OXIDATION BY H_2O_2 AND ENZYME ACTIVITIES OF THE OXIDIZED ENZYME

ABSTRACT

The role of tryptophan residues as endogenous electron donors in cytochrome *c* peroxidase (CCP) was examined by protein steady-state fluorescence. Compound I and more highly oxidized forms of CCP were formed by adding 2, 6 and 20 equiv[‡] of H_2O_2 to 5 μM protein at pH 7.0 in the absence of *exogenous* reducing substrates. Addition of native CCP to 8 M urea at pH 1.5 relieved heme quenching and compound I exhibited 90 ± 4% fluorescence relative to unoxidized CCP, consistent with the loss of 0.7 ± 0.2 tryptophan and the assignment of the primary radical site to Trp191. CCP oxidized with 20-fold excess H_2O_2 exhibited 65 ± 1% relative fluorescence indicating loss of 2.4 ± 0.1 tryptophans. Compound I and the higher oxidized forms of CCP spontaneously decayed to ferric CCP species over ~24 h with the loss of ~0.5 *additional* tryptophan in each case. The 24-h decay product of compound I exhibited 73% activity, 74% H_2O_2 titer and titration led to the further oxidation of ~0.6 tryptophan. However, no further tryptophan oxidation was observed on titration of the 24-h decay products of samples initially oxidized with 6 and 20 equiv of H_2O_2. These samples exhibited 58 and 18% H_2O_2 titer, and 47 and 16% activity, respectively, which shows that radical formation on Trp191 is *not* required for

---

‡ The text of Chapter 4 has been modified from the original publication to convert molar equivalents of H_2O_2 to *redox* equivalents of H_2O_2. Thus, ***in lieu*** of the 1, 3, and 10 equiv of H_2O_2 referred to in the original publication, 2, 6, and 20 *redox* equiv of H_2O_2 have been substituted in Chapter 4.

activity. The fluorescence decrease with time paralleled the decrease in activity of H_2O_2-oxidized CCP using both ferrocytochrome *c* and ferrocyanide as substrates, indicating that tryptophan and activity loss occurred on similar time scales. Since CCP reduced 6 and 20 equiv of H_2O_2 within 5 and 20 min, respectively, but fluorescence and activity loss increased slightly over 24 h, charge migration must occur in the polypeptide during decay, giving rise to 7 - 33% dimer formation along with the loss of the 0.5 additional tryptophan.

INTRODUCTION

Binding of H_2O_2 to ferric heme peroxidases results in heterolytic cleavage of the O-O bond and the formation of oxidized enzyme intermediates. The two- and one-electron oxidized intermediates are termed compound I and compound II, respectively. To regenerate ferric peroxidase, $P(Fe^{III})$, electrons are provided by donor substrates and the enzymic cycle is as follows:

$$P(Fe^{III}) + H_2O_2 \rightarrow \text{compound I } (X^{\bullet}\ Fe^{IV}{=}O) + H_2O \quad (1)$$

$$\text{compound I} + 1e^- \rightarrow \text{compound II} \quad (2)$$

$$\text{compound II} + 1e^- \rightarrow P(Fe^{III}) + H_2O \quad (3)$$

In compound I, the oxidizing equivalents are stored as the oxyferryl state (Fe^{IV}=O) of

the heme iron, and an organic radical, X$^{\bullet}$. In most heme peroxidases, X$^{\bullet}$ is a porphyrin π-cation radical.[1]

Cytochrome *c* peroxidase (CCP), a hemoprotein found in yeast mitochondria, catalyzes the reduction of H_2O_2 by ferrocytochrome *c*. A porphyrin radical is not observed in the stable compound I of CCP so an alternate site for X$^{\bullet}$ had long been sought. Several residues had been implicated as possible radical sites, including Trp51[2-7] Trp191,[4,8] Met172,[2,9] Met230 and Met231.[10,11] Recently, ENDOR measurements on isotopically labeled CCP identified a tryptophan residue as the radical site.[12] Trp191 appeared to be the most likely candidate since the EPR of compound I of the CCP(W191F) mutant does not exhibit the broad signal characteristic of native CCP.[7,13] Also, unlike wild-type CCP, this mutant transiently shows a porphyrin radical on reaction with peroxide.[8] Trp51, which is only 4 Å from the heme, was eliminated as the radical site since Trp51→Phe mutation had no effect on the EPR or ENDOR spectra of compound I.[7]

In the absence of an oxidizable substrate, the Fe^{IV}=O and radical (X$^{\bullet}$) sites of compound I decay slowly to give a product which has an absorption spectrum similar to native ferric CCP.[14] The decay product has lost the 2 oxidizing equiv of compound I but retained ~75% activity.[15] Amino acid analysis showed loss of 0.2 tryptophan, 0.5 tyrosine, and 0.5 phenylalanine at pH 7,[16] suggesting that the 2 latter residues are the major endogenous donors. Moreover, it has been reported that CCP can reduce up to 20 equiv of H_2O_2 without detectable O_2 formation by further oxidation of its amino acid residues.[15] Amino acid analysis indicated that the decay product following

oxidation of CCP with 20-fold excess H_2O_2 (20:1 product) has lost 3.4 tyrosines, 1.5 phenylalanines, and 0.6 tryptophan at pH 7. Peroxide at millimolar concentrations readily oxidizes methionine residues in proteins but not aromatic residues[17]; hence, oxidation of the latter in CCP at low H_2O_2 concentrations ($\leq$ 50 μM) must be mediated by the heme.

CCP is the first enzyme known to use a stable tryptophan radical during its turnover.[18] Since protein emission is dominated by tryptophan, the present study explores the use of steady-state fluorescence measurements to probe the involvement of tryptophan residues in the catalytic cycle of CCP and the loss of these residues in H_2O_2-oxidized CCP. Efficient quenching by the heme results in a fluorescence quantum yield for CCP of only 7% relative to the tryptophan standard, NATA[19] but in 8 M urea at pH 1.5, heme quenching is relieved due to heme dissociation from the polypeptide. Since the seven tryptophans in *denatured* CCP are exposed to an aqueous environment they are expected to possess the same emission quantum yields, allowing fluorescence loss to be equated with tryptophan loss.

However, excitation of tryptophan is also accompanied by tyrosine excitation. Tyrosine and tryptophan have emission maxima at ~303 and ~350 nm in water, respectively, and in the absence of tyrosine to tryptophan energy transfer, the tyrosine contribution to the emission intensity at 350 nm will be negligible. Following correction for inner-filter effects, 1 μM CCP (which contains 7 μM tryptophan) and 7 μM NATA exhibited the same fluorescence intensity in 8 M urea at pH 1.5. This indicates that tyrosine to tryptophan energy transfer, which has a R_o of ~14 Å,[20]

approaches zero efficiency in *denatured* CCP. Denatured alcohol dehydrogenase, which possesses 6 tryptophans and 14 tyrosines, also showed zero energy transfer while the efficiency was 70% in the native state.[20,21] Hence, although CCP possesses 14 tyrosines, which are also likely endogenous donors, tyrosine loss is not expected to affect the emission intensity at 350 nm.

To determine the extent of electron donation from tryptophan residues in compound I and the 6:1 and 20:1 products, fluorescence intensities at 350 nm were measured at various time intervals following oxidation. Enzyme activities, using both ferrocytochrome *c* and ferrocyanide as reducing substrates, were also measured at similar time intervals just prior to denaturation to compare rates of fluorescence loss with activity loss. CCP denaturation in 8 M urea at pH 1.5 occurs within the mixing time (2 - 3 s) which should inhibit protein radical migration *after* sample addition to urea. To probe radical migration to surface residues in oxidized CCP, the extent of peroxide-induced *intermolecular* crosslinking was determined by SDS-PAGE. After 24 h, compound I and CCP oxidized with up to 20:1 H_2O_2 give rise to stable decay products.[14] Activities, H_2O_2 titers, and further loss of tryptophan in the 24-h decay products were examined to ascertain whether Trp191 was necessary for activity since CCP(W191F) has only 0.03% activity.[22] Amino acid analysis of compound I and the 20:1 product was reexamined here to compare tryptophan loss with fluorescence loss.

EXPERIMENTAL PROCEDURES

Materials. Horse heart cytochrome c (Type III), *N*-acetyltryptophanamide (NATA) and guanidinium chloride were obtained from Sigma; ABTS [2,2'-azino-di-(3-ethylbenzthiazoline-6-sulfonate)] was purchased from Boehringer Mannheim as the diammonium salt, and analytical grade urea was purchased from Anachemia. All chemicals were used without further purification. Distilled water (specific resistance 18 MΩ cm) was prepared by a Barnstead Nanopure system. SDS-PAGE was performed on 7.5% acrylamide gels using a Mini Protean II Electrophoresis Dual Slab Cell and silver staining (Bio-Rad). Densitometer tracings of the gels were obtained on a FisherBiotech transmission densitometer. Fluorescence and absorption measurements were carried out on a Shimadzu Model RF 5000 spectrofluorometer and a Hewlett Packard 8451A diode-array spectrophotometer, respectively.

H_2O_2 Oxidation of CCP. A 5-μM CCP stock solution was prepared in 0.1 M sodium phosphate buffer (pH 7.0) assuming $\varepsilon_{408} = 98\ mM^{-1}cm^{-1}$.[23] Stock H_2O_2 solutions (0.2-2 mM) were prepared in the same buffer and added to 5 μM CCP to give the desired H_2O_2:CCP molar ratios. Formation of oxyferryl heme was followed spectrophotometrically at 424 nm.[14]

Enzyme Activity of Oxidized CCP. Activity measurements using ferrocytochrome *c*[24] or ferrocyanide[25,26] as reducing substrates were performed by following substrate oxidation spectrophotometrically (ferrocytochrome *c*, $\Delta\varepsilon_{550} = 18\ mM^{-1}cm^{-1}$; ferrocyanide, $\Delta\varepsilon_{420} = 1.0\ mM^{-1}cm^{-1}$). Activities of H_2O_2-oxidized CCP

species are reported relative to native CCP maintained under the same conditions.

H_2O_2 Turnover and H_2O_2 Titer of Oxidized CCP. ABTS (20 μM) oxidation as monitored at 724 nm was used to determine the extent of H_2O_2 turnover by CCP (5 μM) at various times. The 24-h decay products were titrated with H_2O_2 and the absorbance change at 424 nm monitored to determine the extent of oxyferryl heme formation.

Relative Fluorescence. At various time intervals (15 s - 24 h) after the addition of H_2O_2 to 5 μM CCP in 0.1 M phosphate buffer (pH 7.0), protein samples were diluted with urea to give a final concentration of 1 μM CCP in 8 M urea at pH 1.5. Following 280-mn excitation, fluorescence intensities were measured at 350 nm, which is the emission maximum of CCP in urea. The Raman peak of water was subtracted from all emission spectra, and inner-filter effects were corrected using the formula: [20]

$$F = F_o \,\text{antilog}[(A_{ex} + A_{em})/2] \qquad (4)$$

where F is the corrected fluorescence intensity, F_o the observed intensity, A_{ex} and A_{em} are the absorbances at the excitation and emission wavelengths, respectively. Relative fluorescence intensities ($\%F$) were calculated assuming $\%F = 100$ for unoxidized CCP maintained under the same conditions.

SDS-PAGE of Protein Samples. Crosslinking of CCP following addition of 2, 6 and 20 equiv of H_2O_2 was investigated by SDS-PAGE according to the published procedure.[27] At various time intervals (15 s - 24 h) following addition of H_2O_2 to 5 μM CCP in 0.1 M phosphate buffer (pH 7.0), 10 μl of enzyme were added to 40 μl of 10% (w/v) SDS. Samples were allowed to stand in SDS for 30 min and heated (95 °C) for 5 min prior to loading 0.85 μg protein per sample on the gels which were developed using silver staining. The percent monomer present in oxidized CCP relative to unoxidized CCP was estimated by integration of the densitometer tracings of the gels.

Amino Acid Analysis. Prior to amino acid analysis, 5 μM native CCP, compound I and the 20:1 product were maintained at 22 °C for 24 h. Both base (8N KOH at 110 °C for 14 h) and acid (4 N methanesulfonic acid at 110 °C for 14 h) hydrolysis of the proteins was carried out, and the amino acid content of the products was determined using standard procedures.[28,29]

RESULTS

Relative Fluorescence. Quenching of native CCP emission by the heme is eliminated in 8 M urea at pH 1.5. The fluorescence increase upon denaturation, which is observed within the mixing time (2 - 3 s), is accompanied by a red-shift in emission

maximum to 350 nm, characteristic of tryptophan exposure to an aqueous environment.[20] Furthermore, after correcting for inner filter effects (eq 4), 1 μM CCP, which contains 7 μM tryptophan, and 7 μM NATA exhibited the same fluorescence intensity in 8 M urea at pH 1.5. This is consistent with zero tyrosine to tryptophan energy transfer and zero heme quenching under these conditions. In 8 M urea *at pH 7* residual quenching by the heme was still observed, and the sharp Soret absorption (not shown) indicated that the heme is still coordinated to the CCP polypeptide. It is also of interest that tyrosine emission at 303 nm was not observed for denatured CCP on excitation at 275 nm, the tyrosine absorption maximum.

In phosphate buffer (pH 7.0) both CCP and compound I exhibit emission maxima at 325 ± 2 nm and the 109% relative fluorescence of the latter can be accounted for by red-shifting of the Soret on compound I formation.[19] In contrast, denatured compound I has 90 ± 4% relative fluorescence in 8 M urea (Figure 4.1), indicating loss of emission from 0.7 ± 0.2 of the 7 tryptophans in the protein. Addition of 1 reducing equivalent (ascorbate) before denaturation increased the relative fluorescence to 98 ± 1%, and the addition of a second reducing equivalent resulted in no further increase in fluorescence. Presumably the amino acid radical ($X^{\bullet}$) is reduced before the heme since 1 reducing equivalent did not shift the Soret from the 420-nm maximum for compound I, but a shift to 408 nm, characteristic of ferric CCP, was observed on addition of two reducing equivalents. When 20-fold excess H_2O_2 was added to CCP 15 s prior to denaturation, the relative fluorescence in 8 M urea was 86 ± 3%, indicating that only 1.0 ± 0.2 tryptophan was oxidized in this short time

interval. However, within 5 min, the relative fluorescence had decreased to 75% revealing loss of a second tryptophan whereas the relative fluorescence of compound I remained at 90%. Figure 4.2 summarizes the fluorescence intensities at 350 nm

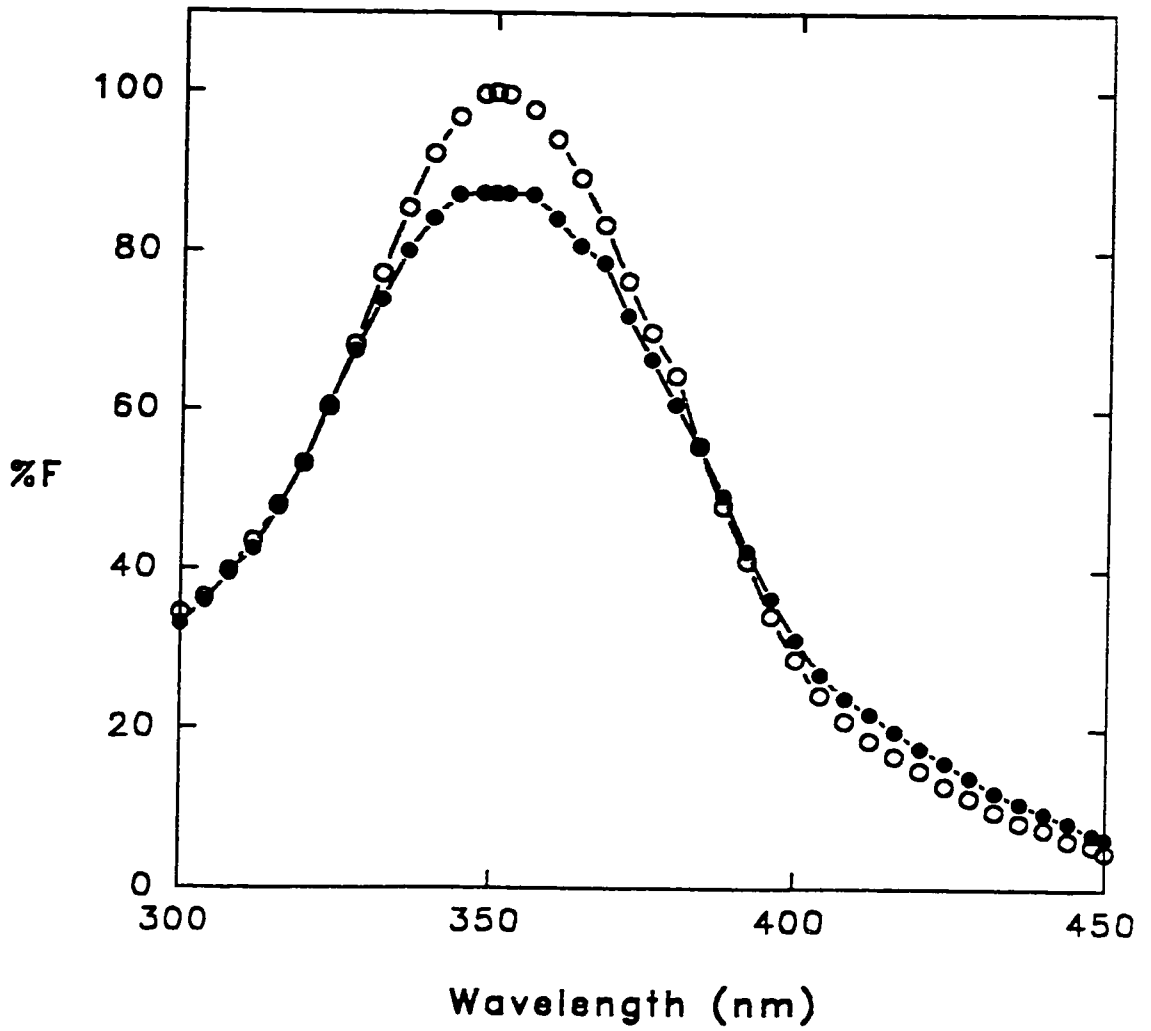

Figure 4.1 Relative fluorescence of 1 μM CCP (open circles) and compound I (closed circles) in 8 M urea at 22 °C on excitation at 280 nm. Slits, 5 nm; scan rate 104 nm/min. Data points are the corrected (eq 4) relative fluorescence intensities, *%F*.

following denaturation of CCP at various intervals after addition of 2, 6 and 20 equiv of H_2O_2. Assuming an equal contribution from each of the seven tryptophans, the decrease in fluorescence was converted to the number of tryptophans lost. Clearly this number *increases* with time and the amount of H_2O_2 added, and ~3 tryptophans are lost in the 20:1 24-h decay product. Essentially identical results (data not shown) were obtained in 6.4 M guanidinium chloride at pH 7.0 but samples in 8 M urea at pH 7.0 were less fluorescent due to heme association with the polypeptide under these conditions.

Enzyme Activity of Oxidized CCP. Activities using ferrocytochrome *c* and ferrocyanide as reducing substrates are shown in panels B and C, respectively, of Figure 4.2. Within 15 s of oxidation, ≥ 85% activity was observed for all samples with both substrates, but the activities of the 6:1 and 20:1 products rapidly decreased in ≤ 20 min. Activities of all samples further decreased over 24 h, and the residual activities using both substrates are listed in Table 4.1.

H_2O_2 Turnover and H_2O_2 Titer of Oxidized CCP. Compound I formed within the mixing time, and addition of ABTS to the CCP-peroxide samples showed that the turnover at pH 7.0 of 6 and 20 equiv of H_2O_2 was complete within 5 and 20 min, respectively. Using the relative absorbance change at 424 nm (the maximum in the ferric and oxyferryl CCP difference spectrum), the 24-h decay products were titrated with H_2O_2 to determine the extent of their ability to re-form oxyferryl heme, and the

Figure 4.2 **(A)** Fluorescence intensities at 350 nm of 1 μM H_2O_2-oxidized CCP in 8 M urea, pH 1.5. CCP (5 μM) was reacted with H_2O_2 in 0.1 M phosphate buffer, pH 7.0, and diluted with urea at various times after addition of H_2O_2. 2:1 H_2O_2:CCP (compound I), circles; 6:1 H_2O_2:CCP, triangles; and 20:1 H_2O_2:CCP, squares. Data points are the averages of 4 measurements. See Figure 4.1 for experimental conditions. **(B)** Ferrocytochrome *c* and (C) ferrocyanide activities in 0.1 M phosphate buffer, pH 7.0, relative to native CCP of the samples in (A) just prior to denaturation.

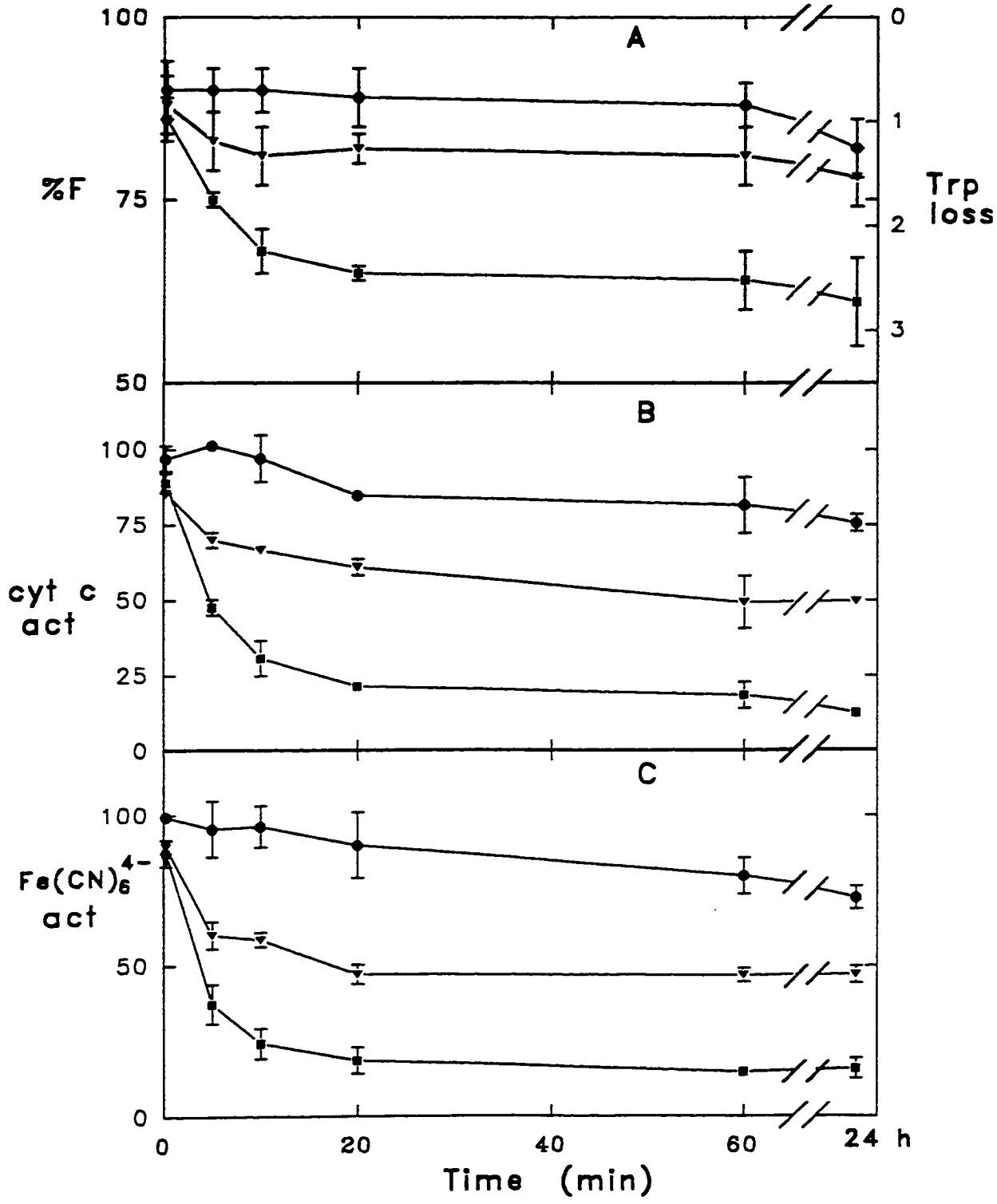
A
B
C
%F
Trp loss
cyt c act
Fe(CN)$_6^{4-}$ act
100
75
50
25
0
1
2
3
0
20
40
60
24 h
Time (min)

Table 4.1 Properties of the 24-h Decay Products of H_2O_2-Oxidized CCP[a]

property (%)[b]	2 equiv H_2O_2	6 equiv H_2O_2	20 equiv H_2O_2
H_2O_2 titer[c]	74 ± 5	58 ± 2	18 ± 0.4
monomer[d]	93	78	77
cyt c act.[e]	73 ± 3	47 ± 2	16 ± 3
$Fe(CN)_6^{4-}$ act.[e]	76 ± 3	50 ± 2	13 ± 2
Trp loss[f]	~0.6	0	0

[a] CCP (5μM) was oxidized with 2, 6 and 20 equiv of H_2O_2 in 0.1 M phosphate buffer, pH 7.0 and properties measured 24 h after oxidation.

[b] Relative to unoxidized CCP maintained under the same conditions.

[c] From H_2O_2 titrations (see text).

[d] From Table 4.2.

[e] Activities from Figure 4.2B and C.

[f] Tryptophan loss at 15 s following addition of 2 equiv of H_2O_2 to the decay products. The loss was estimated from the change in fluorescence of the decay products in 8 M urea (pH 1.5) before and after addition of H_2O_2 (see text).

H_2O_2 titers are also listed in Table 4.1. $\Delta\varepsilon_{424}$ for the decay products is the same as that for native CCP as reported previously for titrations at pH 8.[14]

Soret Absorption. Ferric CCP and compound I exhibit Soret maxima at 408 and 420 nm, respectively (Figure 4.3A). The broad Soret absorption bands observed immediately following addition of ferric CCP, compound I and free hemin to 8 M urea at pH 1.5 are essentially identical (Figure 4.3B). This suggests that the three hemes are in a similar environment and have the same iron coordination and oxidation states. Hence, the protein-bound ferric and oxyferryl hemes are released and the latter is rapidly reduced upon denaturation at pH 1.5.

SDS-Page of Protein Samples. Table 4.2 summarizes the percent monomer in H_2O_2-oxidized CCP at pH 7.0. Gels of compound I and its 24-h decay product showed that essentially all the protein is monomeric whereas the monomeric content of the 6:1 and 20:1 24-h decay products has decreased to ~78%. These results are in marked contrast to those reported previously for CCP oxidized at *pH 4.5* using ≥ 10-fold higher protein concentrations[25,30] where 75, 25 and 0% monomer were observed for the 2:1, 6:1 and 20:1 products, respectively. The significantly higher monomer content observed here is probably due in part to the lower protein concentrations used in this study, but may also arise from the pH dependence of the decay pathways since oxidation of CCP at low and high pH produced different products.[15]

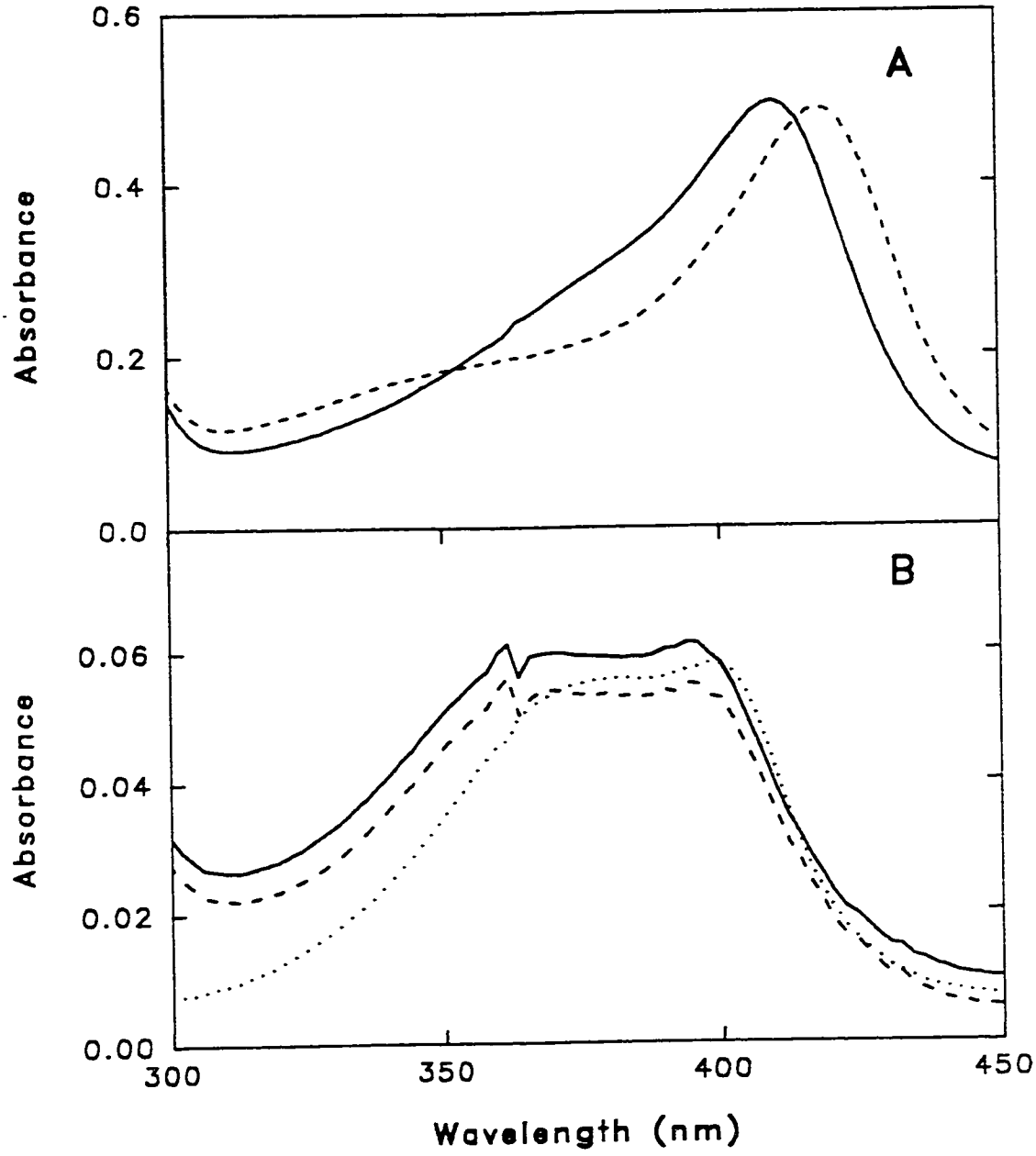

Figure 4.3 Soret absorption of ferric CCP (solid line) and compound I (dashed line). **(A)** 5 μM protein in 0.1 M phosphate, pH 7.0; **(B)** 1 μM protein in 8 M urea, pH 1.5. The dotted line in (B) is the absorption of 0.44 μM hemin.

Amino Analysis of Oxidized CCP. The amino acid composition of CCP and the compound I decay product showed no significant differences but the 20:1 decay product had 2.4 ± 0.3 less tyrosines and 1.7 ± 0.2 less tryptophans than native CCP, in reasonable agreement with the loss of 3.4 tyrosines and 0.6 tryptophan (alkaline hydrolysis) reported previously at pH 7.[16] Thus, compared to the fluorescence measurements, amino acid analysis underestimates tryptophan loss in compound I and the higher oxidized forms of CCP, which may be due to the problems encountered in tryptophan determination.[29]

DISCUSSION

Compound I exhibits 90 ± 4% fluorescence at 350 nm relative to unoxidized CCP in 8 M urea at pH 1.5. This corresponds to the loss of 0.7 ± 0.2 tryptophan and supports the assignment of the radical site ($X^{\bullet}$, eq 1) to a tryptophan residue.[12] The uncertainty in tryptophan loss may be due to reduction of the radical by trace impurities in the urea so that the value of 0.7 may in fact be a lower limit. Upon denaturation, compound II (eq 2) which stores its single oxidizing equivalent as Fe^{IV}=O at pH 7[31] shows 98 ± 1% relative fluorescence; hence, most of the observed fluorescence loss in compound I is due to radical formation and *not* to the rapid reduction of the Fe^{IV}=O heme in urea (Figure 4.3B). Reduction of compound II to ferric CCP before denaturation had no further effect on the fluorescence in 8 M urea.

Table 4.2 Percent Monomer in H_2O_2-Oxidized CCP Samples[a]

	% Monomer[b]		
time	2 equiv H_2O_2	6 equiv H_2O_2	20 equiv H_2O_2
1 s	100	93	95
5 min	100	88	83
1 h	100	89	79
24 h	93	78	67

[a] CCP (5μM) was oxidized with 2, 6 and 20 equiv of H_2O_2 in 0.1 M phosphate buffer, pH 7.0 and denatured at the times indicated.

[b] Percent monomer relative to unoxidized CCP as estimated by integration of densitometer tracings of the gels.

CCP species oxidized with 6 and 20 equiv of H_2O_2 prior to denaturation are significantly less fluorescent than compound I (Figure 4.2A), and loss of 2.8 ± 0.4 tryptophans is observed for the 20:1 24-h decay product. An examination of the 3-D structure of CCP shows a ring of aromatic residues on the proximal side that could channel charge to the heme.[10] There are three tyrosines (187, 229, 236) within 5 Å of Trp191 and a pair of tryptophans (211, 223) within 6-9 Å (Figure 4.4). Oxidation of these residues would be consistent with the fluorescence data (Figure 4.2A) and the amino acid analyses which indicated loss of ~3 tyrosines over 24 h in the 20:1 decay product. Figure 4.2A shows that tryptophan loss is greatest within the 20 min following H_2O_2 addition to CCP, which mirrors the rate of peroxide turnover by CCP; 6 equiv are reduced per mol of enzyme in ≤ 5 min and 20 equiv in ≤ 20 min. The further loss of ~0.5 tryptophan indicates that charge migration occurs in the polypeptide over the period from 1 to 24 h.

Decay of compound I over 24 h clearly does not restore tryptophan fluorescence to 100% (Figure 4.2A); thus, a stable oxidation product of Trp191 or a neighboring tryptophan must be formed during the decay process. Since the 24-h decay product of compound I exhibits 73% ferrocytochrome *c* oxidizing activity, irreversible oxidation of Trp191 would be surprising considering that CCP(W191F) has only 0.03% activity.[22] However, titration with H_2O_2 regenerates the spectrum of compound I and leads to the immediate loss of 0.6 tryptophan (Table 4.1), suggesting that the second oxidizing equivalent ($X^{\bullet}$, eq 1) may also be located mainly on Trp191 in the decay product. H_2O_2 titration of the 6:1 and 20:1 24-h decay products, on the

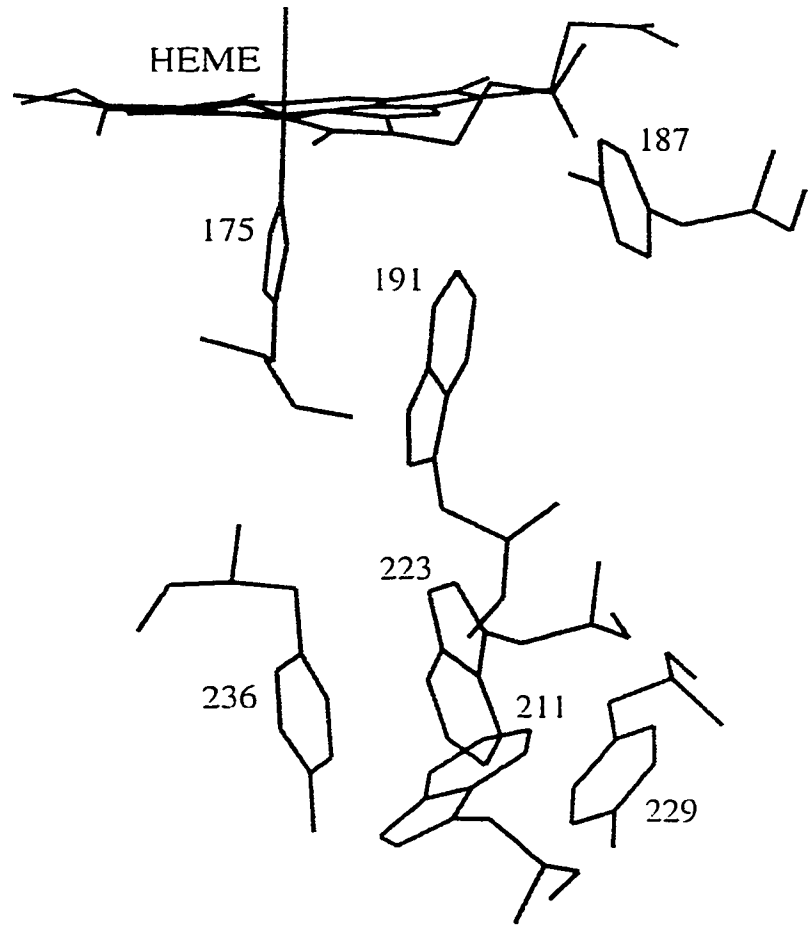

Figure 4.4 Locations of the three tryptophans (191, 211, 223) and three tyrosines (187, 229, 236) relative to the heme and proximal His175 of CCP. This molecular graphics image was adapted from Figure 6 of Edwards et al. (1987)[10] and produced using the MidasPlus software system from the Computer Graphics Laboratory, University of California, San Francisco.[32]

other hand, results in no further oxidation of tryptophan, precluding radical formation on Trp191. Since these species retain 47 and 16% ferrocytochrome *c* oxidizing activity, respectively (Table 4.1), radical formation on Trp191 must *not* be necessary for high ferrocytochrome *c* turnover; this is contrary to expectation considering the negligible ferrocytochrome *c* oxidizing activity of CCP(W191F). Clearly, a stopped-flow investigation of the reaction between H_2O_2 and the decay products would be of interest, particularly since transient porphyrin radical formation was observed for CCP(W191F).[8]

The fluorescence loss in H_2O_2-oxidized CCP parallels the dependence of activity on H_2O_2:CCP ratios and time (Figure 4.2), indicating that tryptophan and activity loss occur on similar time scales. Within 15 s of H_2O_2 addition, $\geq$ 85% activity is observed for all the samples but, like the fluorescence, the activity of the 6:1 and 20:1 products decreases significantly over the 20 min period required for reduction of 20 equiv of H_2O_2 by the enzyme. In all samples activity loss continued over 24 h, as well as the loss of monomer due to protein cross linking (Table 4.1). This is further evidence of charge migration in the polypeptide, which results in the loss of ~ 0.5 additional tryptophan. Both the ferrocytochrome *c* and ferrocyanide oxidizing activities of the 24-h decay products are the same, within experimental error, as the H_2O_2 titers (Table 4.1), which was found previously at pH 8.0[15]; thus, activity loss at pH 7.0 is due to the reduced capacity of the enzyme to react with H_2O_2.

The fluorescence and activity data presented here on oxidized CCP underscore the important role played by tryptophan residues in the redox chemistry of the enzyme.

The loss of activity and H_2O_2 titer with protein fluorescence indicates that tryptophan residues are important in controlling the reactivity of CCP towards H_2O_2. Since ~3 tryptophan residues are lost during the endogenous reduction of peroxide and amino acid analyses reveal loss of ~3 tyrosines, electron donation to H_2O_2 via the heme from the ring of aromatic residues shown in Figure 4.4 is a possibility as suggested previously.[10] HPLC peptide mapping coupled with fluorescence detection and electrospray mass spectrometry are being used to unravel the specific aromatic residues that act as endogenous donors to H_2O_2, and the role of Trp191 in CCP activity.

This study demonstrates that steady-state fluorescence measurements under denaturing conditions are a valuable probe of tryptophan loss in oxidized CCP. The lack of significant fluorescence loss in CCP(W191F) compound I (Chapter 5) provides convincing evidence for the validity of this approach. Amino acid analysis is a much more time consuming, and much less accurate and less sensitive, method for tryptophan determination than fluorescence intensity measurements. Furthermore, the variation in EPR signals following mutation of residues around Trp191 has complicated the assignment of aromatic radicals in CCP mutants[13,33,34]; hence, fluorescence measurements will be useful in distinguishing between tyrosine and tryptophan radicals in these mutants.

ACKNOWLEDGMENTS

We wish to thank Bernard F. Gibbs of the Biotechnology Research Institute (Montreal) for the amino acid analysis. This research was supported by a grant from NSERC (Canada) to A.M.E.

REFERENCES

1 Dawson, J. H. (1989) *Science 240,* 433.

2 Finzel, B. C., Poulos, T. L., & Kraut, J. (1984) *J. Biol. Chem. 259,* 13027.

3 Poulos, T. L., & Finzel, B. C. (1984) *Pept. Protein Rev. 4,* 115.

4 Hori, H., & Yonetani, T. (1985) *J. Biol. Chem. 260,* 349.

5 Goodin, D. B., Mauk, A. G., & Smith, M. (1987) *J. Biol. Chem. 262,* 7719.

6 Fishel, L. A., Villafranca, J. E., Mauro, J. M., & Kraut, J. (1987) *Biochemistry 26,* 351.

7 Scholes, C. P., Liu, Y., Fishel, L. A., Farnum, M. F., Mauro, J. M., & Kraut, J. (1989) *Isr. J. Chem. 29,* 85.

8 Erman, J. E., Vitello, L. B., Mauro, J. M., & Kraut, J. (1989) *Biochemistry 28,* 7992.

9 Goodin, D. B., Mauk, A. G., & Smith, M. (1986) *Proc. Natl. Acad. Sci. U.S A. 83,* 1295.

10 Edwards, S. L, Xuong, N. H., Hamlin, R. C., & Kraut, J. (1987) *Biochemistry 26,* 1503.

11 Hoffman, B. M., Roberts, J. E., Brown, T. G., Kang, C. H., & Margoliash, E. (1979) *Proc. Natl. Sci. U.S.A. 76,* 6132.

12 Sivaraja, M., Goodin, D. B., Smith, M., & Hoffman, B. M. (1989) *Science 245,* 738.

13 Fishel, L. A., Farnum, M. F., Mauro, J. M., Miller, M. A., & Kraut, J. (1991) *Biochemistry 30,* 1986.

14 Erman, J. E., & Yonetani, T. (1975) *Biochim. Biophys. Acta. 393,* 350.

15 Erman, J. E., & Yonetani, T. (1975) *Biochim. Biophys. Acta. 393,* 343.

16 Coulson, A. F. W., & Yonetani, T. (1972) *Biochem. Biophys. Res. Commun. 49,* 391.

17 Neumann, N. P. (1967) *Methods Enzymol. 11,* 485.

18 Prince, R. C., & George, G. N. (1990) *Trends Biochem. Sci. 15,* 170.

19 Fox, T., Ferreira-Rajabi, L., Hill, B. C., & English, A. M. (1993) *Biochemistry 32,* 6938.

20 Lakowicz, J. R. (1983) in *Principles of Fluorescence Spectroscopy,* Plenum: New York, NY.

21 Saito, Y., Tachibana, H., Hayaski, H., & Wada, A. (1981) *Photochem. Photobiol. 33,* 289.

22 Mauro, J. M., Fishel., L. A., Hazzard, J. T., Meyer, T. E., Tollin, G., Cusanovich, M. A., & Kraut, J. (1988) *Biochemistry 27,* 6243.

23 Yonetani, T., & Anni, H. (1987) *J. Biol. Chem. 262,* 9547.

24 Yonetani, T., & Ray, G. S. (1965) *J. Biol. Chem. 240,* 4503.

25 Spangler, B. D. (1984) Ph. D. Dissertation, Northern Illinois University, Dekalb.

26 Jordi, H. C., & Erman, J. E. (1974) *Biochemistry 13,* 3741.

27 Nielsen, T. B., & Reynolds, J. A. (1978) *Methods Enzymol. 48,* 3.

28 Spackman, D. H., Stein, W. H., & Moore, S. (1958) *Anal. Chem. 30,* 1190.

29 Darbre, A. (1986) in *Practical Protein Chemistry - A Handbook,* Wiley: New York, NY.

30 Spangler, B. D., & Erman, J. E. (1986) *Biochim. Biophys. Acta. 872,* 155.

31 Coulson, A. F. W., Erman, J. E., & Yonetani, T. (1971) *J. Biol. Chem. 246,* 917.

32 Ferrin, T. E., Huang., C. C., Jarvis, L. E., & Langridge, R. (1988) *J. Mol. Graphics, 6,* 13.

33 Goodin, D. B., & McRee, D. E. (1993) *Biochemistry 32,* 3313.

34 Houseman, A. L. P., Doan, P. E., Goodin, D. B., & Hoffman, B. M. (1993) *Biochemistry 32,* 4430.

Addendum 1

A requirement in equating the oxidation of Trp residues in compound I and H_2O_2-oxidized CCP with fluorescence loss is that conditions exist under which the fluorescence quantum yield of CCP is 100% relative to the Trp standard, NATA. The steady-state fluorescence spectra of CCP were recorded in 8 M urea as a function of pH to determine whether 100% relative fluorescence can be obtained in denatured CCP.

Stock CCP (5 μM) in 0.1 M sodium phosphate buffer (pH 7.0) was diluted with stock (10 M) urea to give a final concentration of 1 μM CCP in 8 M urea. The pH of the stock urea was varied between 7.0 and 1.5. Fluorescence was monitored as described in Chapter 4, and the steady-state fluorescence intensity at 350 nm following 280-nm excitation of denatured 1 μM CCP (which contains 7 μM Trp), was compared to that of 7 μM NATA under identical conditions.

Table A1.1 summarizes the relative fluorescence at 350 nm of denatured CCP in 8 M urea as a function of pH. The data reveal that the relative fluorescence intensity increases as the pH is decreased from 7.0 to 1.5. In 8 M urea at pH 7.0, the relative fluorescence is ~ 67%, identical to that reported earlier [Fox, T., Ferreira-Rajabi, L., Hill, B. C., & English, A. M. (1993) *Biochemistry 32,* 6938]. In 8 M urea at pH 1.5, however, CCP exhibits 100% relative fluorescence.

The Soret absorption of CCP is sharp in 8 M urea at pH 7.0 but broad in 8 M urea at pH 1.5 (Figure A1.1), and in both cases resembles that of free hemin under the

Table A1.1 Relative Fluorescence of CCP in 8 M Urea vs pH

	% $F_{350\ nm}$ of CCP[a]	
pH	λ_{ex} 280 nm	λ_{ex} 295 nm
7.0	66.5 ± 5	67.2 ± 3
5.0	65.0 ± 5	
4.0	65.0 ± 2	
3.0	60.6	
1.5	100 ± 1	101 ± 2

[a] Relative fluorescence intensity at 350 nm of 1 μM CCP in 8 M urea assuming 100% for 7 μM NATA under identical conditions.

same conditions (Figures 2.4 and 4.3). However, the relative fluorescence intensity of CCP is ~ 100% at pH 1.5 (Table A1.1). Moreover, the half-lives of unfolding of CCP in 8 M urea at pH 7.0 (Chapter 2) and pH 1.5 are ~ 14 and 3 s, respectively, indicating that low pH is more effective in rapidly disrupting the polypeptide and exposing the Trp residues to the aqueous environment.

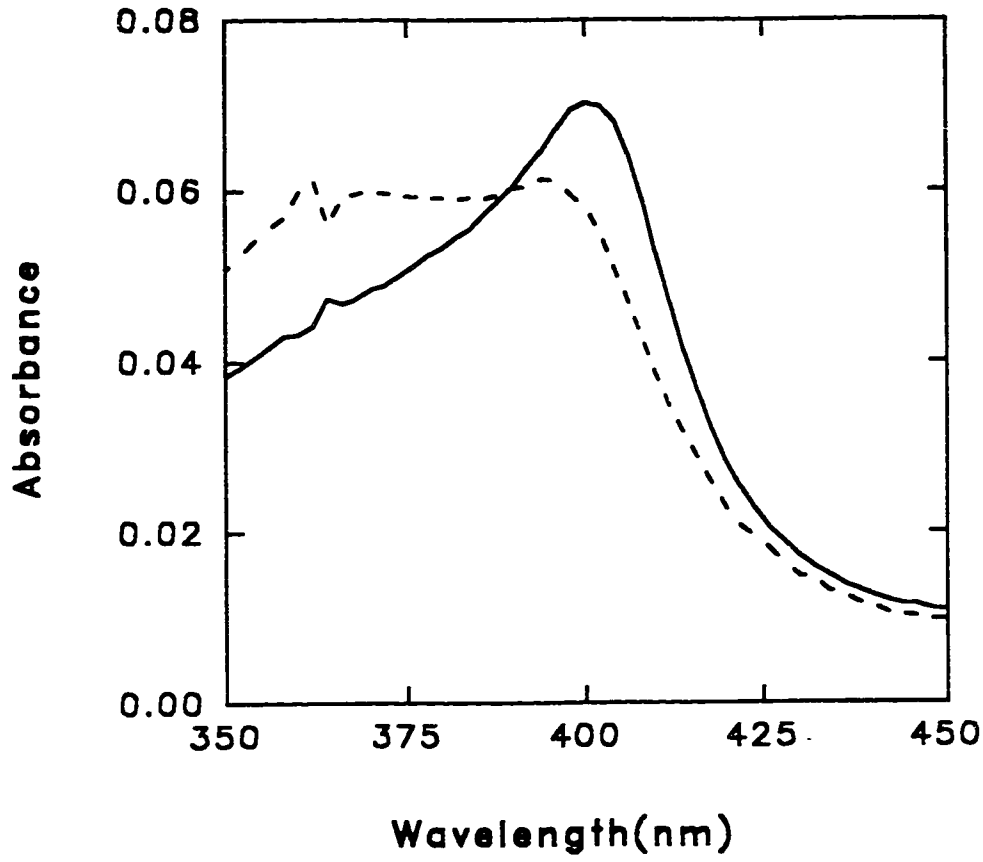

Figure A1.1 Soret absorption of 1 μM CCP in 8 M urea at pH 7.0 (solid line) and pH 1.5 (dashed line).

In the absence of Tyr→Trp energy transfer, the Tyr contribution to the emission intensity at 350 nm will be negligible [Lakowicz, J. R. (1983) in *Principles of Fluorescence Spectroscopy,* Plenum, New York: NY]. Thus, in 8 M urea *at pH 1.5,* zero Tyr→Trp energy transfer and zero heme quenching is assumed to occur since the relative fluorescence of CCP is 100% (Table A1.1) on either 280- or 295-nm excitation. Therefore, the seven solvent exposed Trp residues in *denatured* CCP must possess the same emission quantum yield, allowing fluorescence loss to be correlated with Trp oxidation.

CHAPTER 5

REDOX ACTIVITY OF TRYPTOPHAN RESIDUES IN RECOMBINANT CYTOCHROME *c* PEROXIDASE AND ITS W51F AND W191F MUTANTS

ABSTRACT

Tryptophan oxidation mediated via the heme was initiated by adding 2, 6 and 20 equivalents of H_2O_2 to 5 μM recombinant CCP (CCP(MI)) and its W51F and W191F mutants at pH 7.0. Addition of the proteins to 8 M urea (pH 1.5) relieved heme quenching of Trp fluorescence. CCP(MI)-I, W51F-I, and W191F-I, the two-electron oxidized species (Fe^{IV}=O,$P^{+\cdot}$) formed on addition of 2 equivalents of H_2O_2, exhibited decreased fluorescence relative to the Fe^{III} forms. Loss of 0.7 Trp in CCP(MI)-I and W51F-I, and 0.2 Trp in W191F-I implies that $P^{+\cdot}$ is located on Trp191 in CCP(MI)-I and W51F-I. Spontaneous decay of the Fe^{IV}=O hemes back to Fe^{III}, followed by reaction with 2 more equivalents of H_2O_2 after 24 h, resulted in a *combined* loss of 2.7 (CCP(MI)), 1.5 (W51F) and ~1 (W191F) Trp. Also, addition of 6 equivalents of H_2O_2 to the *resting* Fe^{III} enzymes resulted in loss of ~2 Trps in CCP(MI) but only ~1 in W51F and W191F, suggesting that Trp51 becomes redox active in CCP(MI) when > 2 equivalents of H_2O_2 are reduced. Addition of 20 equivalents of H_2O_2 resulted in a *total* loss of ~4, 2.5, and 2 Trp in CCP(MI), W51F and W191F, respectively. Activity loss largely paralleled Trp loss, and the residual activity of CCP(MI) and W51F exposed to 20 equivalents of H_2O_2 was 5 - 19%, while W191F exhibited ~50% activity. SDS-PAGE analysis revealed that oxidized CCP(MI) and W191F were 60 - 70% monomeric, and W51F 27% monomeric following its reaction with > 2 equivalents H_2O_2. Amino acid analyses confirmed Trp loss and also showed significant Tyr, but *not* Met, loss in the oxidized proteins. Donors to the heme and

pathways of electron migration are proposed based on the combined results.

INTRODUCTION

The identification of a Trp radical in yeast CCP-I was the first instance that a Trp residue[1] was shown to play a redox-active role in an enzyme.[2] Recently, however, a redox-active Trp has been identified in ribonucleotide reductase[3] and, in addition to Trp, a number of other amino acid radicals, including tyrosyl, cysteinyl and glycyl radicals are known to play catalytic roles in enzymatic reactions.[4] Reversible redox activity of protein residues involves the formation of one-electron oxidized free radical species, which are stabilized by the surrounding polypeptide. Thus, a full understanding of the use of protein free radicals in redox catalysis (free radical enzymology) requires characterization of their storage sites, and elucidation of their migration and quenching mechanisms in protein matrices.

The catalysis of two-electron redox chemistry by Fe^{III} heme centres necessitates the generation of radical species. Hence, small plant and fungal heme peroxidases can provide important insight into the reactivity of protein radicals in redox catalysis. Binding of H_2O_2 to the Fe^{III} ion in heme peroxidases (Fe^{III},P) results in heterolytic cleavage of the O—O bond, and formation of a two-electron oxidized intermediate (Fe^{IV}=O,$P^{+\bullet}$), termed compound I (eq. [1]). Reduction of the latter in one-electron steps (eqs. [2] and [3]) back to the resting enzyme occurs via formation of the one-

electron oxidized intermediate (Fe^{IV}=O,P), termed compound II.

$$Fe^{III},P + H_2O_2 \rightarrow Fe^{IV}=O,P^{+\cdot} + H_2O \quad [1]$$

$$Fe^{IV}=O,P^{+\cdot} + 1e^- \rightarrow Fe^{IV}=O,P \quad [2]$$

$$Fe^{IV}=O,P + 1e^- + 2H^+ \rightarrow Fe^{III},P + H_2O \quad [3]$$

In most heme peroxidases $P^{+\cdot}$ is a porphyrin π-cation radical, but a protein-based radical is observed for CCP-I.[5,6] Of the 7 Trps, Trp191, which is in van der Waals contact with the heme (Fig. 1.10), has been identified as the redox-active amino acid residue in CCP-I. The broad EPR signal characteristic of native CCP-I was not observed in the spectrum of W191F-I,[7,8] and this mutant also exhibited a transient porphyrin radical on reaction with peroxide.[9] Trp51, which is only 4 Å from the heme (Fig. 1.10), was eliminated as the radical site since W51F-I exhibited EPR and ENDOR spectra almost identical to those of CCP(MI)-I.[7]

We have shown previously that steady-state protein fluorescence can be used to probe the loss of Trp residues in H_2O_2-oxidized yeast CCP.[10] Since heme is a highly efficient quencher of CCP fluorescence,[11] protein denaturation in 8 M urea at pH 1.5 is required to relieve quenching and allow fluorescence loss to be equated with Trp loss. Furthermore, since denaturation of CCP occurs rapidly in 8 M urea, it is assumed that radical migration does not occur during this process,[10] and that protein-based radicals are converted to stable oxidation products on exposure to the solvent.

The fluorescence measurements are extended here to the recombinant enzyme

(CCP(MI)) and two mutants, W51F and W191F, in which the Trp residues closest to the heme are singly mutated to phenylalanine. In lignin peroxidase (LIP), where Phe46 and Phe193 correspond to Trp51 and Trp191,[12] $P^{\bullet+}$ is a porphyrin π-cation radical in compound I.[13] Since it is more difficult to oxidize the side chain of phenylalanine than the indole side chain of Trp,[14] the rapid transfer of oxidizing equivalents from the porphyrin to a protein-based radical is presumably prevented in LIP-I.[6] Despite the Trp191 → Phe mutation, a porphyrin π-cation radical is only transiently formed ($t_{1/2}$ ~14 ms) in W191F-I.[9] The porphyrin radical is transferred to the protein, resulting in an EPR signal for W191F-I that has been assigned to a tyrosyl radical.[7,8] Hence, an examination of compound I of the two Trp → Phe mutants will provide a test of the EPR data and also demonstrate if fluorescence measurements on the denatured proteins can clearly distinguish between Trp and Tyr radicals.

In the absence of oxidizable substrates, CCP(MI)-I, W51F-I, and W191F-I spontaneously decay to give products with absorption spectra similar to their resting Fe^{III} forms. The half-life of the Fe^{IV}=O heme in CCP(MI)-I and W191F-I is ~3 h,[15] but that of W51F-I is only ~ 3 - 4 s.[16] EPR studies revealed that the protein radical signal in yeast CCP-I decays on a slightly faster timescale than the Fe^{IV}=O center.[17] However, a protein-based radical persists in W191F-I for only ~10 min,[18] clearly indicating that the Fe^{IV}=O heme is not reduced by the removal of a second electron from the EPR-active species. To probe Trp loss due to the combined effects of protein radical decay and endogenous electron transfer to the Fe^{IV}=O heme, the decay products were examined by fluorescence at time intervals between 15 s and 24 h

following the addition of H_2O_2. Furthermore, the 24-h decay products were exposed to another two oxidizing equivalents of H_2O_2 and rapidly unfolded to see if Trp residues were also electron donors in the decay products.

Millimolar H_2O_2 readily oxidizes methionine residues in proteins but not aromatic residues.[19] However, yeast CCP reduces up to 20 equivalents of H_2O_2 at micromolar concentrations using endogenous donors on the polypeptide,[20] including ~ 3 Trps.[10] A mechanism consistent with the reduction of 2 equivalents of H_2O_2 by compound I would be the following:

$$Fe^{IV},P^{+\bullet} \rightarrow Fe^{III},P^{+\bullet},P_x^{\bullet} \quad [4]$$

$$Fe^{III},P^{+\bullet},P_x^{\bullet} + H_2O_2 \rightarrow Fe^{IV}{=}O,P^{+\bullet},P_x^{\bullet},P_y^{\bullet} + H_2O \quad [5]$$

where $P_x^{\bullet}$ and $P_y^{\bullet}$ are additional protein-based radicals generated by the transfer of the two oxidizing equivalents from peroxide via the heme to the polypeptide. Exposure to 6 and 20 equivalents of H_2O_2 was undertaken to estimate the *maximum* number of Trp donors in each of the mutants examined here. As carried out previously with yeast wild-type CCP,[10] amino acid analyses were performed to probe the loss of non-Trp residues, and ferrocytochrome *c* and ferrocyanide oxidizing activities were measured just prior to denaturation to compare fluorescence loss with activity loss. H_2O_2 titres and the extent of radical-mediated *intermolecular* protein cross-linking were also measured. Finally, interpretation of the combined data, in terms of possible sites of protein-based free radical formation and possible radical and electron migration

pathways, is attempted.

EXPERIMENTAL PROCEDURES

Materials. Wild-type recombinant cytochrome *c* peroxidase (CCP(MI)) and its W51F and W191F mutants, prepared as described,[16] were generous gifts from Dr Mark Miller (University of California, San Diego). Horse heart cytochrome *c* (Type III), *N*-acetyltryptophanamide (NATA) and guanidinium chloride were obtained from Sigma; ABTS was purchased from Boehringer Mannheim as the diammonium salt, and analytical grade urea was purchased from Anachemia. All chemicals were used without further purification. Distilled water (specific resistance 18 MΩ cm) was prepared using a Barnstead Nanopure system. SDS-PAGE was performed on 7.5% acrylamide gels using a Mini Protean II Electrophoresis Dual Slab Cell and silver staining (Bio-Rad). Densitometer tracings of the gels were obtained on a FisherBiotech transmission densitometer. Fluorescence and absorption measurements were carried out on a Shimadzu Model RF 5000 spectrofluorometer and a Hewlett Packard 8451A diode-array spectrophotometer, respectively.

H_2O_2 Oxidation. Protein stock solutions of 5 μM were prepared in 0.1 M sodium phosphate buffer (pH 7.0) using ε_{408} ($mM^{-1}cm^{-1}$) values of 102 (CCP(MI)), 141 (W51F)[16] and 109 (W191F).[21] Stock H_2O_2 solutions (0.2 - 2 mM) were prepared in

the same buffer and H_2O_2 concentrations were determined spectrophotometrically by monitoring the CCP-catalyzed oxidation of excess ABTS ($\Delta\varepsilon_{405}$ = 36.8 $mM^{-1}cm^{-1}$). Protein and H_2O_2 stocks were mixed to give the desired ratios. Formation of Fe^{IV}=O heme was followed spectrophotometrically at 424 nm.[17]

Enzyme Activities. Assay solutions contained 180 μM H_2O_2, 25 μM ferrocytochrome *c* or 20 mM ferrocyanide as reducing substrate and 25 nM native or oxidized peroxidase in 0.1 M phosphate buffer (pH 7.0). Activity measurements were performed by following substrate oxidation spectrophotometrically (ferrocytochrome *c*, $\Delta\varepsilon_{550}$ = 18 $mM^{-1}cm^{-1}$ [22]; ferrocyanide, $\Delta\varepsilon_{420}$ = 1.0 $mM^{-1}cm^{-1}$, [23,24]). Activities of the H_2O_2-oxidized enzymes are reported relative to the unoxidized enzymes maintained under the same conditions.

H_2O_2 Turnover, H_2O_2 Titres, SDS-PAGE and Amino Acid Analysis. ABTS (700 μM) oxidation was monitored at 724 nm to determine the time course and extent of H_2O_2 turnover by 5 μM enzyme. The 24-h decay products were titrated with H_2O_2 and the absorbance change at 424-nm monitored to determine the extent of Fe^{IV}=O heme formation. Cross-linking of the proteins following addition of H_2O_2 was investigated by SDS-PAGE,[10] and amino acid analysis were carried out as previously described.[10]

Relative Fluorescence. At various time intervals (15 s - 24 h) after the

addition of H_2O_2 to 5 μM protein in 0.1 M phosphate buffer (pH 7.0), the samples were diluted with urea to give a final concentration of 1 μM protein in 8 M urea at pH 1.5. Following 280-mn excitation, fluorescence intensities were measured at 350 nm, which is the emission maximum of CCP in urea.[11] The Raman peak of water was subtracted from all emission spectra, and inner-filter effects were corrected using the formula:[25]

$$F = Fo \text{ antilog}[(A_{ex} + A_{em})/2] \qquad (6)$$

where F is the corrected fluorescence intensity, Fo the observed intensity, A_{ex} and A_{em} are the absorbances at the excitation and emission wavelengths, respectively. Relative fluorescence intensities ($\%F$) were calculated assuming $\%F = 100$ for unoxidized protein maintained under the same conditions.

RESULTS

Relative Fluorescence. The fluorescence increase, observed within the mixing time (2 - 3 s) upon denaturation of CCP(MI), W51F and W191F in urea, is accompanied by a red-shift in emission maximum to 350 nm, characteristic of Trp exposure to the aqueous environment.[11] After correcting for inner-filter effects (eq. [6]), the proteins exhibit fluorescence intensities in 8 M urea at pH 1.5 equal to that of

Trp model compound NATA, indicating that each of the 6 or 7 Trp residues in the denatured proteins possess the same fluorescence quantum yield as NATA.[10] Heme quenching is totally eliminated under these conditions due to dissociation of the heme from the polypeptide as evidenced by the appearance of free-heme spectra.[10]

Figure 5.1A summarizes the fluorescence intensities at 350 nm following denaturation of CCP(MI) at various time intervals after the addition of 2, 6, and 20 equivalents of H_2O_2. Addition of CCP(MI)-I to 8 M urea at pH 1.5 reveals loss of fluorescence due to heme-mediated Trp oxidation by H_2O_2.[10] CCP(MI)-I formed 15 s prior to denaturation retains 91 ± 3% fluorescence relative to resting CCP(MI), which corresponds to the oxidation of 0.7 ± 0.2 Trp residues. In the 24-h decay of CCP(MI)-I the number of Trps lost increases to 1.4 ± 0.2. Addition of 6 equivalents of H_2O_2 to CCP(MI) 15 s and 5 min prior to denaturation resulted in loss of ~1 and 2 Trps, and when 20 equivalents of H_2O_2 were added for the same time intervals, ~1 and 3 Trps were oxidized; this increased to a total of ~ 4 when the 20:1 sample was denatured after 24 h. Clearly, the number of Trps oxidized increases with time and the amount of H_2O_2 added. Addition of aliquots of the CCP(MI)-H_2O_2 mixtures to an ABTS solution indicated that 3 H_2O_2 were turned over in ~1 min and 10 in ~ 5 min.

Upon denaturation 15 s following its generation, W51F-I exhibits 89 ± 1% relative fluorescence in 8 M urea (pH 1.5), indicating loss of 0.7 ± 0.1 Trps out of a total of 6. Samples of W51F-I denatured over 24 h exhibit loss of 1.0 - 1.3 Trps, and addition of 6 equivalents of H_2O_2 to W51F resulted in oxidized species with essentially the same fluorescence vs time profile as W51F-I (Fig. 5.1B). The

Figure 5.1 Relative fluorescence intensities at 350 nm of 1 μM H_2O_2-oxidized protein in 8 M urea (pH 1.5) at 22 °C. 5 μM protein was reacted with H_2O_2 in 0.1 M phosphate buffer, pH 7.0, and diluted with urea at various times after addition of H_2O_2. Circles, 2 equivalents of H_2O_2 added (compound I); triangles, 6 equivalents of H_2O_2 added; squares, 20 equivalents of H_2O_2 added. Data points are the corrected (eq. [6]) relative fluorescence intensities (*%F*) and represent the averages of 4 measurements. (**A**) CCP(MI), (**B**) W51F and (**C**) W191F. Experimental conditions: 280-nm excitation; slits, 5 nm; scan rate 104 nm/min.

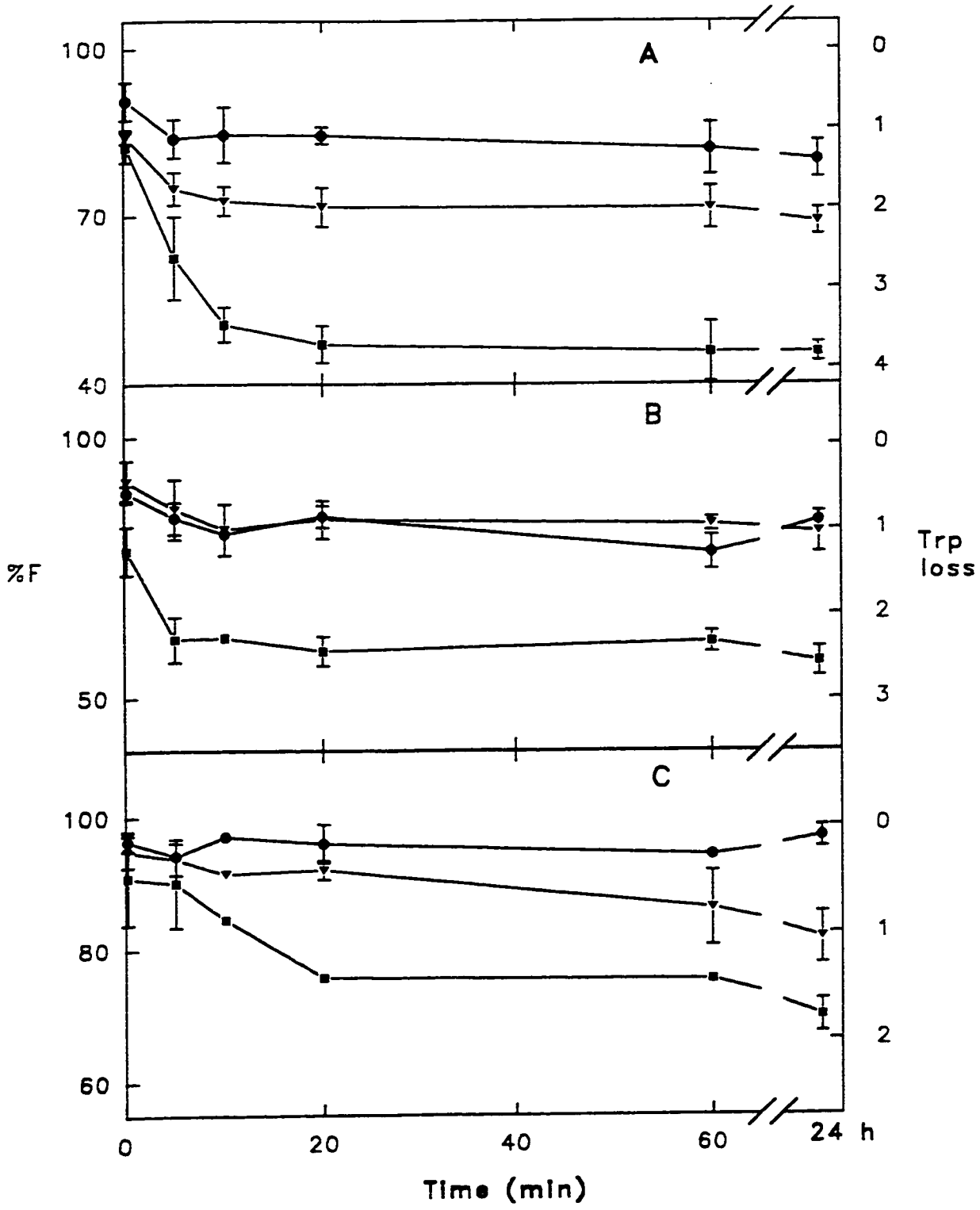
A
B
C
100
70
40
100
50
100
80
60
%F
0
1
2
3
4
0
1
2
3
0
1
2
Trp
loss
0
20
40
60
24 h
Time (min)

fluorescence loss 15 s after the addition of 20 equivalents of H_2O_2 to W51F reveals the immediate loss of ~1 Trp, and at longer times (≥ 5 min), a total loss of ~ 2.5 Trps is observed (Fig. 5.1B).

W191F-I and its 24-h decay product retain 96 - 97% relative fluorescence in 8 M urea (pH 1.5), indicating oxidation of only ~ 0.2 Trp (Fig. 5.1C). The 6:1 and 20:1 W191F samples lose Trp slowly over time, resulting in the oxidation of ~ 1 and 2 Trps, respectively in their 24-h decay products (Fig. 5.1C). Addition of aliquots of the W191F-H_2O_2 mixtures to an ABTS solution indicated that 3 H_2O_2 were turned over in ~1 min and 10 in ~ 30 min.

Enzyme Activities. Using ferrocytochrome *c* as reducing substrate, the activities of CCP(MI) and W51F are shown in Fig. 5.2. CCP(MI)-I and W51F-I formed 15 s before commencing the assays exhibit ~ 96% ferrocytochrome *c* oxidizing activity, but this is reduced to 60 - 70% in the 24-h decay products. Preincubation for 5 - 10 min with 6 equivalents of H_2O_2 further reduces the activity to 50 - 55%, and exposure to 20 equivalents results in 5% activity in W51F and ~19% activity in CCP(MI) (Fig. 5.2 and Table 5.1). W191F has negligible ferrocytochrome oxidizing activity because the presence of Trp191 is necessary for rapid reduction of the heme by ferrocytochrome *c*.[18]

Ferrocyanide oxidizing activities of CCP(MI), W51F and W191F as a function of preincubation time with 2 - 20 equivalents of H_2O_2 are summarized in Fig. 5.3. The overall dependence of activity on the number of oxidizing equivalents added and

on preincubation time is similar to that shown in Fig. 5.2. CCP(MI) and W51F shows similar activity vs preincubation time profiles except that the 6:1 W51F samples lose activity more slowly than the corresponding CCP(MI) samples. The loss in ferrocyanide oxidizing activity of the W191F samples preincubated for only 15 s with H_2O_2 is comparable to that of the other mutants; however, W191F retains considerably greater activity after 24 h, with the 2:1, 6:1 and 20:1 samples exhibiting 86, 77 and 53% activity, respectively, compared to 55%, 25% and 9% for CCP(MI) (Table 5.1).

H_2O_2 Titres. Using the relative absorbance change at 424 nm (the maximum in the difference spectrum of the Fe^{III} and Fe^{IV}=O forms), the 24-h decay products of oxidized CCP(MI) and W191F were titrated with H_2O_2 to determine the extent of their ability to reform Fe^{IV}=O heme (reaction [1]). The decay products of W191F possess the highest titres, and these match the ferrocyanide oxidizing activities closely (Table 5.1). There is also a good correspondence between the titres and ferrocytochrome *c* oxidizing activities for CCP(MI), but its ferrocyanide oxidizing activities are significantly lower (Table 5.1). The instability of the Fe^{IV}=O heme of W51F ($t_{1/2}$ ~ 3-4 s) prevented measurement of its titre; nonetheless, the decay products of this mutant exhibit comparable activity to CCP(MI) with both reducing substrates (Table 5.1).

SDS-PAGE. Table 5.2 summarizes the percent monomer in the H_2O_2-oxidized enzymes at pH 7.0. Gels of CCP(MI)-I and its 24-h decay product showed no polymerized protein, whereas the monomeric content of the 6:1 and 20:1 24-h decay

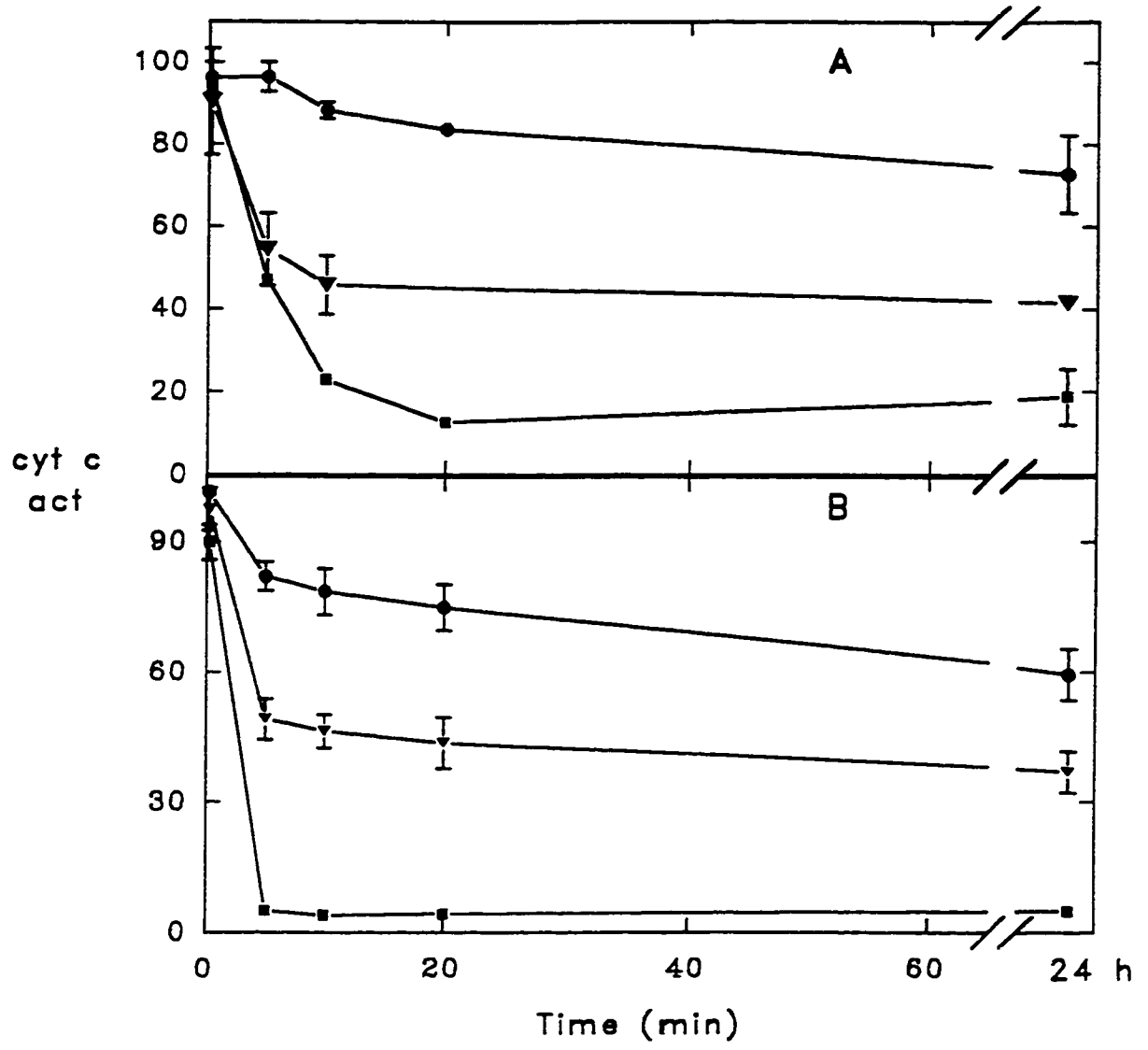

Figure 5.2 Horse heart ferrocytochrome *c* oxidizing activities relative to unoxidized protein in 0.1 M phosphate buffer (pH 7.0) of the **(A)** CCP(MI) and **(B)** W51F samples in Fig. 5.1 just prior to denaturation.

Figure 5.3 Ferrocyanide oxidizing activities relative to unoxidized protein in 0.1 M phosphate buffer (pH 7.0) of the (**A**) CCP(MI), (**B**) W51F and (**C**) W191F samples in Fig. 5.1 just prior to denaturation.

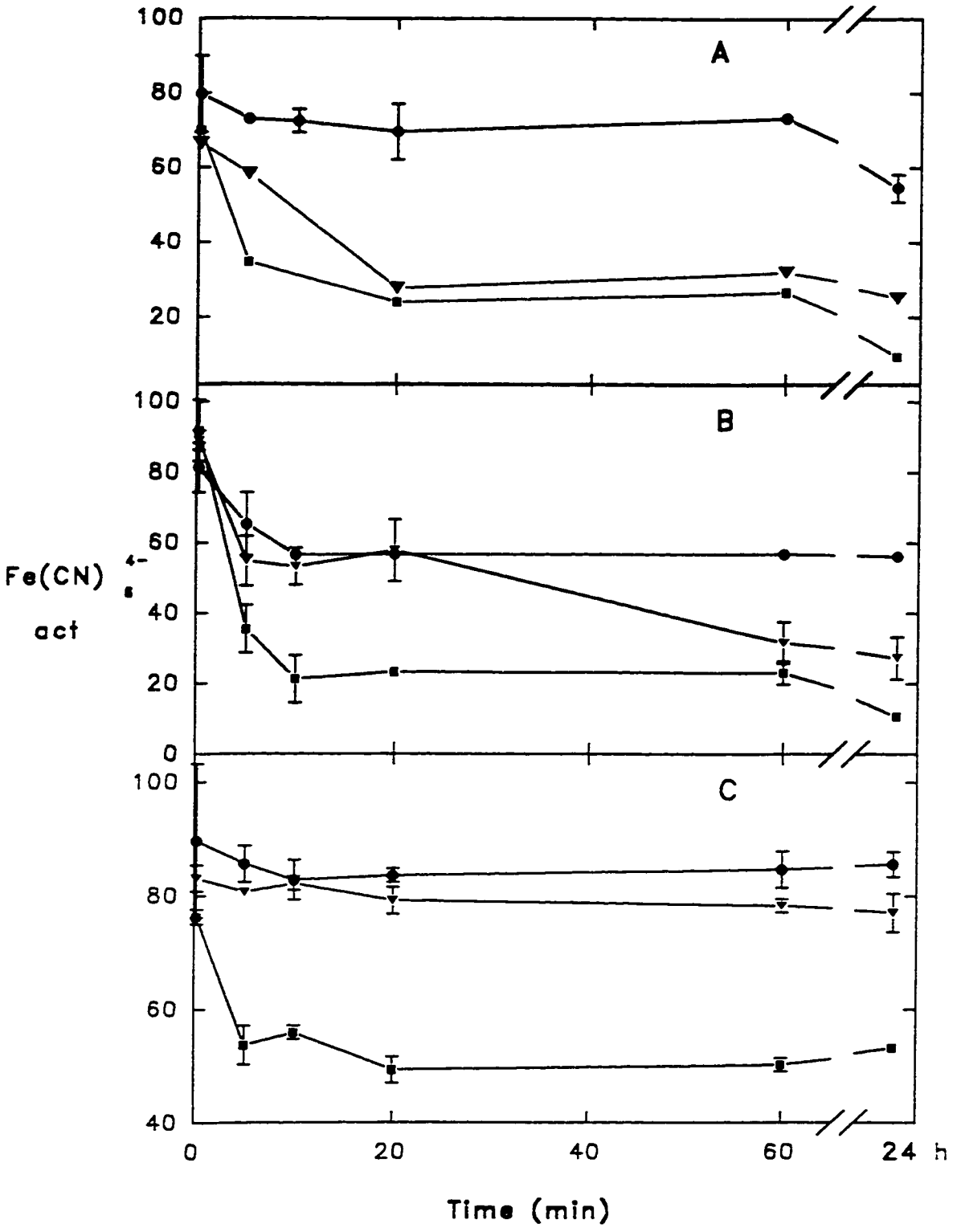
A
B
C
100
80
60
40
20
0
Fe(CN) 4-
6
act
0
20
40
60
24 h
Time (min)

products is 60 - 70%. W51F-I gives rise to 85% monomeric protein when denatured within 15 s, but the monomeric content of its decay product is reduced to 60% within ≥ 1 h. The 6:1 and 20:1 W51F samples show extensive polymerization, with a monomer content of ≤ 28% after 24 h. The percent monomer in oxidized W191F falls within the narrow range of 60 - 80% for all samples (Table 5.2), with the remainder forming dimeric forms exclusively, in agreement with published results.[18]

Amino Acid Analyses. Analyses of the 24-h decay products of CCP(MI) and W191F were carried out (insufficient W51F was available for these analyses). For both proteins the Trp loss was in good agreement with that observed by fluorescence. Loss of 0.7, 1.5, and 4.4 Tyr was observed for the 2:1, 6:1, and 20:1 decay products of CCP(MI), and the 20:1 product also lost 0.8 Met but 0 Cys. The corresponding Tyr losses for W191F were 1.5, 2.0, and 3.8, but no peroxide-induced loss of Met or Cys was observed for this mutant. Although the side chains of Met and Cys residues are readily oxidized, the amino acid analyses suggest that the endogenous donors to the heme are largely Trp and Tyr residues, rather than Met residues (Fig. 1.10) or the single Cys residue in CCP.

DISCUSSION

CCP(MI)-I exhibits 91 ± 3% fluorescence at 350 nm relative to unoxidized

Table 5.1 Properties of the 24-h decay products of H_2O_2-oxidized CCP(MI), W51F, and W191F[a]

	2 equiv. H_2O_2			6 equiv. H_2O_2			20 equiv. H_2O_2		
Property (%)[b]	CCP(MI)	W51F	W191F	CCP(MI)	W51F	W191F	CCP(MI)	W51F	W191F
H_2O_2 titer[c]	72	—[g]	94	54	—[g]	82	18	—[g]	51
Monomer[d]	100	60	67	68	26	65	60	28	65
Cyt *c* act.[e]	73	59	—	42	37	—	19	5	—
$Fe(CN)_6^{4-}$[e]	55	56	86	25	27	77	9	11	53
Trp loss[f]	~1.3	~0.5	~0.7	~1.2	~0.2	0	~0.4	~0.2	0

[a] Properties measured 24 h after oxidation of 5 μM protein in 0.1 M phosphate buffer (pH 7.0).

[b] Relative to unoxidized samples maintained under the same conditions.

[c] From H_2O_2 titrations (see text).

[d] From Table 5.2.

[e] Activities from Figs. 5.2 and 5.3.

[f] Trp loss 15 s following addition of 2 equivalents of H_2O_2 to the decay products. The loss was estimated from the change in fluorescence of the decay products in 8 M urea (pH 1.5) before and after the addition of H_2O_2 (see text)

[g] Fe^{IV}=O forms of W51F are too unstable to measure the H_2O_2 titres spectrophotometrically.

Table 5.2 Percent monomer in H_2O_2-Oxidized CCP(MI), W51F, and W191F [a]

	% Monomer[b]								
	2 equiv. H_2O_2			6 equiv. H_2O_2			20 equiv. H_2O_2		
Time	CCP(MI)	W51F	W191F	CCP(MI)	W51F	W191F	CCP(MI)	W51F	W191F
15 s	100	85	78	100	60	65	100	68	70
5 min	100	73	70	69	35	66	68	25	60
1 h	100	60	65	72	26	70	67	28	65
24 h	100	60	67	68	26	65	60	28	65

[a] 2, 6, and 20 equivalents of H_2O_2 were added to 5 μM protein in 0.1 M phosphate buffer (pH 7.0) and the samples were denatured at the times indicated.

[b] Percent monomer relative to unoxidized samples as estimated by integration of the densitometer tracings on the gels.

CCP(MI) in 8 M urea at pH 1.5, corresponding to the loss of 0.7 ± 0.2 Trp. This result is the same as that observed for yeast wild-type CCP,[10] and supports the assignment of Trp191 as the redox-active residue in CCP-I and CCP(MI)-I.[1] W51F-I exhibits the same Trp loss (0.7 ± 0.1) as CCP(MI)-I, but the fluorescence loss in denatured W191F-I is negligible (Fig. 5.1C). These results are consistent with the assignment of the EPR signals to a tyrosyl radical in W191F-I and an indolyl radical in W51F-I,[7,8] and confirm that Tyr- and Trp-based radicals can be distinguished by the fluorescence method employed here.

Dissipation of the oxidizing equivalent (Fe^{IV}=O,$P^{+\cdot}$) stored in compound I increases the Trp loss in CCP(MI)-I and W51F-I to ~1.4. The Fe^{III} heme of the decay products reacts rapidly with H_2O_2, and this leads to the immediate loss of 1.3, 0.5, and 0.7 extra Trps in CCP(MI), W51F and W191F (Table 5.1), corresponding to a *combined* loss of 2.7, 1.5, and 0.9 Trps, respectively. Oxidation of Trp51 on addition of H_2O_2 to the decay product of CCP(MI)-I is likely since Trp51 → Phe mutation significantly decreases Trp oxidation on the addition of H_2O_2 to the decay product of W51F-I. Trp51 is also a possible electron donor in the 24-h decay product of W191F-I given that reaction with H_2O_2 results in the loss of ~0.7 Trp (Table 5.1).

Addition of 6 equivalents of H_2O_2 to the *resting* enzymes prior to denaturation results in the loss of ~2 Trps in CCP(MI) and ~1 in each of the mutants (Fig. 5.1). This provides further evidence that oxidizing equivalents generated at the heme are transferred to Trp191 and Trp51 in CCP(MI) by a mechanism such as that given in eqs. [4] and [5]. The ABTS results reveal that CCP(MI) and W191F turn over 6

equivalents of H_2O_2 in less than 1 min, and the amino acid analyses show loss of 1.5 and 2 Tyr residues in CCP(MI) and W191F, respectively, in addition to the Trps oxidized in these proteins. To reduce 6 equivalents of H_2O_2 would require that three oxidized aromatic residues act as two-electron donors. However, additional donors may have gone undetected, given the experimental errors associated with amino acid analyses and the fluorescence measurements (see error bars in Fig. 5.1). LC-MS characterization of the oxidized proteins using an electrospray source is under way to determine the nature and location of the modified residues.

After standing for 24 h, the 6:1 decay products were reacted with more H_2O_2. The results revealed that an additional Trp was oxidized in CCP(MI) (Table 5.1), to give a *combined* loss of > 3 Trps. No extra Trps were oxidized in the mutants (Table 5.1), where only one Trp was initially oxidized (Fig. 5.1). Thus, both Trp191 → Phe and Trp51 → Phe mutation must shut down pathways of endogenous electron transfer to the heme that access redox-active Trp residues in the wild-type enzyme.

Following exposure to 20 equivalents of H_2O_2 a maximum Trp loss of ~4, 2.5, and 2 is observed for CCP(MI), W51F and W191F, respectively (Fig. 5.1). Amino acid analysis shows that ~4 Tyr residues were lost in both CCP(MI) and W191F, and ~1 Met in CCP(MI), and the ABTS results reveal that the 20 equivalents of H_2O_2 are turned over by CCP(MI) and W191F in 5 and 30 min, respectively. Thus, in the absence of catalatic activity ($2H_2O_2 \rightarrow O_2 + 2H_2O$), 20 electrons would have to be transferred to peroxide via the heme. Two-electron oxidation of the 9 residues found to be lost in CCP(MI) would supply 18 electrons, but only 12 electrons would be

available from the 6 residues lost in W191F. It has been shown previously that yeast wild-type CCP can turn over 20 equivalents of H_2O_2 with no detectable oxygen evolution, which eliminates turnover via catalatic activity.[20] It is possible that CCP(MI) also turns over 20 equivalents of H_2O_2 by utilizing endogenous donors, but this is less likely for W191F, and possible catalatic activity of this mutant is under investigation. It is noteworthy that an extra Trp is oxidized in the 20:1 decay product of CCP(MI) compared to the yeast enzyme[10]; furthermore, CCP(MI) turns over 20 equivalents of H_2O_2 almost five times faster than yeast CCP.[10] Hence, despite the very similar X-ray structures of the two wild-type proteins,[26] they may not utilize a common set of pathways for endogenous electron donation to the heme.

Oxidation of amino acid residues significantly reduces the ability of CCP(MI), and that of W191F to a lesser extent, to undergo reaction with H_2O_2 (eq. [1]). This is reflected in the H_2O_2 titres of the 24-h decay products listed in Table 5.1. Since one of the oxidizing equivalents of peroxide is transferred to the protein in reaction [1], depletion of endogenous donors around the heme (Fig. 1.10) may inhibit further reaction with peroxide. In addition, oxidation of the distal His52 could prevent Fe^{IV}=O formation, since this residue plays a key role in the heterolytic cleavage of peroxide, and His52 $\rightarrow$ Leu mutation results in a 10^5-fold decrease in the rate of reaction [1].[27,28] Amino acid analysis shows loss of 0.3 - 0.6 His in the decay products of CCP(MI) and 0.1 - 0.4 His in those of W191F. Thus, the slightly greater His loss in the wild-type enzyme, coupled with the greater loss of redox-active aromatic residues, may account for the lower H_2O_2 titres of the CCP(MI) decay products.

The ferrocytochrome *c* oxidizing activities of the 24-h decay products of CCP(MI), and the ferrocyanide oxidizing activities of the W191F products are similar to their H_2O_2 titres (Table 5.1). Hence, the decreased activities of these species can be attributed to the same factors that prevent Fe^{IV}=O heme formation. However, the ferrocyanide oxidizing activities of the CCP(MI) decay products are ~10 - 20% lower than the corresponding ferrocytochrome *c* oxidizing activities (Table 5.1), unlike oxidized yeast CCP where both activities were found to be the same.[10] Ferrocyanide and ferrocytochrome *c* are oxidized at different sites on CCP. The small molecule diffuses up the peroxide-access channel and is oxidized at the δ-*meso* heme edge.[29] Reconstitution of CCP with δ-*meso*-substituted heme groups blocks ferrocyanide oxidation and selectively inhibits the ferrocyanide oxidizing activity of the enzyme.[29] Retardation of ferrocyanide oxidation would thus be possible by diminishing access to the heme in the decay products by a mechanism such as radical-mediated *intra*molecular cross-linking in the neighborhood of the substrate channel.

Oxidation of ferrocytochrome *c* involves complex formation between the proteins. A putative electron transfer path via Trp191 has been proposed based on the X-ray structure of the CCP—cyt *c* complex,[18,30] in which the heme edges are separated by at least 17 Å.[18] It has been demonstrated that formation of an indolyl radical at Trp191 is necessary for the efficient ferrocytochrome *c* oxidizing activity of CCP(MI).[18] Since Trp loss is observed for the three CCP(MI) decay products (Table 5.1), it is possible that Trp191 is not 100% *irreversibly* oxidized in the fractions with ferrocytochrome *c* oxidizing activity. However, it is also possible that new

ferrocytochrome *c* oxidation sites open up in the decay products, which do not require that Trp191 remains unaltered.

A comparison of Figs. 5.1, 5.2, and 5.3 indicates that the time course of activity loss is similar to that for fluorescence loss. Both change rapidly over the first 10 - 20 min, and then slowly over the next 24 h. Hence, fluorescence is a good probe of the time course of other changes, in addition to Trp loss, induced in CCP(MI) and its mutants following reaction with peroxide.

Table 5.2 summarizes the radical-mediated *inter*molecular cross-linking in CCP(MI) and its mutants. The percent dimer observed in the oxidized W191F samples falls within the range of 20 - 40% at all time intervals, irrespective of the extent of H_2O_2 turnover. Approximately 30% dimerization of W191F-I has been reported previously,[18] which is roughly the average of the values listed for this mutant in Table 5.2. CCP(MI) exhibits a similar amount of dimerization as W191F, and also a small fraction of polymerization to higher molecular weight species, following the loss of 2 or more Trps (exposure to 6 equivalents of H_2O_2 for $\geq$ 5 min). The reaction of metmyoglobin with H_2O_2 also produces protein-based radicals, and a Tyr151-Tyr151 intermolecular cross-link has been established in sperm whale myoglobin.[31] Tyrosine radicals readily dimerize, so the dityrosine bond in myoglobin is assumed to arise from radical formation at Tyr151, which is 12 Å from the heme. Peptide mapping of the dimer formed in H_2O_2-oxidized yeast CCP indicated that an intermolecular cross-link is localized between residues 32 and 48,[23,32] a sequence that includes Tyr36, Tyr39, and Tyr42. These three Tyr residues are highly solvent

exposed and are within 5 - 14 Å from the heme (Fig. 1.10); hence, cross-linking in W191F and CCP(MI) is likely to involve dityrosine formation between these Tyr-rich regions. It is of note that ≤ 40% of oxidized CCP(MI) and W191F undergo cross-linking (Table 5.2). This suggests that the radical migration pathway(s) leading to cross-linking are shut down once alternate pathways are chosen, or that the proteins are heterogeneous. Variation in the extent of post-translational processing of the N-terminal Met^{33} in CCP(MI) and its mutants has been detected by electrospray MS (G. Tsaprailis, unpublished results), and the effects of such heterogeneity are under investigation. W51F-I exhibits similar cross-linking behavior to W191F-I (Table 5.2), but on exposure to 6 equivalents of H_2O_2, extensive conversion to higher molecular weight species is observed.

The fluorescence, activity, and cross-linking data presented here on oxidized CCP(MI) and its Trp mutants underscore the important role played by Trp residues in the redox chemistry of the enzyme. Previously, we had suggested that a ring of aromatic residues on the proximal side of the heme of yeast CCP act as donors to peroxide[10]; these residues include the 3 proximal Trps (191, 211, 223) and 3 Tyr residues (187, 229, 236) (Fig. 1.10). The fluorescence results obtained here support the loss of the 3 proximal Trps in recombinant CCP(MI), and the distal Trp51 appears to be also oxidized on addition of more than 2 equivalents of H_2O_2 to CCP(MI), as discussed previously. At least 4 Tyr residues are oxidized in CCP(MI) and these could include three from the proximal side, and one from sequence 32 - 48, which is likely to be involved in intramolecular cross-linking.

Mutation of Trp191 → Phe results in immediate cross-linking on W191F-I formation. Thus, electron transfer from a Tyr residue in sequence 32 - 48 to the porphyrin is likely to occur in W191F-I. Since Trp loss is observed following addition of > 2 equivalents of H_2O_2 to W191F, oxidation of Trp51 may follow that of the initial Tyr. It is difficult to speculate on the identity of the remaining Tyr and Trp residues oxidized in W191F; however, their oxidation does not lead to further cross-linking of the protein.

Mutation of Trp51 → Phe gives rise to a protein that undergoes extensive cross-linking following addition of > 2 equivalents of H_2O_2. Loss of 1 Trp on denaturation of W51F-I suggests than Trp191 is the first protein-based radical formed, but formation and dissipation of additional protein radicals in this mutant results in over 70% polymerization of the protein.

The ability of CCP to reduce more than 2 equivalents of H_2O_2 in the absence of its donor substrate may be important under conditions of oxidative stress in yeast.[34] Another of CCP's proposed functions is the regulation of mitochondrial respiration rates by controlling the flow of reducing equivalents to cytochrome *c* oxidase, which CCP does by competing for the same reducing substrate, ferrocytochrome *c*.[34] To carry out both of these functions, the presence of Trp51 and Trp191 is critical. Mutation of the former results in an enzyme that undergoes extensive cross-linking, presumably due to radical migration to its surface. Exposed radicals in vivo would lead to damage of other cellular components. Removal of Trp191 leads to a "well-behaved" mutant, but one with negligible ferrocytochrome *c* oxidizing activity.

ACKNOWLEDGMENTS

We wish to thank Dr Mark Miller (UCSD) for providing us with the CCP(MI), W51F and W191F proteins used in this study. This research was supported by a grant form the Natural Sciences and Engineering Research Council of Canada (NSERC) to A.M.E.

REFERENCES

1 Sivaraja, M., Goodin, D. B., Smith, M., & Hoffman, B. M. (1989) *Science 245,* 738.

2 Prince, R. C., & George, G. N. (1990) *Trends Biochem. Sci. 15,* 170.

3 Bollinger, J. M., Jr., Tong, W. H., Ravi, N., Hyunh, B. H., Edmondson, D. E., & Stubbe, J. (1994) *J. Am. Chem. Soc. 116,* 8024.

4 Sigel, H., & Sigel, A. (1994) *Metal Ions in Biological Systems: Metalloenzymes Involving Amino Acid-Residue and Related Radicals,* Vol. 30, Marcel Dekker: New York, NY.

5 Dawson, J. H. (1989) *Science 240,* 433.

6 English, A. M., Tsaprailis, G. (1995) *Adv. Inorg. Chem. 43,* 79.

7 Scholes, C. P., Liu, Y., Fishel, L. A., Farnum, M. F., Mauro, J. M., & Kraut, J. (1989) *Isr. J. Chem. 29,* 85.

8 Fishel, L. A., Farnum, M. F., Mauro, J. M., Miller, M. A., & Kraut, J. (1991) *Biochemistry 30,* 1986.

9 Erman, J. E., Vitello, L. B., Mauro, J. M., & Kraut, J. (1989) *Biochemistry 28,* 7992.

10 Fox, T., Tsaprailis, G., & English, A. M. (1994) *Biochemistry 33,* 186.

11 Fox, T., Ferreira-Rajabi, L., Hill, B. C., & English, A. M. (1993) *Biochemistry 32,* 6938.

12 Poulos, T. L., Edwards, S. L., Wariishi, H., & Gold, S. L. (1993) *J. Biol. Chem. 268,* 4429.

13 Marquez, L., Wariishi, H., Dunford, H. B., & Gold, M. H. (1988) *J. Biol. Chem. 263,* 10549.

14 Isied, S. S. (1991) in *Metal Ions in Biological Systems: Electron Transfer Reactions in Metalloproteins* (Sigel, H., & Sigel, A., Eds.,) Vol. 27, pp 1-56, Marcel Dekker: New York, NY.

15 Erman, J. E., Vitello, L. B., Miller, M. A., & Kraut, J. (1992) *J. Am. Chem. Soc. 114,* 6592.

16 Fishel, L. A., Villafranca, J. E., Mauro, J. M., & Kraut, J. (1987) *Biochemistry 26,* 351.

17 Erman, J. E., & Yonetani, T. (1975) *Biochim. Biophys. Acta 393,* 350.

18 Miller, M. A. , Vitello, L. B., & Erman, J. E. (1995) *Biochemistry 34,* 12048.

19 Neumann, N. P. (1967) *Methods Enzymol. 11,* 485.

20 Erman, J. E., & Yonetani, T. (1975) *Biochim. Biophys. Acta 393,* 343.

21 Mauro, J. M., Fishel, L. A., Hazzard, J. T., Meyer, T. E., Tollin, G., Cusanovich, M. A., & Kraut, J. (1988) *Biochemistry 27,* 6243.

22 Yonetani, T., & Ray, S. G. (1965) *J. Biol. Chem. 240,* 4503.

23 Spangler, B. D. (1984) Ph.D. Dissertation, Northern Illinois University, Dekalb.

24 Jordi, H. C., & Erman, J. E. (1974) *Biochemistry 13,* 3741.

25 Lakowicz, J. R. (1983) *Principles of Fluorescence Spectroscopy* Plenum: New York, NY.

26 Wang, J., Mauro, J. M., Edwards, S. L., Oatley, S. J., Fishel, L. A., Ashford, V. A., Xuong, N., & Kraut, J. (1990) *Biochemistry 29,* 7160.

27 Erman, J. E., & Vitello, L. B. (1992) *J. Am. Chem. Soc. 114,* 6592.

28 Erman, J. E., Vitello, L. B., Miller, M. A., Shaw, A., Brown, K. A., & Kraut, J. (1993) *Biochemistry 32,* 9798.

29 Pelletier, H., & Kraut, J. (1992) *Science 258,* 1748.

30 DePhillis, G. D., Sishta, B. P., Mauk, A. G., & Ortiz de Montellano, P. R. (1991) *J. Biol. Chem. 266,* 19334.

31 Wilks, A., & Ortiz de Montellano, P. R. (1992) *J. Biol. Chem. 267,* 8827.

32 Spangler, B. D., & Erman, J. E. (1986) *Biochim. Biophys. Acta 872,* 155.

33 Sherman, F., Stewart, J. W., & Tsunasawa, S. (1985) *BioEssays 3,* 27.

34 English, A. M. (1994) in *Encyclopedia of Inorganic Chemistry* (King, R. B. , Ed.,) Vol. 4, pp 1682-1697, Wiley: Chichester, England.

CHAPTER 6

MECHANISTIC INSIGHTS FROM MASS SPECTRAL ANALYSIS INTO THE ANTIOXIDANT PROPERTIES OF YEAST CYTOCHROME *c* PEROXIDASE

All aerobic organisms produce hazardous reactive oxygen species such as hydrogen peroxide (H_2O_2).† Catalase and glutathione peroxidase (GPx) are generally recognized as the major enzymes involved in the enzymatic detoxification of H_2O_2. However, not all aerobes possess catalase activity nor can all utilize glutathione for the enzymatic catabolism of H_2O_2, suggesting that other enzymes must play a role in protecting specific organisms against H_2O_2 cytotoxicity. Cytochrome *c* peroxidase (*Cc*P), which was first reported in yeast,[1] is one such enzyme. Recently, it has been proposed that *Cc*P may represent a major antioxidant enzyme in certain parasites such as the trematode *Schistosoma mansoni*[2] and the nematode *Brugia malayi*.[3] The reported resistance of adult *S. mansoni* worms to H_2O_2-mediated killing *in vitro*, and presumably also *in vivo*, is attributed to the presence of *Cc*P and GPx in the worms[4] since catalase is absent.[5]

The catalysis of two-electron redox chemistry such as $H_2O_2 + 2H^+ + 2e^- \longrightarrow 2H_2O$ by Fe^{III} heme centres necessitates the generation of radical species. Binding of H_2O_2 to ferric heme peroxidases (Fe^{III},P) results in heterolytic cleavage of the O-O bond, and formation of a two-electron oxidized intermediate (Fe^{IV}=O,$P^{+\bullet}$), termed compound I (eq 1). Reduction of the latter in one-electron steps (eqs 2 & 3) back to

---

† This Chapter has been formatted to comply with the guidelines outlined in *Science*. The structure of this Chapter is therefore different from that of Chapters 2 to 5. Furthermore, the *experimental procedures* in this chapter appear in the body of the figure captions rather than as a separate subsection.

the resting enzyme occurs via formation of the one-electron oxidized intermediate (Fe^{IV}=O,P), termed compound II.

$$Fe^{III},P + H_2O_2 \rightarrow Fe^{IV}=O,P^{+\cdot} + H_2O \quad (1)$$

$$Fe^{IV}=O,P^{+\cdot} + 1e^- \rightarrow Fe^{IV}=O,P \quad (2)$$

$$Fe^{IV}=O,P + 1e^- + 2H^+ \rightarrow Fe^{III},P + H_2O \quad (3)$$

In most heme peroxidases $P^{+\cdot}$ is a porphyrin π-cation radical,[6,7] but a protein-based radical on Trp191, which is in van der Waals contact with the heme, is observed for yeast C*c*P (YC*c*P) compound I.[8,9] This was the first instance that a Trp residue was shown to play a redox-active role in an enzyme,[10] and the X-ray structure of the complex between recombinant YC*c*P [C*c*P(MI)] and cytochrome *c* reveals that the latter is bound at the surface of C*c*P(MI) to maximize electron transfer to the Trp191 radical following reduction of H_2O_2.[11] To date, YC*c*P is the only known *monoheme* peroxidase with ferrocytochrome *c* oxidizing ability.

Over 20 years ago it was reported that YC*c*P can reduce up to 20 equivalents of H_2O_2 in the absence of a reducing substrate by using endogenous donors on its polypeptide.[12] No evolution of O_2 was detected which eliminated the possibility of catalatic activity ($2H_2O_2 \rightarrow O_2 + 2H_2O$) and, since apoYC*c*P does not reduce H_2O_2 under the same conditions, reduction must be mediated via the heme. A mechanism consistent with the reduction of 2 equivalents of H_2O_2 by *compound I* is the following:

$$Fe^{IV}=O,P^{+\bullet} + 2H^+ \rightarrow Fe^{III},P^{+\bullet},P_x^{\bullet} + H_2O \quad (4)$$

$$Fe^{III},P^{+\bullet},P_x^{\bullet} + H_2O_2 \rightarrow Fe^{IV}=O,P^{+\bullet},P_x^{\bullet},P_y^{\bullet} + H_2O \quad (5)$$

Electron transfer to the $Fe^{IV}=O$ heme results in formation of $P_x^{\bullet}$ in eq (4), and reaction of H_2O_2 with the newly-formed Fe^{III} heme leads to the generation of an additional protein-based radical ($P_y^{\bullet}$) as shown in eq 5. YC*c*P can undergo reactions 4 and 5 until ~20 equivalents of H_2O_2 are reduced before destruction of the heme becomes apparent.[12]

Figure 6.1 reveals that a number of readily oxidizable residues (Tyr, Trp, Met) surround the heme in YC*c*P. Previously, we have shown by protein fluorescence and amino acid analysis that multiple Tyr and Trp residues are lost in H_2O_2-oxidized YC*c*P,[13] in C*c*P(MI) and in mutants (W51F and W191F) where the Trp residues closest to the heme (Figure 6.1) are singly mutated to Phe.[14] The affect of oxidation on the residual activity and the extent of radical-mediated intermolecular crosslinking in C*c*P(MI) and its mutants was reported.[14]

H_2O_2-MEDIATED CROSSLINKING

Table 6.1 summarizes the radical-mediated *inter*molecular dimerization of C*c*P(MI) and its mutants. No dimerization of oxidized C*c*P(MI) is observed within 1 h unless the enzyme is exposed to >2 equivalents of H_2O_2, which results in ~30% homodimer formation. The percent homodimer observed in the oxidized W191F

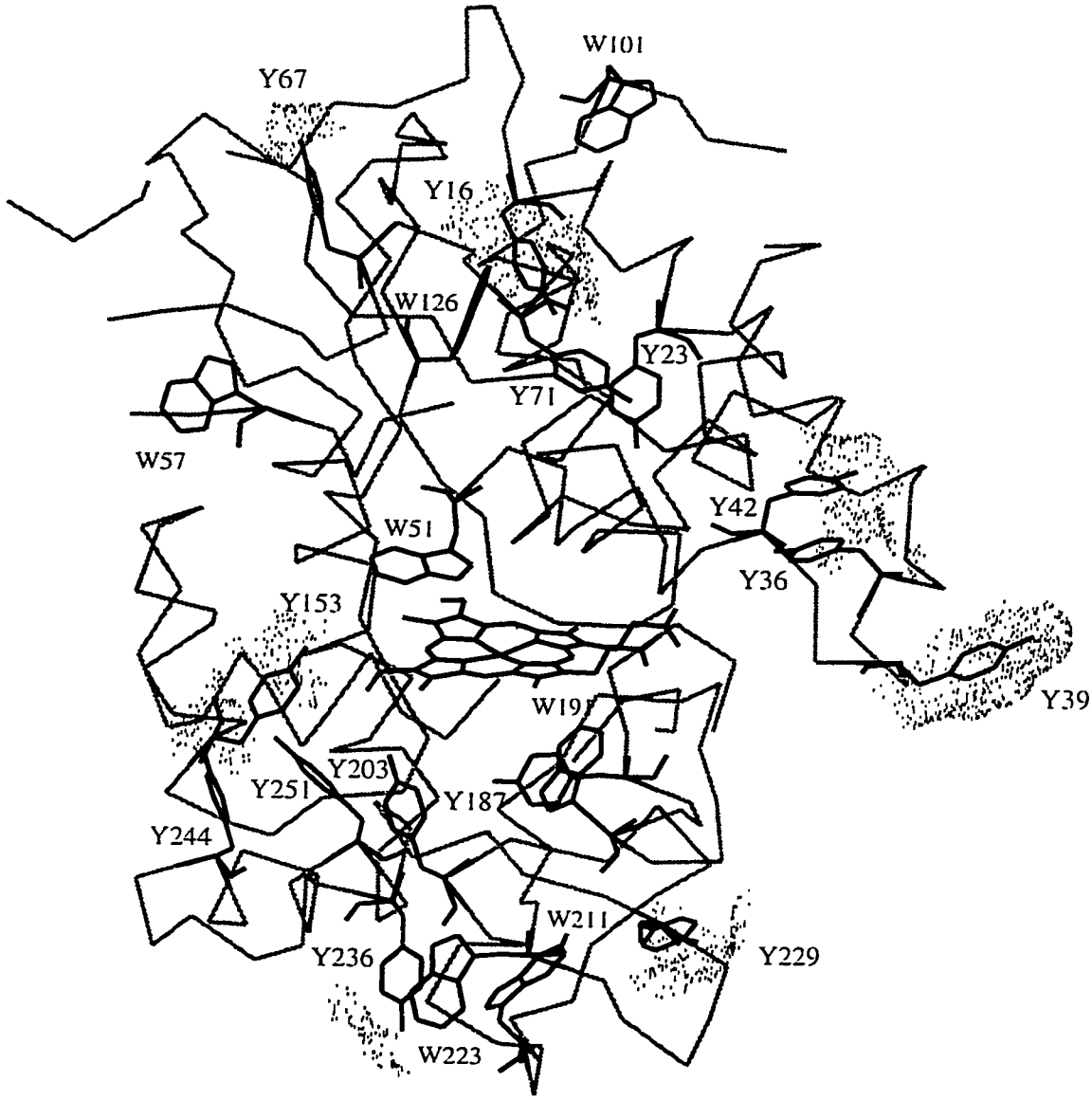

Figure 6.1 The C_α backbone of *Cc*P(MI) showing the location of the 7 Trp (W) and 14 Tyr (Y) residues relative to the heme. The solvent-exposed surfaces of the most exposed Tyr residues are shown as dots and were calculated using the Conolly algorithm available with the Insight II software package (v. 95.0; BIOSYM Technologies Inc., San Diego). The *Cc*P(MI) coordinates are from Ref. 26.

samples within 1 h is 30-35% irrespective of the extent of H_2O_2 turnover, and these values are in agreement with the ~30% dimerization in W191F compound I reported previously.[15] Since the extent of homodimer formation in oxidized *Cc*P(MI) and W191F is relatively constant (Table 6.1), the radical migration pathway(s) leading to crosslinking must be shutdown once alternate migration pathways are chosen. The W51F mutant exhibits extensive crosslinking on H_2O_2-oxidation and formation of higher molecular weight polymeric species is also observed.

Peptide mapping of the dimer formed in H_2O_2-oxidized Y*Cc*P at pH 4.5 indicated that an intermolecular crosslink is localized between residues 32 and 48,[16,17] a sequence that includes Tyr36, Tyr39 and Tyr42. These three Tyr residues are solvent exposed and are within 5 - 14 Å of the heme (Figure 6.1); hence, crosslinking in Y*Cc*P is likely to involve dityrosine formation between these tyrosine-rich regions.

To determine the site(s) of the crosslinking in *Cc*P(MI) and W191F at neutral pH, the homodimers were separated from the monomeric forms by gel-permeation FPLC (Figure 6.2). Tryptic digestion of both the monomer and dimer peaks was carried out and the digests were analyzed by HPLC with electrospray mass spectral detection (LC-MS). The results of peptide mass mapping of the monomeric and dimeric forms of W191F oxidized with 2 equivalents of H_2O_2 are shown in Figure 6.3. Changes were observed in the chromatograms above scan number 600; additional peaks resulting from T_6—T_6 and T_6—T_{26} crosslinking were observed in the dimer map but not in that of the monomer. As expected, the crosslinked peptides contain solvent-exposed Tyr36, 39, 42 (T_6) and Tyr229, 236 (T_{26}) (Figure 6.1); the T_6—T_6 crosslinked

Table 6.1 Crosslinking in H_2O_2-Oxidized *Cc*P(MI), W51F and W191F within 60 min[a]

	% dimer		
Sample	2 equiv H_2O_2	6 equiv H_2O_2	20 equiv H_2O_2
*Cc*P(MI)[b]	0	28	33
+ *cyt c*[c]	✓	✓	✓
W191F[b]	35	30	35
+ *cyt c*[c]	✓	✓	✓
W51F[b]	40	74	72
+ *cyt c*[c]	X	X	X

[a] The indicated equivalents of H_2O_2 were added to 5 μM protein in 0.1 M phosphate buffer (pH 7.0) and the samples were left standing for 60 min at room temperature. Crosslinking of the proteins on H_2O_2 oxidation was investigated by SDS PAGE.[13]

[b] Percent homodimer (*Cc*P-*Cc*P; MW 70 kDa) formation is relative to that in unoxidized samples as estimated by integration of the densitometer tracings of the gels on a Fisher-Biotech transmission densitometer.

[c] Check mark (✓) indicates the formation of a *Cc*P-cyt *c* heterodimer (MW 47 kDa) as determined by SDS PAGE on H_2O_2-oxidation of 5 μM *Cc*P in the presence of 25 μM ferricytochrome *c* in 0.1 M phosphate buffer, pH 7.0.

Figure 6.2 Gel Permeation Chromatography of the H_2O_2-Oxidized W191F Mutant. W191F (5 μM) was reacted in 75 mL of 0.1 M NaPi buffer (pH 7.0) with 2 equivalents of H_2O_2 to form compound I, and allowed to stand at room temperature overnight. The W191F compound I decay product was concentrated to ~ 250 μM in a Amicon stirred ultrafiltration cell with a YM-10 membrane (10000 MW cut off). Gel permeation chromatography was carried out on a Pharmacia Superose 12 FPLC column equilibrated with 50 mM NaPi/0.2 M KCl (pH 7.0). The sample (25 - 130 nmol per run) was eluted in the same buffer at a flow rate of 0.3 mL/min. The fractions eluting at the same volume on multiple runs were pooled. SDS-PAGE on a 10% gel confirmed that peaks A and B were the dimeric and monomeric forms of H_2O_2-oxidized W191F, respectively. The concentration of the pooled fractions (A and B) was determined using the Bradford protein assay.[27]

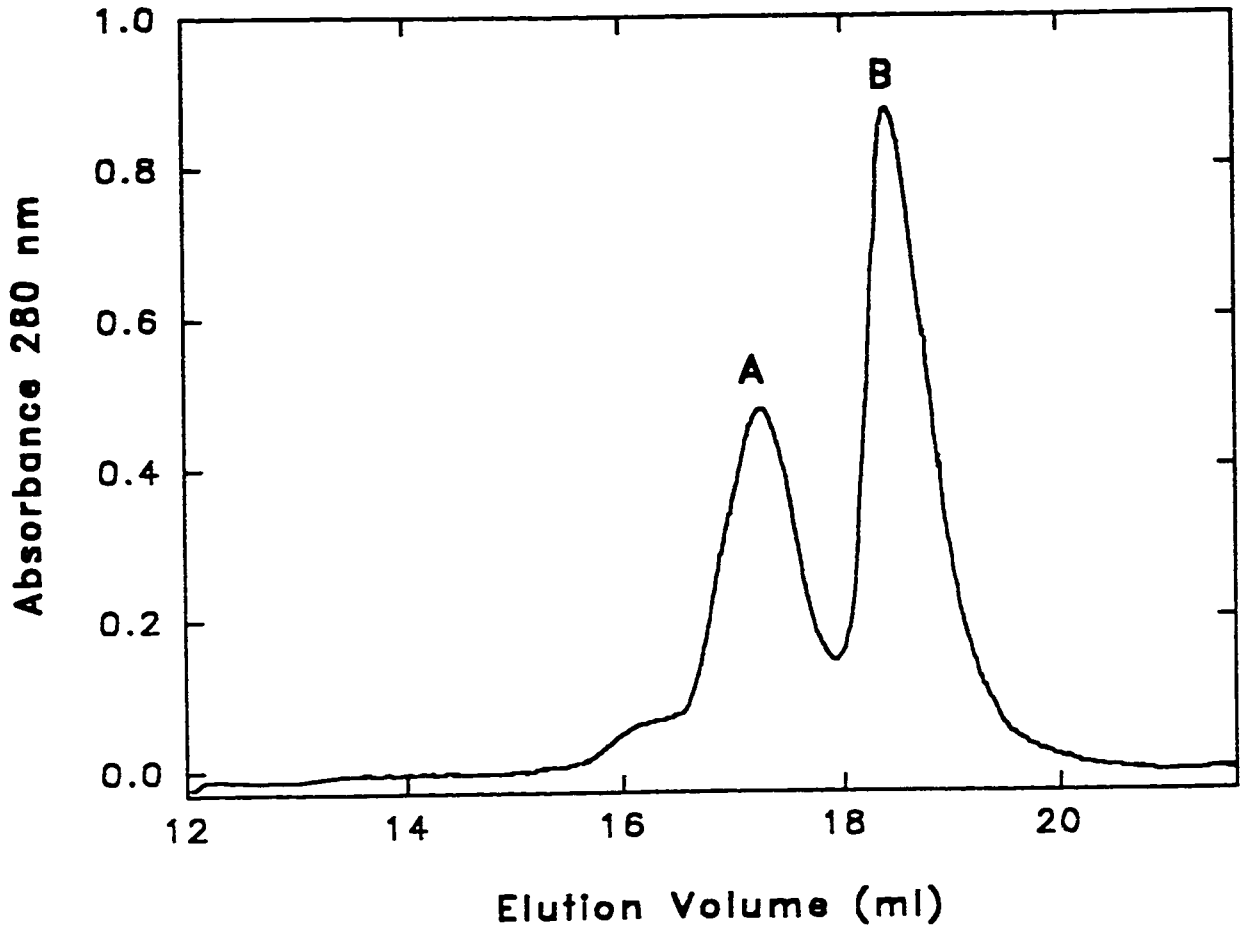
1.0
0.8
0.6
0.4
0.2
0.0
Absorbance 280 nm
A
B
12
14
16
18
20
Elution Volume (ml)

peptide is in higher abundance, presumably because Tyr39 is the most exposed tyrosine in *Cc*P(MI). Interestingly, ***no*** T_{26}—T_{26} crosslink was observed, indicating that radical formation on T_6 is necessary for dimer formation.

Since no dimerization is detectable in *Cc*P(MI) oxidized with 2 equivalents of H_2O_2 (Table 6.1), enzyme treated with 20 equivalents of H_2O_2 was used for gel permeation and LC-MS analysis. The gel permeation results on H_2O_2-oxidized *Cc*P(MI) were the same as those for W191F (Figure 6.2). The *Cc*P(MI) dimer mass map, although poor in quality due to MS technical problems, revealed that a number of peptides were missing including T_{26} (Tyr229,236), T_{23} (Trp191, Tyr187,203), T_3 (Tyr16), and T_1 which had the initial Met processed. It is of note that all these missing peptides, with the exception of T_1, contained oxidizable aromatic residues which are likely endogenous donors to the heme.[13,14]

ANALYSIS OF *Cc*P SPIN ADDUCTS BY LC-MS

Previously, we have shown that LC-MS can be used to identify the adducts formed by trapping the protein-based radicals formed in H_2O_2-oxidized horse heart metmyoglobin with the spin trap, 2-methyl-2-nitrosopropane (MNP).[18] Reduction of the spin adducts with ascorbate resulted in derivatives that were stable under the conditions used to carry out peptide mass mapping by LC-MS.[18] Addition of MNP to the reactions between 20 μM W191F with 2 and 20 equivalents of H_2O_2 resulted in no detectable changes in the mass of the mutant. This indicates that saturated MNP

Figure 6.3 Peptide Mass Mapping of (**A**) Monomeric and (**B**) Dimeric Forms of H_2O_2-Oxidized W191F Mutant. Peaks A and B (3 and 6 nmol, respectively) from the gel permeation chromatograph (Figure 6.2) were loaded onto a Vydac reversed phase C18 4.6- x 250-mm HPLC column, and the heme-free forms were eluted with a 10 - 50% CH_3CN gradient in 0.05% TFA at 1 mL/min over 20 min. The apoproteins (~ 200 µg) were lyophilized and resuspended in 0.1 M NaPi/10% CH_3CN at pH 7.0. Sequencing-grade trypsin (Boehringer Mannheim) was added at a sample:trypsin ratio of 50:1 (w/w) and digestion was carried out at 37 °C for 4 h, and terminated by freezing in Liq. N_2. The tryptic peptides (3-4 µg) were separated on a Vydac reversed phase C18 1- x 250-mm column with a 0 - 60% CH_3CN gradient in 0.05% TFA at 40 µL/min over 100 min. The LC-MS system consisted of a Hewlett Packard 1090 HPLC and a Finnigan SSQ 7000 single quadrupole mass spectrometer fitted with an electrospray ionization source. The needle spray voltage was 4.5 kV and on-line acquisition of mass spectra was performed a rate of 5 s/scan. Native tryptic peptides T_{32} , T_{33} , T_6 and T_{26}, are labelled as well as the crosslinked peptides, T_6—T_6 and T_6—T_{26}, in the reconstituted ion chromatograms (RIC) in **A** and **B**.

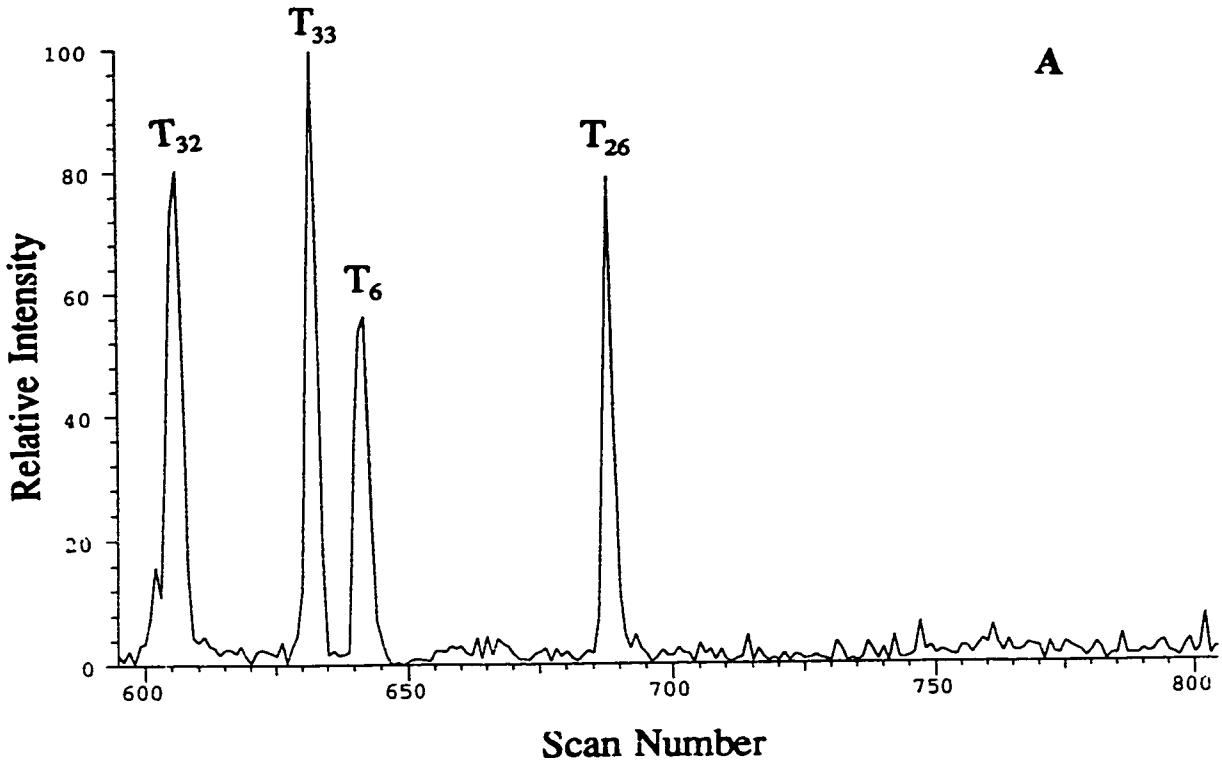
A
T_{33}
T_{32}
T_{26}
T_6
Relative Intensity
100
80
60
40
20
0
600
650
700
750
800
Scan Number

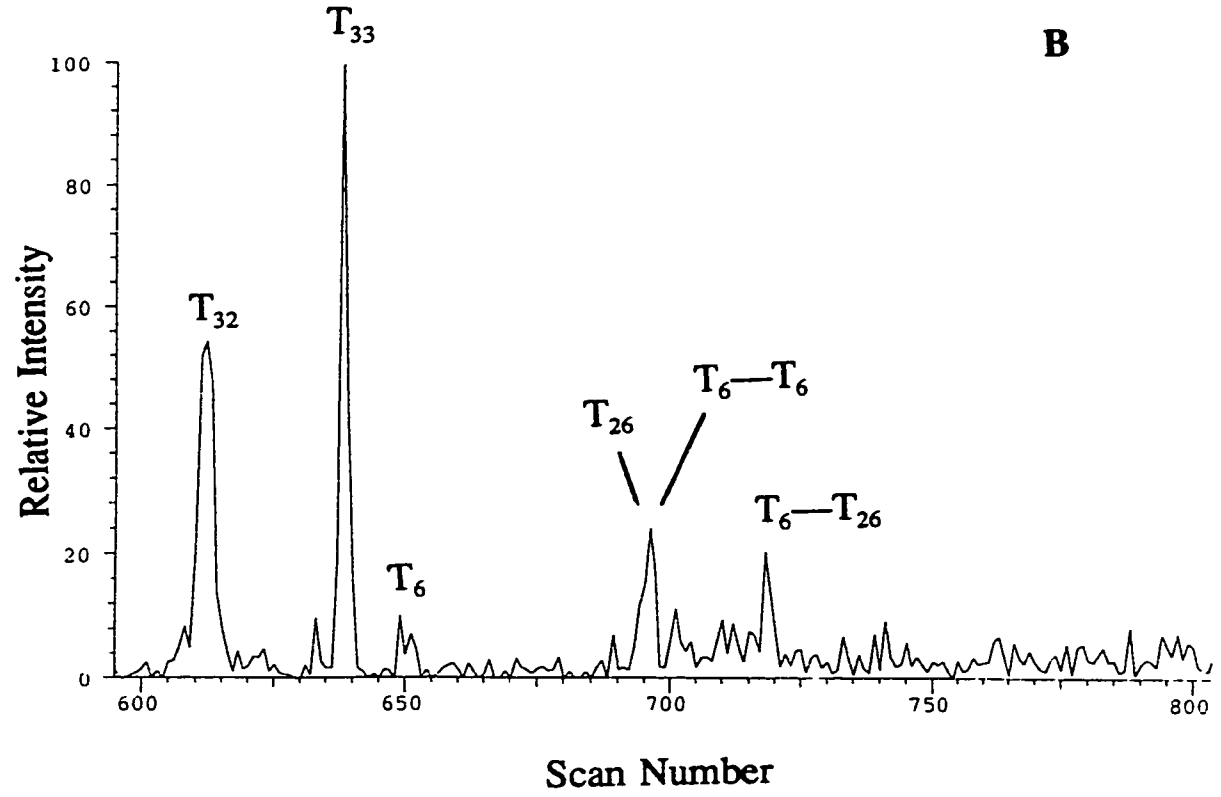
B
T_{33}
T_{32}
T_6—T_6
T_{26}
T_6—T_{26}
T_6
Relative Intensity
100
80
60
40
20
0
600
650
700
750
800
Scan Number

cannot compete with dimerization in 20 μM W191F.

When MNP is added to C*c*P(MI)/H_2O_2 reactions, mass changes are observed in the undigested protein (data not shown) and in a number of Tyr-containing tryptic peptides. Figure 6.4A shows that T_{26} is extensively modified in C*c*P(MI) oxidized with 20 equivalents of H_2O_2 in the presence of MNP. Sequencing of this peptide by MS (Figure 6.4B) reveals that spin-adduct formation occurs on Tyr236, which has an increased mass of 72 as observed previously for the Tyr-MNP spin adduct in myoglobin.[18] Mass changes of +72 Da are also observed for ~ 50% T_{21} which contains Tyr153, and for a small fraction of T_6 which contains Tyr36, 39 and 42. Hence, spin adduct formation can clearly compete with dityrosine formation in oxidized C*c*P(MI). This is presumably due to the fact that the Tyr236 radical is less reactive than the radical(s) in T_6 (Tyr36, 39 and/or 42) in dityrosine formation, which is considered a possible marker of organismal oxidative stress.[19] Hence, radical translocation in C*c*P(MI) should result in less cellular damage compared to radical translocation in W191F or in W51F, which in the latter mutant leads to extensive dimerization and polymerization indicative of highly reactive surface radicals. It is also noteworthy that 25 μM ferricytochrome *c* can compete with homodimer formation in H_2O_2-oxidized C*c*P(MI) and W191F, but not in the W51F mutant (Table 6.1). Since cytochrome *c* docks to C*c*P(MI)[11] between Tyr229 and Tyr39 (Figure 6.1), the lack of heterodimer formation in the W51F/cytochrome *c* complex suggests that radical formation on Tyr39 may not be extensive in W51F.

Figure 6.4 Mass Spectral Analysis of MNP Spin Adducts Formed in H_2O_2-Oxidized C*c*P(MI). A stock (23 mM) 2-methyl-2-nitrosopropane (MNP; Aldrich) solution was prepared from the MNP dimer in 50 mM NaPi buffer (pH 7.4) pre-treated with Chelex resin (BioRad) which also contained 50 µM diethylenetriamine-*N,N,N',N'',N''*-pentaacetic acid (DETPA). Stock (50 µl) C*c*P(MI) in 0.1 M NaPi buffer (pH 7.0) was added to the MNP-containing buffer to yield final C*c*P(MI) and MNP monomer[28] concentrations of 20 µM and 11 mM, respectively. Oxidation of C*c*P(MI) was initiated by the addition of 2 or 20 equivalents of H_2O_2. At 10 min following the addition of H_2O_2, ascorbate and HCl were added and the reaction mixture (~ 340 µg of protein) was injected onto a reversed phase C18 4.6- x 250-nm column (Vydac) and the protein separated from its heme and buffer salts with a 10-50% CH_3CN gradient in 0.05% TFA at 1 mL/min over 20 min. ApoC*c*P(MI) was lyophilized and resuspended in 0.1 M NaPi (pH 7.0) and ~50 µg was digested with 20:1 (w/w) trypsin at 37 °C for 2 h. Digestion was stopped by freezing in Liq. N_2, and 2-4 µg was separated on a Vydac microbore C18 1- x 250-nm column with a 0-60% CH_3CN gradient in 0.05% TFA at 40 µL/min over 100 min. On-line LC-MS of the digests (**A**) was carried out as described in Figure 6.3. MNP spin adduct formation was observed in peptide T_{21} which coeluted with native T_{21} (scan 381-386; not shown), in T_6 and in T_{26}. On-line CID sequencing of modified T_{26} (**B**) was performed in the capillary/skimmer region of the SSQ with the capillary at 67 mV and the tube lens at 120 mV. The +1, +2 and +3 ions fragment in this region and were analyzed in Q1. The fragment ions (*b* and *y*) are shown in panel (**B**) along with the sequence of T_{26} and the modified Tyr residue (Y^*).

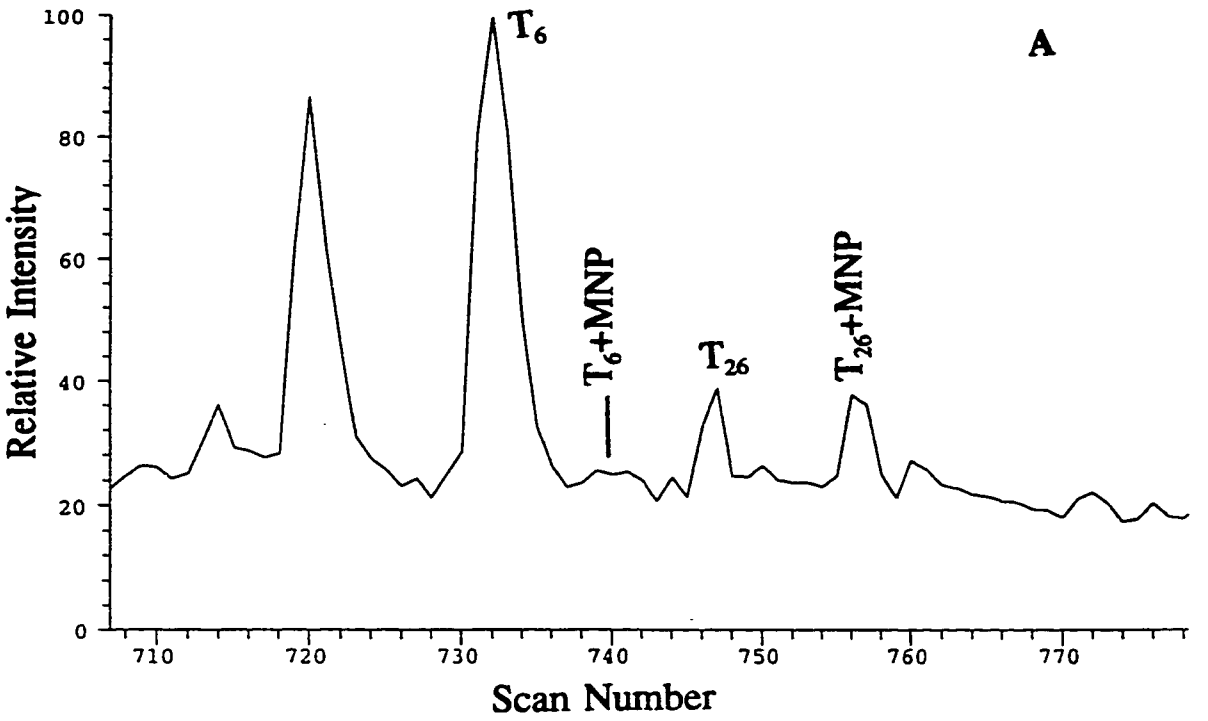
A
T6
T6+MNP
T26
T26+MNP
Relative Intensity
Scan Number
100
80
60
40
20
0
710
720
730
740
750
760
770

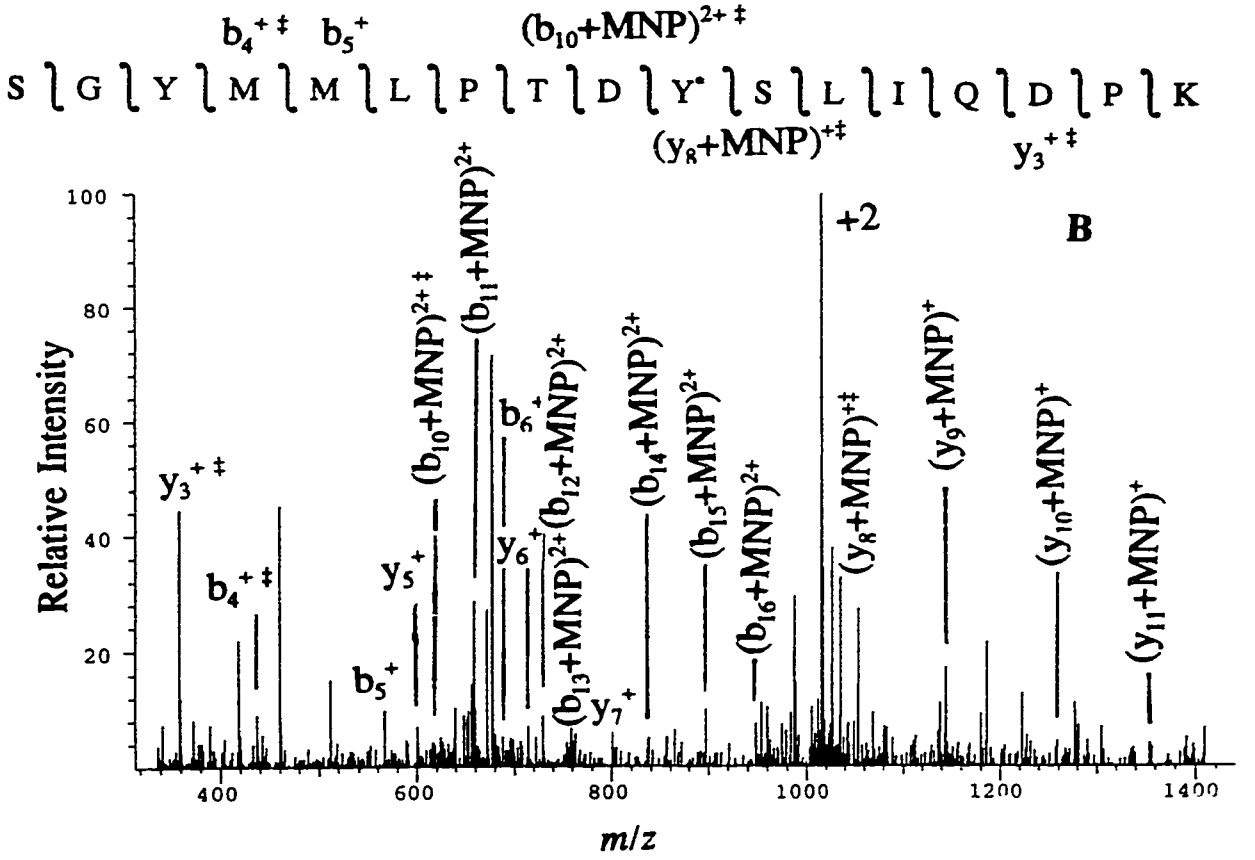
b4+‡ b5+
(b10+MNP)2+‡
S G Y M M L P T D Y* S L I Q D P K
(y8+MNP)+‡
y3+‡
B
+2
Relative Intensity
m/z
y3+‡
b4+‡
b5+
y5+
(b10+MNP)2+‡
(b11+MNP)2+
b6+
y6+
(b12+MNP)2+
(b13+MNP)2+
y7+
(b14+MNP)2+
(b15+MNP)2+
(b16+MNP)2+
(y8+MNP)+‡
(y9+MNP)+
(y10+MNP)+
(y11+MNP)+
100
80
60
40
20
400
600
800
1000
1200
1400

PROTECTION AGAINST OXIDATIVE DAMAGE IN YEAST

Heme-free apoYC*c*P is rapidly converted to holoYC*c*P during the adaptation of yeast to oxygen.[20] Heme insertion is oxygen induced, and the levels of apoYC*c*P in anaerobically growing yeast are similar to those of the holoenzyme found under aerobic conditions.[21] Although the adaptive formation of C*c*P in yeast is a striking example of how a cell can rapidly manufacture an active hemoprotein in response to oxygen, little attention has been given to the antioxidant role of YC*c*P. C*c*P activity has also been identified in a number of bacteria with the diheme enzyme from *Pseudomonas aeruginosa* being the best characterized,[22] but again little attention has been paid to the function of C*c*P in bacteria.

The ability of YC*c*P to reduce more than 2 equivalents of H_2O_2 in the absence of its donor substrate, ferrocytochrome *c*, may be important in the rapid adaptation of yeast to aerobic conditions. Expression of most of the heme proteins in *Saccharomyces cerevisiae* is regulated by oxygen.[23] However, unlike YC*c*P, *de novo* synthesis of catalase and cytochrome *c* is cycloheximide sensitive, indicating that expression of these proteins is transcriptionally controlled.[21] Thus, accumulation of YC*c*P under aerobic growth is likely to occur before its reducing substrate, ferrocytochrome *c*. Hence, the demonstrated ability of C*c*P(MI) to store a number of oxidizing equivalents on its polypeptide with minimal crosslinking could be very important at this juncture. It is also relevant that H_2O_2-oxidized C*c*P(MI) retains ~20% activity[14] even after reducing 20 equivalents of peroxide. Thus, YC*c*P likely plays a

key role in enzymatic detoxification of H_2O_2 before catalase accumulates in the cell.

Clearly, Trp51 and Trp191 are key residues in *Cc*P(MI). The MS data presented here on oxidized *Cc*P(MI) and its W191F mutant underscore the important role played by these residues in the redox chemistry the enzyme. Mutation of Trp191 → Phe results in immediate crosslinking on compound I formation, and the high yield of T_6—T_6 peptide indicates that this likely arises from rapid Tyr → porphyrin electron transfer in W191F compound I. Bound ferricytochrome *c* can compete with the rapid dityrosine formation (Table 6.1) but not freely-diffusing MNP. It is difficult to speculate on the identity of the residues oxidized in the monomeric form(s) of W191F but their oxidation obviously does not lead to further crosslinking of the protein. However, reoxidation of the FPLC-collected monomer (Peak B; Figure 6.2) should be carried out to verify this.

Mutation of Trp51 → Phe gives rise to a protein that undergoes extensive crosslinking following addition of > 2 equivalents of H_2O_2. Loss of 1 Trp on denaturation of W51F-I suggests than Trp191 is the first protein-based radical formed,[14] but formation and dissipation of additional protein radicals in this mutant results in over 70% polymerization of the protein.

Another of YC*c*P's proposed functions is the regulation of mitochondrial respiration rates by controlling the flow of reducing equivalents to cytochrome *c* oxidase by competing for the same reducing substrate, ferrocytochrome *c*.[24] For this function as well as H_2O_2 detoxification, the presence of both Trp51 and Trp191 is critical. Mutation of the former results in an enzyme that undergoes extensive

crosslinking, presumably due radical migration to its surface. Exposed radicals *in vivo* would lead to damage of other cellular components. For example, oxidation of metmyoglobin with H_2O_2 also produces highly reactive protein-based radicals,[18] which may play a role in cell damage during reperfusion of the heart.[25] Removal of Trp191 in CcP(MI) results in less extensive crosslinking but this mutant exhibits negligible ferrocytochrome *c* oxidizing activity.[15]

ACKNOWLEDGMENTS

We wish to thank Dr Mark Miller (UCSD) for providing us with the CcP(MI), W51F and W191F proteins, and the transformed *E. coli* cells that were used to isolate CcP(MI) and W191F for this study.

REFERENCES

1 Altschul, A. M., Abrams, R., & Hogness, T. R. (1940) *J. Biol. Chem. 136,* 777.

2 Campos, E. G., Smith, T. M., & Prichard, R. K. (1995) *Comp. Biochem. Physiol. B. 111,* 371.

3 Ou, X., Thomas, R., Chacon, M. R., Tang, L., & Selkirk, M. E. (1995) *Exp. Parasitolol. 80,* 530.

4 Smith, J. M., Mkoji, G. M., & Prichard, R. K. (1989) *Am. J. Trop. Med. Hyg. 40,* 186.

5 Mkoji, G. M., Smith, J. M., & Prichard, R. K. (1988) *Int. J. Parasitol. 18,* 667.

6 Dawson, J. H. (1989) *Science 240,* 433.

7 English, A. M., & Tsaprailis, G. (1995) *Adv. Inorg. Chem. 43,* 79.

8 Scholes, C. P., Liu, Y., Fishel, L. A., Farnum, M. F., Mauro, J. M., & Kraut, J. (1989) *Isr. J. Chem.* 29, 85.

9 Sivaraja, M., Goodin, D. B., Smith, M., & Hoffman, B. M. (1989) *Science 245,* 738.

10 Prince, R. C., & George, G. N. (1990) *Trends Biochem. Sci. 15,* 170.

11 Pelletier, H., & Kraut, J. (1992) *Science 258,* 1748.

12 Erman, J. E., & Yonetani, T. (1975) *Biochim. Biophys. Acta. 393,* 350.

13 Fox, T., Tsaprailis, G., & English, A. M. (1994) *Biochemistry 33,* 186.

14 Tsaprailis, G., & English, A. M. (1996) *Can. J. Chem. 74,* 2250.

15 Miller, M. A., Vitello, L. B., & Erman, J. E. (1995) *Biochemistry 34,* 12048.

16 Spangler, B. D., & Erman, J. E. (1986) *Biochim. Biophys. Acta 872,* 155.

17 Spangler, B. D., Ph. D. Dissertation, Northern Illinois University, Dekalb, 1984.

18 Fenwick, C. W., & English, A. M. (1996) *J. Am. Chem. Soc. 118,* 12236.

19 Giulivi, C., & Davies, K. J. A. (1993) *J. Biol. Chem. 268,* 8752.

20 Sels, A. A., & Cocriamont, C. (1968) *Biochem. Biophys. Res. Commun. 32,* 192.

21 Djavadi-Ohaniance, L., Rudin, Y., & Schatz, G. (1978) *J. Biol. Chem. 253,* 4402.

22 Ellfolk, N., Rönnberg, M., & Österlund, K. (1991) *Biochim. Biophys. Acta 1080,* 68.

23 Zitomer, R. S., & Lowry, C. V. (1992) *Microbiol. Rev. 56,* 1.

24 English, A. M. (1994) in *Encyclopedia of Inorganic Chemistry: Iron: Heme Proteins, Peroxidases, & Catalases,* (King, R. B., Ed.,) Vol. 4., pp 1682-1697, John Wiley & Sons: Chistester, England.

25 Kelman, D. J., DeGray, J. A., & Mason, R. P. (1994) *J. Biol. Chem. 269,* 7458.

26 Wang, J., Mauro, J. M., Edwards, S. L., Oatley, S. J., Fishel, L. A., Ashford, V. A., Xuong, N. -H., & Kraut, J. (1990) *Biochemistry 29,* 7160.

27 Bradford, M. (1976) *Anal. Biochem. 72,* 248.

28 Makino, K., Moriya, F., & Hatano, H. (1985) *J. Chromatogr. 332,* 71.

Addendum 2

In order to apply LC-MS methodology to future investigations of H_2O_2-oxidized HRP, peptide mass mapping of the native protein was carried out. Grade I lyophilized HRP from Boehringer Mannheim was used to prepare 200 µM stock protein in 0.1 M sodium phosphate buffer (pH 7.0). ApoHRP (~ 140 µg) was formed by heme removal on a reversed phase C18 4.6- x 250-nm HPLC column (Vydac) with a 10 - 50% CH_3CN gradient in 0.05% TFA at 1 mL/min over 20 min. The apoHRP was lyophilized and resuspended in 0.1 M sodium phosphate buffer at pH 7.0. Sequencing-grade trypsin from Boehringer Mannheim was added at a sample:trypsin ratio of 10:1 (w/w) and digestion was carried out at ambient temperature for 16 - 24 h. Digestion was quenched by freezing in Liq. N_2 and ~ 3 µg was separated on a Vydac microbore phenyl 1- x 250-nm column with a 5 - 95% CH_3CN/isopropanol (70/30; v/v) gradient in 0.1% acetic acid/0.05% TFA at 40 µL/min over 120 min. On-line mass spectrometric detection (LC-MS) of the peptides was carried out as they were eluted from the column. The LC-MS system was the same as that described in Chapter 6. A spray voltage of 4.4 kV was used and data acquisition was performed at a rate of 5 s/scan.

The LC-MS RIC map of the tryptic peptides of HRP is shown in Figure A2.1. A total of 23 peaks with an ion current above 10% are labeled. The individual mass spectra at the scan numbers corresponding the to peaks in the RIC were analyzed. Based on the sequence of HRP (Figure A2.2) and the predicted masses of its tryptic

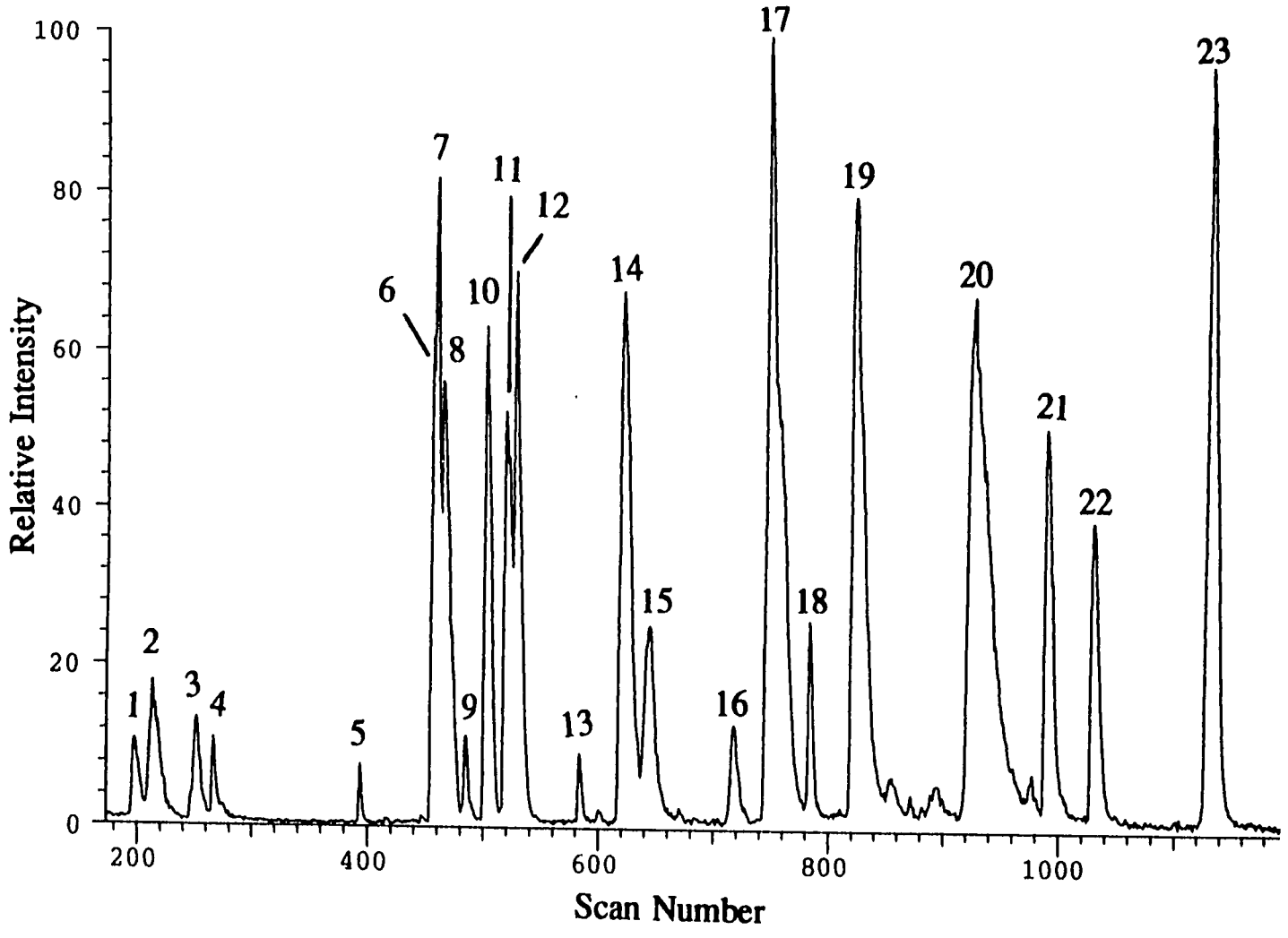

Figure A2.1 LC-MS RIC of the tryptic digest of HRP. The peaks 10% above the baseline are labelled (1-24). The assignment of the peptides based on their masses is shown in Table A2.1.

1	ELTPTFYDNS	CPÑVSNIVRD	TIVNELRSDP	RIAASILRLH	FHDCFVNGCD
51	ASILLDÑTTS	FRTEKDAFGN	ANSARGFPVI	DRMKAAVESA	CPRTVSCADL
101	LTIAAQQSVT	LAGGPSWRVP	LGRRDSLQAF	LDLANANLPA	PFFTLPQLKD
151	SFRNVGLÑRS	SDLVALSGGH	TFGKNQCRFI	MDRLYÑFSNT	GLPDPTLÑTT
201	YLQTLRGLCP	LNGÑLSALVD	FDLRTPTIFD	NKYYVNLEEQ	KGLIQSDQEL
251	FSSPÑATDTI	PLVRSFAÑST	QTFFNAFVEA	MDRMGNITPL	TGTQGQIRLN
301	CRVVNSNS				

Figure A2.2 Amino acid sequence of HRP based on the amino acid sequence studies [Wellinder, K. G. (1979) *Eur. J. Biochem. 96,* 483]. Cysteines (C) involved in the 4 disulfides (11-91, 44-49, 97-301, and 177-209) are marked, as are the 8 sites (Ñ) of carbohydrate attachment.

Table A2.1 Assignment of HRP Tryptic Peptides

Peak[a]	Observed $[MH]^+$ [b]	Predicted $[MH]^+$ [c]	Residues[d]
1	1842.6	1842.8	154-159*
2	541.3	541.4	119-123
3	1022.6	1022.5	66-75
4	1381.6	1380.7	63-75
5	681.1	681.3	179-183
6	935.3	935.5	225-232
7	1185.4	1185.6	233-241
8	743.3	743.5	32-38
9	2612.6	---	40-62, 116-138, 266-288[e]
10	959.3	959.5	20-27
11	803.3	803.4	76-82
12	1587.1	1586.8	284-298
13	1475.4	1475.8	160-174
14	4222.4	4239.8	1-19...85-93*[f,g]
15	3400.3	---	---
15	3254.8	---	274-302[e]
16	5064.7	---	78-125[e]
17	3671.8	3671.7	242-264*
17	3893.0	3893.6	39-62*[f]
18	2850.4	---	100-126,101-126, 130-154,177-201, 187-212[e]
19	3047.6	3047.5	94-118...299-302[f]
20	10674.0	---	26-123,65-164, 121-217,122-218[e]
21	3353.4	3353.4	265-283*
22	2534.0	---	84-108,89-114[e]
23	2744.0	2744.5	125-149
24	---	---	---

[a] Peak labels from Figure A2.1. [b] Calculated from the mass spectra. [c] Predicted from the sequence of HRP. [d] Residues are listed in Figure A2.2. [e] Unassigned peptides. [f] Disulfide-linked peptide(s). [g] Tentatively assigned glycosylated/disulfide-linked T_1—T_{10}, but since HRP is known to contain a modified N-terminus, the mass of the carbohydrate may differ from 1170.4 Da. * Glycosylated peptides.

peptides, all but 3 peptides (1 of which is disulfide linked) were identified. Seven peptides were not assigned, and some of these may contain different degrees of glycosylation which would prevent exact mass determination. The assignment of the peptides is shown in Table A2.1.

HRP (MW ~ 34 kDa) has 308 amino acid residues, contains 2 bound Ca^{2+} ions, and 4 disulfide bridges. It is made up of a single polypeptide chain that carries 8 neutral *N*-linked carbohydrate side-chains, which have the average composition of (*N*-acetylglucosamine)$_2$ (mannose)$_3$ (fucose) (xylose) [Wellinder, K. G. (1979) *Eur. J. Biochem. 96,* 483]. Based on this average, the masses of the glycosylated peptides are expected to increase by 1170.4 Da . Trypsin cleaves specifically at Lys and Arg residues [Darbre, A. (1986) in *Practical Protein Chemistry- A Handbook,* Wiley & Sons: Chichester, England] and ideally 28 HRP tryptic peptides, 7 of which are linked by disulfide bridges, are expected based on the sequence in Figure A2.2. The peptide mass mapping analysis (Table A2.1) shows that 5 peptides were identified with a carbohydrate moiety of mass 1170.4 Da. The unidentified glycopeptides likely contain carbohydrates of mass < 1170.4 Da and may give rise to a number of the unidentified peptides. Furthermore, 5 disulfide-linked peptides are easily identifiable and these contain the predicted oxidized cross-linked cysteines.

The results in Table A2.1 underscore the advantages of LC-MS in peptide mapping. LC-MS has the clear advantage of mass resolving power even when the peptide maps suffer from low chromatographic resolution. In conclusion, the LC-MS results in Table A2.1 reveal that peptide mass mapping of H_2O_2-oxidized HRP and/or

otherwise modified HRP is highly feasible.

CHAPTER 7

GENERAL CONCLUSIONS AND SUGGESTIONS FOR FUTURE WORK

The plant peroxidase superfamily consists of evolutionary-related peroxidases from bacteria, fungi, and plants. The two most widely studied peroxidases are CCP and HRP. Both peroxidases unfold in denaturants in two distinct steps as monitored by fluorescence but loss of their secondary structure as monitored by UV/CD occurs in a single step (Chapter 2). The $N \rightleftharpoons I$ fluorescence-sensitive transition in CCP(MI) involves the heme cavity indicating flexibility of the heme. Such flexibility may be important in heme uptake by the apoprotein, which is the dominant form *in vivo* when yeast are grown under anaerobic conditions. Furthermore, since CCP is able to store many oxidizing equivalent on its polypeptide (Chapters 4 and 5), its enhanced conformational flexibility over that of HRP might be of importance in the generation and translocation of radicals. The conformational change involving the Trp117-containing loop, which is responsible for the fluorescence-detectable $I \rightleftharpoons U$ transition of HRP has no obvious functional role but is likely a consequence of the structural elements (2 bound Ca^{2+} ions and 4 disulfide bridges) present in HRP. These structural elements are also responsible for the greater kinetic stability of HRP compared to CCP(MI). Cations would be counterproductive in radical stabilization in CCP since it has been observed that a region of negative electrostatic potential has been built into this peroxidase to stabilize the Trp191 radical [Miller, M. A., Han, G. W., & Kraut, J. (1994) *Proc. Natl. Acad. Sci. U.S.A. 91*, 11118].

The effects of cyanide ligation on the conformational states of CCP(MI) (Chapter 3), provide additional evidence for conformational flexibility in CCP since a $N \rightleftharpoons I$ transition also occurs in CCP-CN and resembles its acid $\rightleftharpoons$ alkaline transition. It

is likely that the $N \rightleftharpoons I$ transition of both unligated and CN^--ligated CCP(MI) arises from partial tertiary structure collapse. An $I \rightleftharpoons U$ transition above 4 M GdHCl is not observed in HRP-CN, presumably because excess free CN^- causes disulfide cleavage. The higher unfolding cooperativity as well as the decreased kinetic stability of HRP-CN compared to HRP, support such speculation.

Protein steady-state fluorescence in 8 M urea at pH 1.5 results in 100% relative fluorescence for yeast CCP and this allows fluorescence loss to be equated with Trp loss (Chapter 4). The role of Trp residues as endogenous electron donors in CCP compound I and in H_2O_2-oxidized CCP was examined. Loss of fluorescence is observed in denatured compound I equal to the loss of ~ 1 Trp, supporting the assignment of Trp191 as the amino acid radical in CCP. Further H_2O_2-oxidation of the polypeptide in the absence of ferrocyt *c* results in the total loss of ~ 3 Trps in the 20:1 decay product and amino acid analysis also reveals the loss of ~ 3 Tyrs. Charge migration must occur in the polypeptide of CCP since further activity and fluorescence loss occurs over 24 h. The residual ferrocyt *c* (16 - 73%) and ferrocyanide oxidizing activities (13 - 76%) of the H_2O_2-oxidized CCP decay products correlate with their H_2O_2 titers (18 - 74%), indicating that activity loss is due to the reduced capacity of the enzyme to react with H_2O_2. Charge migration to the surface also occurs and results in *intermolecular* crosslinking such that 7 - 33% of the H_2O_2-oxidized protein forms dimers. Nonetheless, CCP exhibits a remarkable ability to store oxidizing equivalents while maintaining some activity and this may be related to its proposed role as an antioxidant enzyme in yeast (Chapter 6).

The redox activity of Trp residues in CCP(MI) and its W51F and W191F mutants was investigated (Chapter 5) by the same methodologies used for yeast CCP (Chapter 4). Loss of 1 Trp in compound I of CCP(MI) and W51F but ~ 0 Trps in W191F compound I strongly suggests that $P^{+\cdot}$ is located on Trp191 (eq 1.3). Reoxidation of the compound I decay products of CCP(MI), W51F and W191F results in immediate loss of 1.3, 0.5 and 0.7 extra Trps, respectively, implying that Trp51 is a possible electron donor in the decay product. Addition of 6 equivalents of H_2O_2 results in loss of ~ 2 Trps in CCP(MI) but only ~ 1 in W51F and W191F, suggesting that Trp51 becomes redox active in CCP(MI) when > 2 equivalents of H_2O_2 are reduced. An additional Trp is oxidized in the decay product of CCP(MI) following addition of 6 equivalents of H_2O_2 but not in W51F or W191F, indicating that both Trp→Phe mutations shut down pathways of endogenous electron transfer. Further oxidation of Trps on reaction with 20 equivalents of H_2O_2 results in a total loss of ~ 4, 2.5 and 2 Trps in CCP(MI), W51F and W191F, respectively. Amino acid analysis of the 20:1 decay products also shows loss of up to 4.4 Tyrs and 0.8 Met in CCP(MI) and 3.8 Tyrs in W191F. The residual activities of CCP(MI) and W51F exposed to 20 equivalents of H_2O_2 are 5 to 19% while W191F retains ~ 50% ferrocyanide oxidizing activity after 24 h. The high activity of H_2O_2-oxidized W191F is not surprising considering the lower overall loss of Trp and Tyr residues compared to that of CCP(MI). It is possible that W191F may use catalatic activity in turning over 20 equivalents of H_2O_2, which would be consistent with its constant degree of dimerization (~ 30%). Charge migration to the surface in CCP(MI) requires treatment

with > 2 equivalents of H_2O_2 but, like W191F, results in only ~ 33 % dimer formation. Radical migration is greatly facilitated by the Trp51→Phe mutation since over 70% of the H_2O_2-oxidized W51F undergoes polymerization.

Mass spectral analysis was used to gain insight into the antioxidant properties of CCP (Chapter 6). Two sites of *intermolecular* crosslinking in the decay product of W191F compound I were found by peptide mass mapping (LC-MS). A comparison of the tryptic peptides of the monomer and dimer forms of W191F shows that residues 30-48 and 227-243 are involved in crosslinking and that radical formation on residues 30-48 is necessary for dimer formation. The addition of a spin trap (MNP) to W191F prior to reaction with H_2O_2, followed by tryptic digestion and LC-MS analysis, reveals that no surface radicals are trapped in W191F indicating that the spin trap *cannot* compete with dimerization. However, following oxidation of C*c*P(MI) with 20 equivalents of H_2O_2 in the presence of MNP the tryptic peptides that contain Tyr36, 39, 42 (T_6), Tyr153 (T_{21}), and Tyr229, 236 (T_{26}) are modified. Sequencing of modified T_{26} by on-line CID reveals that spin-adduct formation occurs on Tyr236. Since T_{26} is less reactive than T_6 in dityrosine formation in W191F [and presumably also in CCP(MI)], radical formation of Tyr236 should result in less cellular damage *in vivo*.

Future Work

The present studies (Chapters 2 to 6) on CCP and HRP reveal some very

interesting insights into structure-function relationships in heme peroxidases. Equally important, this work raises new questions and highlights opportunities for future work. The following studies are proposed:

(1) Examine the conformational state(s) of APX in denaturants. It would be of interest to compare the results with those of CCP(MI) and HRP in Chapters 2 and 3 since APX contains a single proximal cation so the stabilizing effects of cation binding could be evaluated. Interestingly, APX has a Trp residue in an analogous position to that of CCP(MI) but forms a porphyrin cation radical in compound I.

(2) Follow up on the speculation that excess free CN^- modifies the disulfides of HRP, leading to the observed effects on its conformational state in denaturants as well as to its kinetic instability relative to unligated HRP. On-line LC-MS analysis of proteolytic digests (Addendum 2) of HRP-CN should be of value towards this goal.

(3) Complement the denaturant-induced denaturation studies of CCP-CN and HRP-CN with a thermally-induced denaturation study using FTIR.

(4) Investigate whether steady-state fluorescence is a useful probe in determining if redox-active Trp residues exist in APX and HRP on their reaction with excess H_2O_2 in the absence of exogenous electron donors.

(5) While yeast CCP does not evolve O_2 in reducing 20 equivalents of H_2O_2, W191F is more likely to demonstrate "catalase-like" activity based on its Trp loss and crosslinking pattern. Therefore, possible O_2 evolution during the reaction of W191F with > 2 equivalents of H_2O_2 should be investigated using a Clark oxygen electrode.

(6) Mutation of the distal Trp51 results in extensive translocation of radicals to the surface of CCP on its reaction with H_2O_2 as evidenced by extensive crosslinking of W51F. During the present study, insufficient W51F was available to separate the polymeric forms of H_2O_2-oxidized W51F. Separation of some of these forms and peptide mass mapping, similar to that performed for CCP(MI) and W191F, should be carried out to locate the crosslinking sites.

(7) The crosslinking and the spin trapping experiments performed on CCP(MI) and W191F revealed that certain surface-exposed Tyr residues are redox-active and transfer electrons to the Fe^{IV}=O. These Tyrs should be singly-modified with NO_2 and purified to homogeneity since it would be of interest to measure the electron transfer rates from pulse-radiolytically generated Tyr-$NO_2^{\bullet -}$ to the Fe^{IV}=O heme.

(8) Tyr→Phe mutants (Y36F, Y39F, Y42F, Y236F, etc.) should be used to specifically shutdown radical migration pathways to reactive Tyrs in CCP. The effects of these mutations on endogenous donation to H_2O_2 should be examined.